A LIQUID-NITROGEN-COOLED MASER WITH SPECIAL BROAD-BAND FEATURES

by

Robert D. Pringle

Thesis presented for the Degree of Doctor of Philosophy of the University of Edinburgh in the Faculty of Science.

August, 1966

CONTENTS

	Introduction	1
Chapter 1	The Principle of the Stimulated Emission Amplifier	5
1.1	Spontaneous Emission	5
1.2	Stimulated (or Induced) Absorption	6
1.3	Stimulated (or Induced) Emission	6
1.4	Inversion Ratio and Negative Spin Temperature	8
1.5	Spontaneous Emission and Noise	10
Chapter 2	Maser Materials and Pumping Systems	13
2.1	Two-Level Systems	14
2.2	Multi-Level Pumping Systems	16
2.3	"Push-Pull" Pumping	24
2.4	The Zero-Field Maser	30
Chapter 3	Ruby as a Maser Material at Liquid Nitrogen Temperature	35
3.1	Transition Probabilities	35
3.2	Magnetic Q, Q_m	39
3.3	Optimisation of $(n_3 - n_2)/\Delta\nu_L$	41
3.3.1	Spin-Spin Relaxation Time, τ_2	45
3.3.2	Spin-Lattice Relaxation Time, τ_1	46
3.3.3	Cross-Relaxation	48
3.4	Signal Saturation	61
Chapter 4	Cavities and Travelling-Wave Structures for Masers	65
4.1	Cavity Masers	65
4.2	Travelling-Wave Masers	72
4.2.1	Gain and Bandwidth in Travelling-Wave Masers	73

Chapter 5	Reactance Compensation in Cavity Masers	78
Chapter 6	Design and Construction of a Two-Cavity Maser	93
6.1	Methods of Cavity Construction	93
6.2	Maser Cavity	102
6.3	Coupling Cavity	109
6.4	Adjustment of Coupling Slots	110
6.5	The Tapered Waveguide Sections	112
Chapter 7	Ancillary Equipment	119
7.1	The d.c. Magnetic Field	119
7.2	Pump Frequency Equipment (K-band)	121
7.2.1	K-band Bridge Circuit	121
7.2.2	Low-Power Swept-Frequency K-band Circuit	123
7.2.3	High-Power K-band Pump Circuit	125
7.3	Signal-Frequency (X-band) Equipment	128
7.3.1	Maser Gain Measurement	131
7.3.2	Maser Bandwidth Measurement	132
Chapter 8	Results and Conclusions	136
8.1	Pump Power	136
8.2	Maser Performance	138
8.2.1	Alignment of the Cavities	138
8.2.2	Feedback and Probe Coupling to the Maser	139
8.2.3	Photographs Showing the Alignment of the Two-Cavity Maser	141
	References	158
	Acknowledgements	166

INTRODUCTION

General

Great value attaches to efficient, high-capacity communication systems. Commercial prospects are excellent for any nation or company which can control and operate new channels made possible by satellite relays. Distances are very great but power supplies available at the satellite station are very small and therefore ground receivers of the highest possible sensitivity are required. The revenue from such systems is directly proportional to channel capacity and hence to bandwidth and therefore this must be made as large as possible if the maximum yield is to be obtained from the very large capital investments involved.

The signal level which can be detected is governed in the first instance by the background noise temperature, and here nature has bestowed upon the designers of communication systems the gift of a low-noise window extending approximately from 3 to 10 Gc/s. In this frequency range the background noise temperature for an antenna beamed at a high angle of elevation is only a few degrees Kelvin and the detectable signal level is determined for all practical purposes by the noise temperature of the receiver.

The development of the maser amplifier has enabled this low-noise region of the spectrum to be exploited. Since amplification by stimulated emission was first demonstrated by C. H. Townes and his associates in 1955 the maser has been developed into the "near-ideal" amplifier. Liquid-helium-cooled

travelling-wave masers have noise temperatures of 3 or 4°K which, with gains of 30-35 dB, enable receiving systems with overall noise temperatures as low as 30°K to be built and most of this residual noise temperature comes from the aerial itself and the waveguides connecting it to the maser. While they do not realise the full potential of the carrier frequencies the achievable bandwidths (of the order of 25 Mc/s) are commercially attractive and are ample even for colour television channels.

In view of the practical difficulties and the cost involved in producing and using liquid helium, interest has been shown in masers cooled with liquid nitrogen. There are fundamental reasons why such masers could never attain the high performance of the liquid-helium-cooled maser, but there are applications where the extremely low noise temperature of the latter is not required. By designing specially for the higher temperature masers can be built with noise temperatures less than 100°K which, at the present time can be challenged only by certain types of parametric amplifier.

There are two basic types of maser. The active maser material interacts with the microwave signal field either in a cavity or in a slow-wave structure. Hitherto all liquid-nitrogen-cooled masers have been of the single cavity type and it is not possible to overcome the disadvantages of this type by changing to the travelling-wave type structure as has been done at liquid helium temperatures. The chief disadvantage of the single cavity maser is that the voltage-gain-bandwidth

product, which is constant, is typically 10 to 20 Mc/s and with this simple cavity maser even this limited performance cannot be manipulated to full advantage since the voltage-gain-bandwidth product does not remain constant if the bandwidth is increased much beyond 1 Mc/s. Furthermore the frequency response of such an amplifier is Lorentzian which means that even within this limited bandwidth the shape of the response curve is not ideal for communications purposes.

Work done at liquid helium temperatures in the United States on "Reactance Compensation" has shown that both the bandwidth and the shape of the response curve can be improved by the addition of a passive coupling cavity between the input waveguide and the maser cavity. Reasonably flat bandwidths of the order of the transition line width of the active material were achieved at 14 dB gain (too low for a practical liquid-helium-cooled maser). While it is obvious that such spectacular performances are not possible at liquid nitrogen temperature, it is the purpose of this investigation to determine both theoretically and in practice to what extent this principle can be applied at this higher temperature.

Layout of Thesis

After briefly considering the principles involved and the difference between liquid helium temperature and liquid nitrogen temperature operation in Chapter 1, the choice of ruby as the most suitable material is justified in Chapter 2. Chapter 3 contains a detailed discussion of the parameters which determine the choice of the best pumping mode and the best chromium

concentration for operation at 77°K. The two basic microwave structures for masers are considered in Chapter 4 and it is shown that despite their attractive bandwidth characteristics, slow-wave structures are not suitable for masers operating at 77°K. It is concluded that at this temperature a cavity maser must be used.

In Chapter 5 the various improvements that have been made to the bandwidth characteristics of cavity masers by the method of "reactance compensation" are considered and it is reasoned that the approach most likely to produce an improved performance at 77°K is to have one active maser cavity coupled to the input waveguide by a passive coupling cavity. Calculations of the expected performance of such a device are presented using the best reported values for the various parameters involved. Chapter 6 describes the design and construction of the cavities and the special tapered guide sections required to couple into them. A brief description of the associated equipment and measurement techniques is given in Chapter 7 and Chapter 8 contains the actual results. These show how the gain and bandwidth can be adjusted while maintaining a flat gain v. frequency characteristic. The bandwidth is close to the expected value though the observed gains are rather low. The possibility of this being due to too high a signal input level is discussed.

In conclusion it is claimed that the method of reactance compensation has been shown to produce a gain v. frequency characteristic which is near to the ideal for communications purposes.

CHAPTER ONE

The Principle of the Stimulated Emission Amplifier

The theory governing the principle of stimulated emission was first developed by Einstein[1] in his historic paper "Zur Quantentheorie der Strahlung" in which he considered the phenomenon of emission and absorption of radiation in the light of Planck's Radiation Formula[2].

Einstein considered the simple case of an assembly of molecules each of which can be in one of two energy levels with energies E_1 and E_2 ($E_1 < E_2$). The ratio of the populations n_{1o} and n_{2o} in thermal equilibrium at temperature T is given by the Boltzmann Distribution

$$n_{2o} = n_{1o} \exp\left(-\frac{E_1 - E_2}{kT}\right) = n_{1o} \exp\left(-\frac{h\nu_{12}}{kT}\right)$$

Even in the absence of an applied field of frequency ν_{12} there will be a field of this frequency caused by the continuous processes of emission and absorption of radiation. There are three such processes:

1.1 Spontaneous Emission

In any system with molecules in an excited state there is a finite probability of emission of a quantum of the appropriate energy, leaving the molecule in the ground state. This process is proportional only to the number of molecules in the upper energy level, n_2, and is therefore called "spontaneous emission". Thus the rate of change of n_2 due to this process is

$$\left(\frac{dn_2}{dt}\right)_{\text{spontaneous}} = -A\, n_2 \qquad (A = \text{constant})$$

1.2 Stimulated (or Induced) Absorption

This represents the probability of a molecule in level 1 absorbing a quantum of radiation from the radiation field and being excited into level 2. The probability of this occurring is proportional to the number of molecules in the lower level and to the energy density $\mu(\nu)$ of the radiation field at the appropriate frequency ν_{12}. For zero applied electromagnetic field there will be a field of energy density $\mu_0(\nu)$. The rate of change of n_2 due to this process which is called "stimulated" or "induced" absorption is

$$\left(\frac{dn_2}{dt}\right)_{\text{stimulated absorption}} = \mu(\nu).\, B.\, n_1 \qquad (B = \text{constant})$$

1.3 Stimulated (or Induced) Emission

Einstein reasoned that there must be an emission process analogous to stimulated absorption and it was this new postulate which provided a theory which agreed with the experimentally-observed facts. The probability of a molecule in the upper energy level emitting a quantum of energy is increased by the presence of an incident radiation field of the appropriate frequency ν_{12}. The probability of stimulated emission is proportional to the number of molecules in the upper energy state and the energy density of the incident field

$$\left(\frac{dn_2}{dt}\right)_{\text{stimulated emission}} = -\mu(\nu).\, C.\, n_2 \qquad (C = \text{constant})$$

For the system in equilibrium with its surroundings at temperature T the populations of the levels are constants and therefore the total rate of change of n_2 is zero. The energy density of the field is $\mu_0(\nu)$. Therefore

$$\frac{dn_2}{dt} = - A\, n_2 + B.\, n_1 .\, \mu_0(\nu) - C.\, n_2 .\, \mu_0(\nu) = 0$$

Inserting the Boltzmann relation and rearranging.

$$\mu_0(\nu) = \frac{A}{Be^{\frac{h\nu}{kT}} - C}$$

Comparing this with the experimentally fitted radiation formula of Planck

$$\mu_0(\nu) = \frac{8\pi\nu^3}{C^3} \cdot \frac{h\nu}{e^{\frac{h\nu}{kT}} - 1}$$

indicates that $A/B = \frac{8\pi h\nu^4}{C^3}$ and B = C. B = C implies that for any molecule in the upper state the probability of stimulated emission is exactly the same as the probability of stimulated absorption for any molecule in the lower state. This conclusion is of fundamental importance in the quantum theory in general and in the theory of masers in particular. Another such principle, which no attempt will be made to prove here, is that photons emitted as a result of stimulated emission are in phase with the photons causing the stimulation. Clearly this is necessary if stimulated emission is to be used to obtain amplification.

In a system of molecules in thermal equilibrium there are more molecules in the lower energy state than in the upper state and hence a beam of radiation of the appropriate fre-

quency passing through the system will be attenuated since more quanta will be absorbed from the beam by the system than will be emitted into it. If, however, the system is in a state such that $n_2 > n_1$ a greater number of quanta will be emitted into the beam than will be absorbed from it and amplification of the beam results. This is an oversimplified case and in practice whatever type of enclosure is used for the system will involve losses and the condition for amplification is then that $n_2 > n_1$ by an amount greater than that corresponding to the losses.

1.4 Inversion Ratio and Negative Spin Temperature

To describe quantitatively the degree of "inversion" as this emissive state is called, an "inversion ratio", I, is defined thus:

$$\text{Inversion ratio, } I = \frac{n_2 - n_1}{n_{1o} - n_{2o}}$$

where n_2 and n_1 are the populations of the upper and lower states respectively in the inverted state and n_{2o} and n_{1o} are the populations for thermal equilibrium as before.

Alternatively n_1 and n_2 may be inserted in the Boltzmann equation to define a parameter T_s. T_s then has the dimensions of temperature and describes the degree of inversion. For an inverted system, since $n_2 > n_1$, T_s is negative and is called the "negative spin temperature". (The word "spin" occurs because most maser systems involve energy levels of electron spins.)

The above theory applies to any system governed by the Boltzmann Distribution interacting with any electromagnetic field of the appropriate frequency. It will be advantageous to obtain some idea of the orders of magnitude of certain parameters for the particular frequency and temperatures involved in X-band maser design.

Planck's Constant $h = 6{\cdot}625 \times 10^{-34}$ Joule-sec.

Boltzmann's Constant $k = 1{\cdot}38 \times 10^{-23}$ Joule/°K.

Frequency ν = 10 Gc/s $= 10^{10}$ c/s.

The following table shows $h\nu/kT$ and the fraction of the total population n_t in each of the two levels at 1·5°K (liquid helium under reduced pressure), 4·2°K (liquid helium at atmospheric pressure), 77°K (liquid nitrogen) and 290°K (room temperature)

(The suffix $_o$ denotes population at thermal equilibrium)

T (°K)	$h\nu/kT$	n_{1o}/n_t	n_{2o}/n_t	$(n_{1o} - n_{2o})/n_t$
1·5	0·32	0·58	0·42	0·16
4·2	0·09	0·523	0·477	0·046
77	0·006	0·5014	0·4986	0·0028
290	0·0016	0·5003	0·4997	0·0006

The problem of how to achieve the condition $n_2 > n_1$ required for maser action will be discussed in later chapters when it will be seen that the fraction $(n_2 - n_1)/n_t$ can, under certain conditions, be made larger than the fraction $(n_{1o} - n_{2o})/n_t$ (i.e. inversion ratios greater than unity are possible) but it

will always be of the same order. From this it is immediately obvious why masers are usually operated at liquid helium temperatures. The 1·5°K temperature has been quite widely used in laboratory systems but most masers which have been employed in practical systems were operated at 4·2°K. It is seen that the population difference is about 4·5% at 4·2°K compared with about 0·25% at 77°K. Since the maser performance is directly dependant on the population difference $n_2 - n_1$ this limits the performance at the higher temperature. The obvious remedy of increasing the total number of participating molecules cannot be applied indiscriminately although it will be shown that some of the loss in performance can be recouped in this way.

1.5 Spontaneous Emission and Noise

This process must be considered firstly because it produces radiation at the signal frequency which is of random phase and secondly because it is a relaxation mechanism. It can be shown[3] that for electron spin systems of the type used in most masers

$$A = \frac{8\pi^3 \mu_0}{3hc^3} (g\beta)^2 \nu_{12}^2$$

where g is the spectroscopic splitting factor,

β is the Bohr magneton,

$(g\beta)$ is the magnetic dipole moment.

For a frequency of 10 Gc/s $A \sim 10^{-11}$ sec^{-1} i.e. for an electron spin in the upper energy level the mean lifetime is of the order of 10^{11} sec. A maser of the type to be considered would

contain of the order of 10^{19} spins and therefore the spontaneous emission rate would be at the most about 10^{8} photons/sec.

At 10 Gc/s the photon energy $h\nu$ is $6{\cdot}625 \times 10^{-24}$ Joule and at 10^{8} per second this corresponds to a noise power of the order of 10^{-17} watts. This is in theory the only source of noise in the maser and the small magnitude of this explains the low noise features of masers. In practice there are finite losses in the microwave system which give rise to a noise power dependent on the temperature. Equivalent noise temperatures of the order of 100°K have been measured for liquid-nitrogen-cooled masers. Even with a bandwidth of only 1 Mc/s this thermal noise corresponds to a noise power (kTB) of the order of 10^{-15} watts and this increases proportionately with bandwidth. Thus even for the limited bandwidths already achieved the thermal noise is of the order of 100 times greater than the spontaneous emission noise and hence the latter may be disregarded.

Spontaneous emission is also a relaxation process. It has already been mentioned that the emissive condition ($n_2 > n_1$) can never be an equilibrium condition and a system in such a condition will always be subject to relaxation processes which tend to restore it to thermal equilibrium. Spontaneous emission is the most fundamental of these processes. If a system is perturbed from its equilibrium state then, in the absence of any stronger relaxation mechanism, spontaneous emission will re-establish the equilibrium state.

In practical masers, however, there are other processes which constitute a much stronger coupling to the surroundings and in fact at microwave frequencies, particularly for magnetic dipole moments of electron spins, spontaneous emission makes a negligible contribution to the total relaxation.

At optical frequencies, the formula for the spontaneous emission probability, A, is similar except that the dipole moment is usually an atomic electric dipole moment and the frequency is about 5 orders of magnitude greater. Since $A \propto \nu^4$ the spontaneous emission probability is vastly increased and this, the most fundamental relaxation process, is also the predominant one.

The design of a maser divides naturally into two sections. Firstly a material with a suitable system of energy levels must be chosen and secondly a microwave structure must be designed which will allow suitable interaction between the material, the microwave signal field which is to be amplified and any other fields required to achieve and maintain the emissive condition.

CHAPTER TWO

Maser Materials and Pumping Systems

The first demonstration of the principle of stimulated emission was the ammonia beam gas maser of Townes et al.[4,5] but such masers are not suitable for use as amplifiers despite their inversion mechanism being capable of producing very low negative "spin" temperatures at room temperature since this mechanism can only operate where the mean free path of the molecules in the beam is large compared with the diameter of the beam. This limits the output power to a level too low even for a preamplifier. Furthermore the frequency is dictated by molecular constants of the system which would be an inconvenient restriction on the design of an amplifier although this combined with the very narrow line width has led to the development of gas masers as frequency standards.

The search for suitable systems in which the inversion required for maser amplification could be achieved and maintained centred at an early stage on paramagnetic electron spin systems. The emissive condition can never be an equilibrium one and hence a system in the emissive state will always tend to relax to equilibrium. The levels used in solid state masers are obtained by Zeeman splitting of electron spin levels by an applied d.c. magnetic field. This removes the degeneracy in electron spin states which exists in the absence of such a preferred direction, making states which had previously the same energy separate to an extent which corresponds

to microwave transition frequencies for readily available fields of the order of a few Kilogauss. Any departure from the equilibrium population distribution will tend to relax exponentially to the equilibrium state once the perturbing mechanism is removed and this decay is characterised by a time constant $\tau_{\parallel}$, the "spin-lattice" relaxation time - so called because it describes the strength of the coupling between the spins and the supporting host lattice.

2.1 Two-Level Systems

Two-level Systems are necessarily pulsed because a system of only two energy levels cannot be pumped into an emissive state by a strong incident microwave field and be simultaneously amplifying a weak microwave signal at the same frequency. Another reason is that a two-level system cannot be pumped into an emissive state by application of a continuous microwave field however great its power. All methods of producing inversion in a two-level system are pulsed. From the thermal equilibrium state with $n_2 < n_1$ energy is absorbed from the pumping field until $n_1 = n_2$ when the levels are said to be "saturated". It is impossible, however, to make n_2 exceed n_1 by any continuous method involving only two levels and all methods of inverting such systems are pulsed. The two-level maser depends for success of operation on the relaxation time being long enough to allow the emissive state to persist for a finite time after the pumping has been completed. To permit this the only suitable spins are those of very loosely bound electrons in solids. Ordinary dilute paramagnetic salts cannot be used because the electrons are too tightly bound to the atoms and hence in turn

to the lattice which shortens the spin lattice relaxation times. Suitable energy level systems are found in the paramagnetism of conduction electrons in semi-conductors (not metals because the high electron density would cause too much interaction between spins) and F-centres. An F-centre is the type of lattice defect where a lattice site is occupied by an electron instead of by an atom.

The first attempt to produce a two-level maser was by Combrisson, Honig and Townes[6] using silicon doped with phosphorus or arsenic. The inversion mechanism was the principle of "adiabatic fast passage" developed by Bloch[7] in his work on nuclear magnetic resonance. Despite a spin-lattice relaxation time estimated to be in the 5 to 30 sec. range at liquid helium temperatures amplification was not observed. It was not surprising, therefore, that experiments by the same team using a paramagnetic salt, $SiF_6.6H_2O$ doped with 0·05% Mn^{2+} (which has a higher spin density than in the above case), also failed since in this case the spin-lattice relaxation time was estimated to be 10^{-2} to 10^{-4} seconds.

Chester, Wagner and Castle[8] obtained amplification (and oscillation) using single crystals of quartz and MnO in which F-centres had been created by neutron irradiation. Using adiabatic fast passage to obtain inversion a voltage-gain-bandwidth product ($\sqrt{GB}$) of 5 Mc/s was observed for gains of 8 to 21 dB at X-band. The amplification obtained was in pulses of about 1 millisecond duration but the gain was decreasing exponentially throughout this period. This demonstrated that two-level solid-state masers could be operated successfully

but the fact that the $\sqrt{GB}$ product is not constant (or even approximately constant) for the duration of the pulse makes such systems totally unsuitable for communications purposes. Two-level masers were considered in spite of their necessarily pulsed mode of operation because it was felt that it might be possible to use them in conjunction with a pulse-code-modulation system such as delta-modulation but this exponential decay of the $\sqrt{GB}$ product precludes any such application. Furthermore all two-level masers have been operated at liquid helium temperatures and although the coupling of the spins to the lattice is weaker than in paramagnetic salts, the spin lattice relaxation times will be much shorter at 77°K. This means that the available amplifying time will be shortened and the decay of the $\sqrt{GB}$ product will be accelerated. Consequently two-level masers which are unsuitable at liquid helium temperatures are a fortiori unsuitable at liquid nitrogen temperature.

2.2 Multi-Level Pumping Systems

Multi-level pumping was first suggested by Bloembergen[9] in 1956 and has since been employed in all maser amplifiers produced with usable performance. The first and most important advantage is that continuous operation is possible. The second advantage is that the eminently suitable Zeeman splitting of dilute paramagnetic salts can be made use of since the continuous pumping employed allows the system to tolerate the shorter spin-lattice relaxation times. In multi-level systems the energy for inverting the signal transition is

supplied at a frequency different from the signal frequency. This "pump" frequency is usually, but not necessarily, greater than the signal frequency.

Bloembergen's original suggestion was for a three-level system. There are two possible configurations:

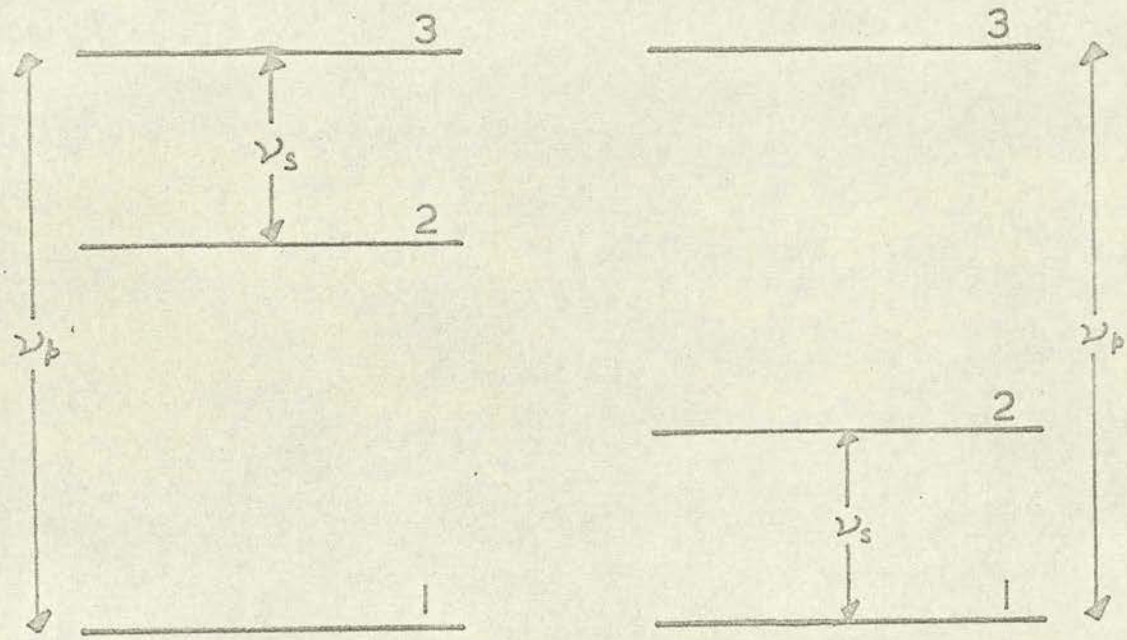

Three-level Pumping

Fig. 2.1

In both cases levels 1 and 3 are saturated by the pump field. In 2.1 (a), from the Boltzmann Distribution, assuming relaxation times between all pairs of levels to be of the same order inversion occurs provided that

$$\exp\left(\frac{E_2 - E_1}{kT}\right) + \exp\left(-\frac{E_3 - E_2}{kT}\right) > 2$$

$$\text{i.e.} \quad \exp\frac{h(\nu_p - \nu_s)}{kT} + \exp\left(-\frac{h\nu_s}{kT}\right) > 2$$

At liquid nitrogen temperature and X-band $\frac{h\nu_s}{kT} \doteq \cdot 006$ and it is legitimate to use the linear approximation to the exponentials, therefore this condition for inversion becomes

$$\nu_p > 2\nu_s$$

Normally the relaxation times are of the same order and this is the required condition for inversion. Bloembergen has shown that if the relaxation times are not of the same order, this condition must be modified to

$$\frac{\nu_p - \nu_s}{(\tau_1)_{21}} > \frac{\nu_s}{(\tau_1)_{32}}$$

where $(\tau_1)_{21}$ is the spin lattice relaxation time for the level 2 to level 1 transition and $(\tau_1)_{32}$ is similarly defined.

The condition for inversion in the system shown in 2.1 (b) is

$$\frac{\nu_p - \nu_s}{(\tau_1)_{32}} > \frac{\nu_s}{(\tau_1)_{21}}$$

The first experimental demonstration of the feasibility of Bloembergen's proposed pumping scheme was by Scovil, Feher and Seidel[10] in 1957. They used the second of the above configurations. The active material was a 0·5% concentration of gadolinium in lanthanum ethyl sulphate. The lanthanum ion is diamagnetic i.e. once the outer valence electrons are removed in ionic bonding all shells are complete. The

gadolinium ions (which in this case occupied 1 in every 200 lanthanum-type lattice sites) are the paramagnetic ions since they have an unfilled shell (the third outermost after ionisation). This shell contains seven electrons whose spins are unpaired and since the spin of an electron is $\frac{1}{2}$ the total spin S of the system is $\frac{7}{2}$ which, when the d.c. magnetic field is applied, yields $2S + 1 = 8$ energy levels. The electric field of the crystal has only a small effect since the unpaired electrons in the 4f shell are screened by the completely filled 5s and 5p shells. Such screening is typical of rare earth ions but for Gd^{3+} the effect of the crystal field is further reduced since the orbital angular momentum is zero. The first order effect of the crystal field on the spin of a paramagnetic ion is through the mechanism of spin-orbit coupling and therefore there are only higher order crystal field effects present if the orbital angular momentum is zero.

The derivation of the splitting of the energy levels from the Hamiltonian operator for a given ion and lattice is treated in some detail in the two standard text-books on masers (Vuylsteke[1] and Siegman[3]). It will, however, be worthwhile considering briefly the form of the Hamiltonian. For Gd^{3+} in lanthanum ethyl sulphate the Hamiltonian can be represented as follows: (for d.c. field parallel to the c-axis of the crystal)

$$\mathcal{H} = g\beta\, \underline{H}_0 \cdot \underline{S} - 2K_1\{S_z^2 - \tfrac{1}{3}S(S+1)\} + K_1(S_x^2 - S_y^2)$$

g is the spectroscopic splitting factor (1·99 in this case)

β is the Bohr magneton

H_0 is the applied magnetic field (in the z-direction)

S is the total effective spin of the ion (suffixes denote quantised components of S)

K_1 is a constant describing the effect of the crystal field on the ion

K_1 is small for the reasons discussed above.

Gd^{3+} therefore behaves very like a free ion (for which the Hamiltonian would be simply the first term on the right-hand side). The second term represents the higher order effects of the crystal field which, though small, are enough to cause non-uniformity of splitting without which ν_{12} would be equal to ν_{23} and maser action would not be possible. The third term represents admixture of the energy states which is also essential since it allows the $\Delta S_z = \pm 2$ transitions which are normally forbidden and upon which the pumping depends. The normal (unperturbed) quantum theory selection rules allow only $\Delta S_z = 0$ or ± 1 which includes the signal transition.

The energy levels for an applied field of 2·85 Kilogauss are shown in Fig. 2.2. Since ν_p is not in this case greater than $2\nu_s$, it is required that $(\tau_1)_{32}$ be much less than $(\tau_1)_{21}$ so that the increase in population of level 2 due to relaxation from level 3 is greater than the decrease in population of level 2 due to relaxation to level 1. This was achieved by adding a 0·2% concentration of cerium (Ce^{3+}) ions to the crystal and is due to cross-relaxation which will be discussed more fully later.

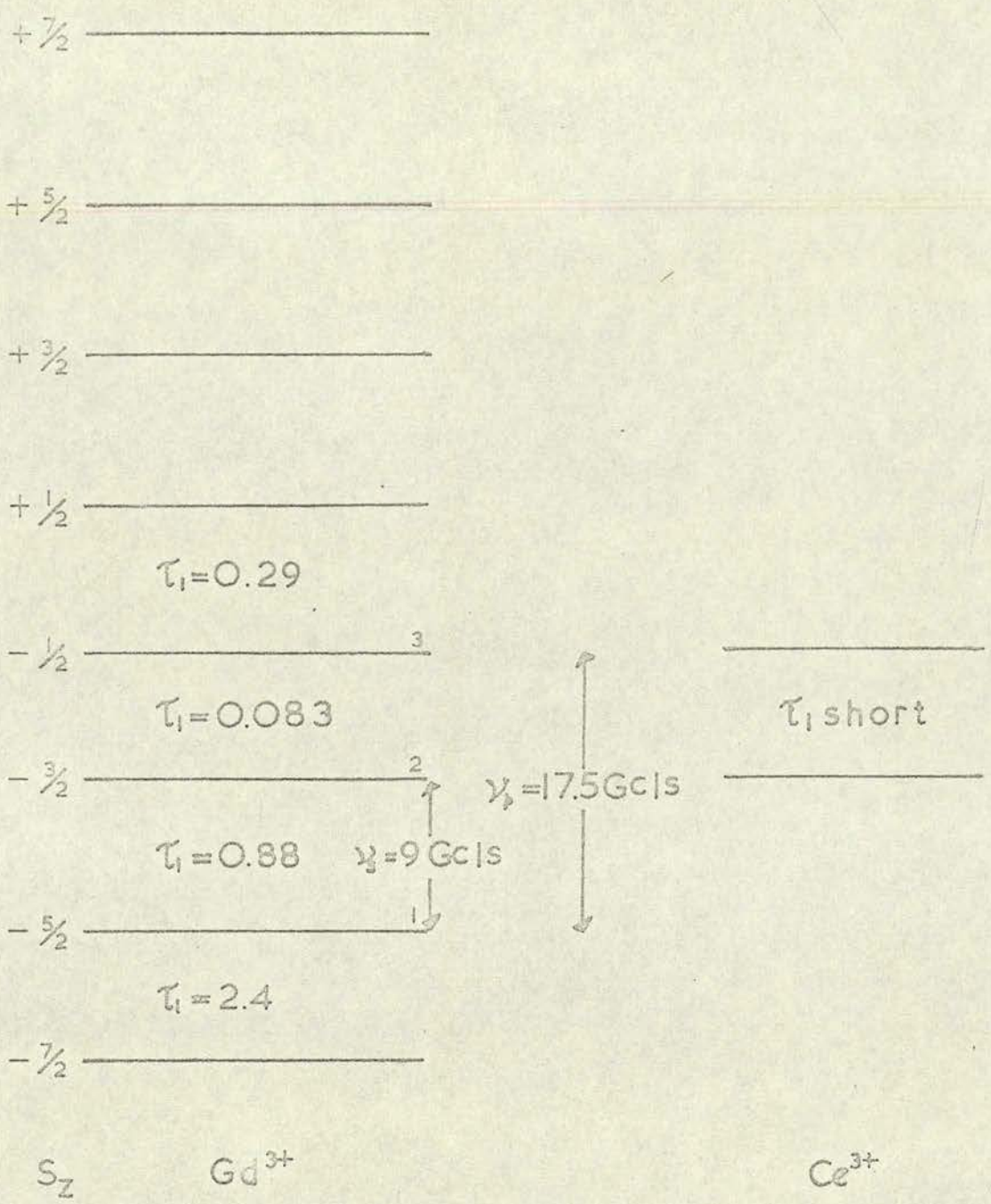

Energy levels of Gd^{3+} and Ce^{3+}
in lanthanum ethyl sulphate
(τ_1 in sec.$\times 10^{-4}$)

Fig. 2.2

The most serious disadvantage of gadolinium ethyl sulphate is that there are 8 energy levels of which only 3 are used. To a first approximation, therefore, only 3/8 of the active ions are being used. Since a compromise is always being sought between having as high a concentration of ions as possible in the maser and having them far enough apart to prevent excessive line broadening by "spin-spin" interaction, this redundancy of more than half the active ions is undesirable since it reduces the effective concentration of participating spins to which the strength of the maser action is directly proportional. Such redundancy is to be avoided in maser materials in general but in choosing a material for operation at 77°K this is particularly important because, as was discussed in Chapter One, the population difference involves only about ¼% of the total number of ions instead of about 4½% at liquid helium temperature.

A further disadvantage of this material is that it is unstable at room temperature which requires that it be kept refrigerated at all times. This original experiment did not actually produce a working maser amplifier but oscillation was obtained showing that with suitable coupling of the cavity this should be possible. Notwithstanding the above difficulties this material was used successfully in the first travelling-wave maser in 1959[12] and a good performance was obtained although even at that time the superior properties of ruby for maser action were realised.

The first three-level maser to perform as an amplifier

was built by McWhorter and Meyer[13] and used potassium cobalticyanide (diamagnetic) doped with 0·5% potassium chromicyanide (paramagnetic). This maser had its signal frequency at S-band but is of interest since the active ion was chromium which has only 4 Zeeman levels. Chromium is in the iron transition group which have the 3d shell incomplete. In the chromium ion this is the outermost shell and consequently the electrons in it are not screened from the effect of the crystal field by other shells. The electron orbits in this case are not free to orient themselves in the d.c. magnetic field but are "locked into" specific orientations by the strong crystal electric field. This is called "quenching" and it leads to "spin-only" paramagnetism i.e. only the electron spins (which have no electric moment) are free to participate. The total electron spin of chromium is $S = \frac{3}{2}$ (three unpaired electrons each of spin $\frac{1}{2}$) which gives $2S + 1 = 4$ Zeeman levels. Thus in this maser there is only one unused energy level.

To avoid having even one redundant level, McWhorter and Meyer tried at considerable length to build a similar maser with the Ni^{3+} ion in zinc fluorosilicate but failed since adequate pump power to combat the very short spin-lattice relaxation times ($\sim 10^{-4}$ sec.) of this material was not available. A further disadvantage is that the line width of this material is inhomogeneously broadened by a distribution of electric fields. It has been suggested that the very short relaxation times of this material are due to its spectroscopic

splitting factor g, which has a value of about 2.3. For a free spin g is 2 and for many paramagnetic salts it is close to 2 but slightly below it. In general g is anisotropic due to crystal field effects. It is generally accepted that a value of g much different from 2 implies considerable spin-orbit and hence spin-lattice interaction with attendant short relaxation times. Attempts to build masers with this ion at 1·4 and 2·8 Gc/s. failed. The reason why so much trouble was taken by McWhorter and Meyer and by other research workers (including Bloembergen himself) to make use of such a seemingly awkward salt is that apart from the g-factor the Ni ion appears ideal for three-level maser operation. It has no nuclear magnetic moment (which would broaden the line) and it has total spin unity which gives $2S + 1 = 3$ Zeeman levels and hence there are no unused energy levels. Also the splitting leaves one level unchanged which makes tuning easier. There is no published record of any subsequent masers with the nickel ion.

2.3 "Push-Pull" Pumping

Interest in the nickel ion may well have decreased due to the success achieved with 4-level pumping in chromium-doped ruby. This system uses all 4 levels of the chromium ion and hence removes the need for a 3-level ion. The use of ruby as a maser material was first suggested by Makhov, Kikuchi, Lambe and Terhune[14]. The 4-level system is actually a combination of the two configurations of the three level system. The energy level spacing is as shown in Fig. 2.3 and the operating principle is briefly as follows:

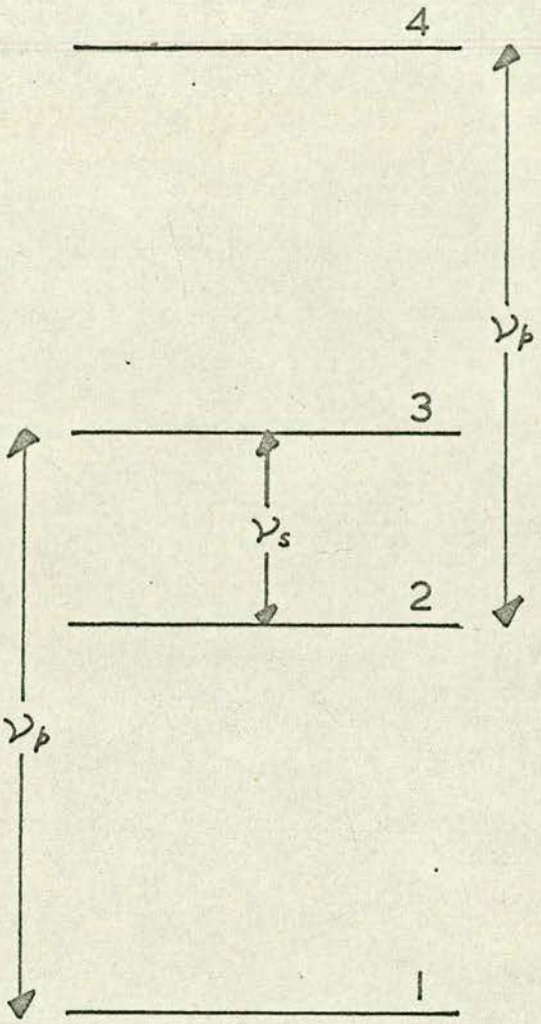

Four-level "Push-pull" Pumping

Fig.2.3

$$E_4 - E_2 = E_3 - E_1$$

and consequently applying a microwave field at the corresponding frequency will pump spins from E_1 to E_3 which inverts E_3 with respect to E_2 as before. The same field also pumps spins from E_2 to E_4. The inversion produced across the signal transition E_3 to E_2 is better than by any previously described method since spins are not only being pumped into the upper signal level but are also being pumped out of the lower signal level. For obvious reasons this scheme is sometimes called "push-pull" pumping.

Synthetic ruby (Al_2O_3) is used as a diluent for the Cr^{3+} ions and the electric field of this crystal is such that, if the d.c. magnetic field is applied at an angle of $54^{\circ}44'$ to the crystal axis the required 1-3 and 2-4 degeneracy is obtained for all values of the d.c. field. Since the advantages of this material were realised a great deal of work has been done on the paramagnetic resonance of chromium doped ruby to extend the previously available data of Geusic[15] and now computed data is available (Chang and Siegman)[16] and Schulz-Du-Bois[17] has published iso-frequency plots for a whole range of frequencies including 9·3 and 23·9 Gc/s.

Vuylsteke[11] has shown that the Hamiltonian for Cr^{3+} in Al_2O_3 is of the general form:

$$\mathcal{H} = g\beta \underline{H}_0 \cdot \underline{S} - D\{S_z^2 - \tfrac{1}{3}S(S+1)\} + E(S_x^2 - S_y^2)$$

(D and E are constants)

Geusic[15] showed that for ruby E = 0. S = $\frac{3}{2}$ for Cr^{3+} and

therefore

$$\mathcal{H} = g\beta\, \underline{H}_0 \cdot \underline{S} - D\{S_3^2 - \tfrac{5}{4}\}$$

Using this and the appropriate wave functions the elements of the Hamiltonian matrix are found and diagonalisation of this matrix yields the secular equation: (The energy level spacings are expressed in terms of frequency ν)

$$\nu^4 - 2(\nu_D^2 + \tfrac{5}{4}\nu_0^2)\nu^2 + 2\nu_0^2\nu_D(1 - 3\cos^2\theta)\nu$$

$$+ \nu_D^4 + \tfrac{9}{16}\nu_0^4 + \tfrac{1}{2}\nu_D^2\nu_0^2(1 - 6\cos^2\theta) = 0$$

ν_D is a constant of the crystal = 5·79 Gc/s. (Geusic[15])

$$\nu_0 = \frac{g\beta H_0}{h}$$ (θ = angle between H_0 and c-axis).

It is seen that for $\theta = \text{arc cos } \frac{1}{\sqrt{3}} = 54^\circ 44'$, the equation is quadratic in ν^2 which yields the symmetric splitting which is required for push-pull pumping. For this orientation

$$\nu = \pm\{(\nu_D^2 + \tfrac{5}{4}\nu_0^2) \pm \nu_0\sqrt{(3\nu_D^2 + \nu_0^2)}\}^{\frac{1}{2}}$$

The signal frequency is at X-band and the pump frequency at K-band for an applied field of about 4 Kilogauss. Fig. 2.4 shows the variation of the frequency spacing of the levels for an appropriate range of values of the applied field. This graph was drawn using data computed from the above by Reitbock[18] using a value of 5·73 Gc/s. for ν_D which is the value for 77°K.

It is important to realise that although 1-3 and 2-4 degeneracy exists for all values of the applied field, the $\Delta S_3 = \pm 2$ transitions corresponding to the pump frequency transitions are only "allowed" transitions when the

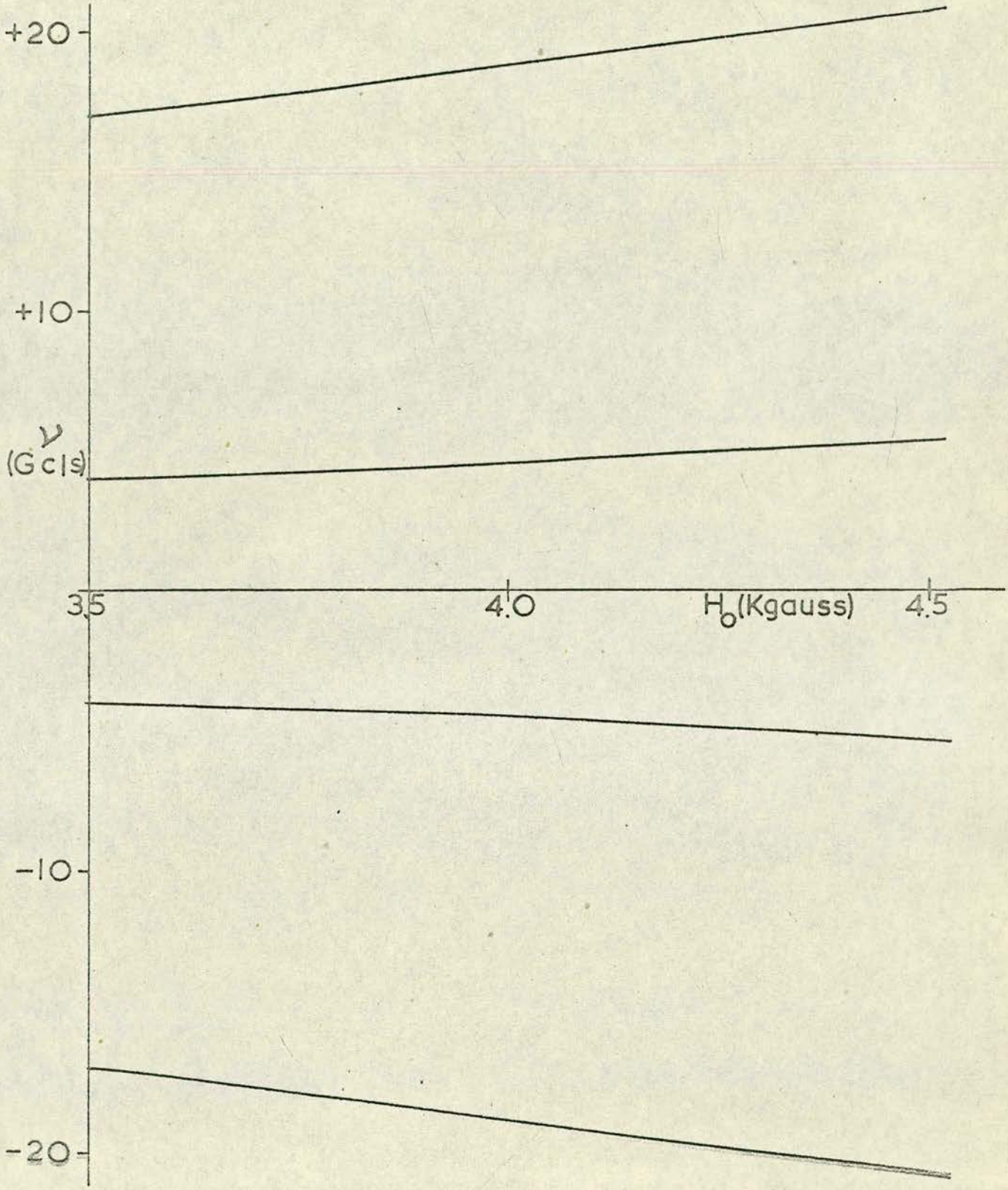

Energy levels of Cr^{3+} in Al_2O_3 ($\theta = 54°44'$)

Fig. 2.4

perturbation on the ions due to the applied magnetic field is of the same order as the perturbation due to the crystalline electric field. This causes suitable superposition of the state functions to allow such transitions. The "zero-field splitting" of the energy levels is $2\nu_D$ which is of the order of 10 Gc/s. and this represents the magnitude of the crystalline field perturbation and hence the required d.c. magnetic field produces a perturbation of the same order for the pump frequencies at K-band. Kikuchi, Lambe, Makhov and Terhune[19] conducted a series of tests (at 4·2°K) on single and push-pull pumping at powers of up to 120 mW and concluded that the push-pull mode gives improvement by a factor of 4.

Apart from this prime advantage of providing the most efficient pumping scheme, ruby is fortunately suitable in almost all other aspects. It is chemically stable at all temperatures up to 1000°C. It is hard and can be cut and ground to an accurately rectangular parallelipiped which is useful since in the later developments of cavity masers the crystal is plated and itself forms the cavity. The thermal conductivity of ruby is high and this is important, particularly if, as may be necessary at liquid nitrogen temperature, high pump powers are being used. The pump energy resonating in the material tends to raise its temperature and in a material with high thermal conductivity this causes the refrigerant to boil off and it has to be replenished which presents no serious difficulty. If, however, the maser material is of low conductivity the pump power may raise the

temperature at the centre of the crystal and set up a temperature gradient between the centre and the sides leaving the latter at the temperature of the refrigerant. This would be most undesirable since the thermal relaxation times would vary throughout the material.

After the original demonstration of the suitability of ruby as a maser material, Morris, Kyhl and Strandberg[20] built a tunable X-band maser using 0·01% chromium doped ruby. This maser was very successful, exhibiting a voltage-gain-bandwidth product of 43 Mc/s at 4·2°K. Subsequently improved cavity and travelling-wave structures have increased the attainable voltage-gain-bandwidth products as will be shown later. All the X-band masers which have been reported with improved performances since then have used 4-level pumping in chromium doped ruby.

The above examples are discussed to bring out the requirements of a good maser material and in a design study for a liquid nitrogen maser ruby emerges very quickly as the most suitable possibility. Some time after the start of this project an excellent and very comprehensive list of maser materials was published (Siegman[3]) and in it there is no material which would appear to be more suitable than ruby for a liquid nitrogen maser.

2.4 The Zero Field Maser

The only other material that was seriously considered was iron doped Al_2O_3 which offers the possibility of operation without the necessity for the applied d.c. magnetic field.

King and Terhune[21] used this material (0·1% Fe^{3+} in Al_2O_3) successfully in a maser. The spin of the Fe^{3+} ion is $\frac{5}{2}$ (5 unpaired electrons) and the cubic crystalline electric field causes splitting and superposition of spin states as shown in fig. 2.5. The mixing causes the transitions between the top pair of levels and the bottom pair of levels to be allowed without the necessity for a large perturbation due to the magnetic field. This splitting and mixing by the crystalline field occurs only for ions with a spin of 2 or over, which explains why this is not found with the chromium ion. The magnetic field was small (~100 gauss) and was used only to tune the maser. The diagram in Fig. 2.5 is for $\theta = 0$ and variation of θ changes the rate of splitting of the energy states with the applied magnetic field which also aids tuning. In a packaged system, for instance, a small fixed field could be applied and the tuning effected by rotation. This maser was operated at a signal frequency of 12·3 Gc/s and was pumped at 31·8 Gc/s. The zero-field splittings are actually 12·07 and 19·13 Gc/s. which places a lower limit on the signal frequency of 12·07 Gc/s. which is rather high for the low noise "window" between 3 and 10 Gc/s. In the maser of King and Terhune the voltage-gain-bandwidth product ($\sqrt{G}B$) was 15 Mc/s but no mention is made in the short letter describing this maser about what steps, if any, were taken to establish the optimum concentration.

Nagy and Friedman[22,23] have recently reported $\sqrt{G}B$ products as high as 165 Mc/s with no d.c. field at all and up to

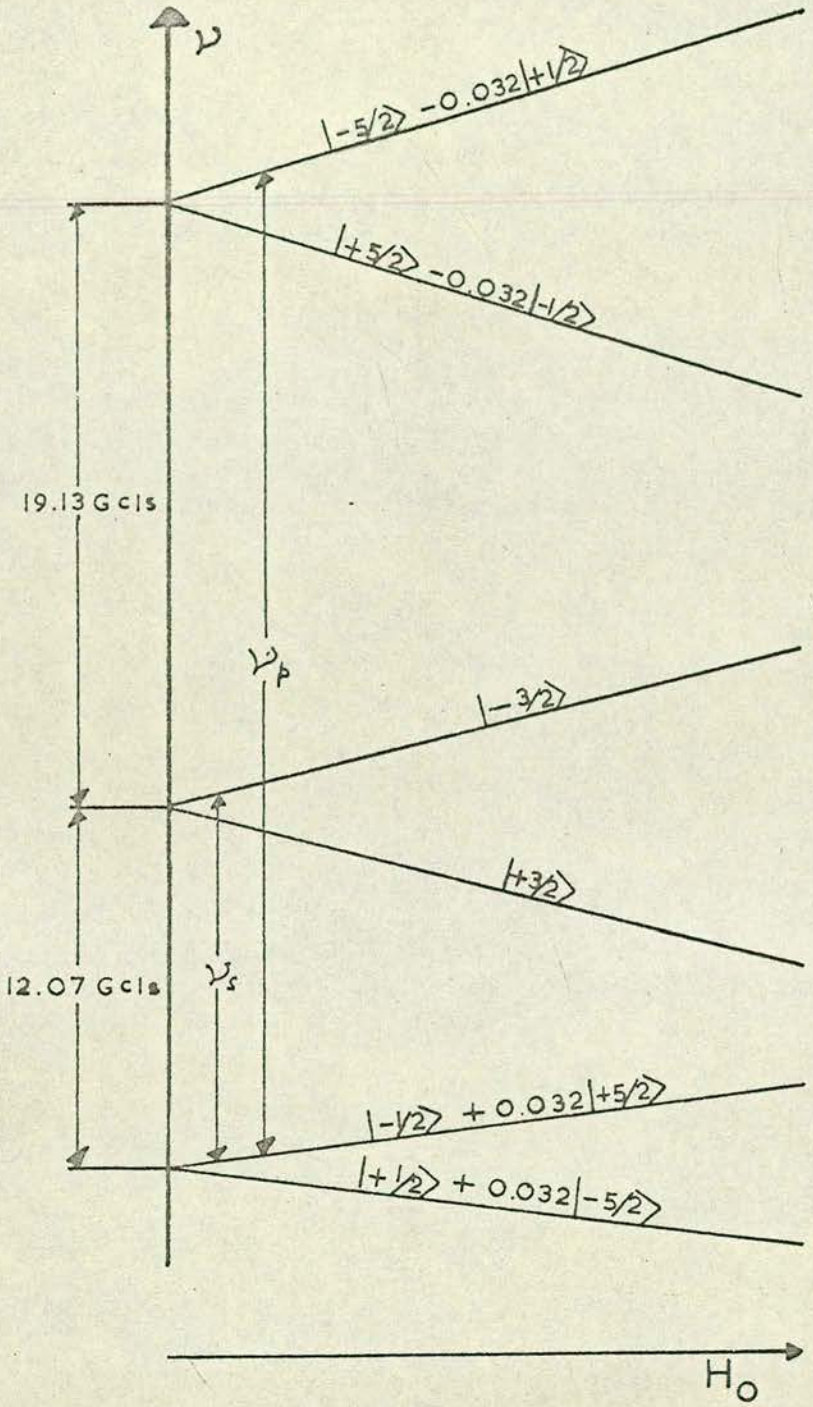

Energy levels of Fe^{3+} in Al_2O_3

Fig. 2.5

250 Mc/s with fields of only 5-10 gauss. They have also reported operation with this material in powdered form.

For a liquid-nitrogen-cooled maser, however, advantageous though it would be to dispense with the need for a large d.c. magnetic field, the limitation of this material to 3-level pumping is a serious drawback. No maser has been operated in the 3-level mode at 77°K but by analogy with measurements on ruby at 4·2°K it is reasonable to suppose that a 3-level system would require at least 4 times as much pump power as a 4-level system. Since 4-level ruby masers operating at 77°K required several watts of power for saturation it is possible that to saturate the pump transition of a 3-level system in Fe^{3+}-doped Al_2O_3 at 77°K might require more than the maximum available power (~10 watts). In the absence of any relevant experimental results indicating the possibility of success it was considered that it would be unwise to try to use this material.

Bearing in mind possible communications applications, a further objection to this material is that the signal frequency could not be lower than 12 Gc/s which is too high to take advantage of the low noise "window" from 3-10 Gc/s.

In view of its extreme suitability, therefore, it was decided to employ ruby as the active material. To its many advantages which have already been extolled in Section 2.3 must be added that of availability. In the last few years high quality crystals of ruby have become more readily available because of the extensive development work

necessitated (and financed) by the demand for ruby laser rods and the very high quality they require.

CHAPTER THREE

Ruby as a Maser Material at Liquid Nitrogen Temperatures

3.1 Transition Probabilities

For any system of energy levels, the power dP emitted from or absorbed by any two energy levels i and j in a volume dV is:-

$$dP = h\nu_{ij} W_{ij} |(n_i - n_j)| dV \qquad (E_j > E_i)$$

For a maser this will be power absorbed in the case of the pump transition and power emitted in the case of the signal transition but the expression is the same. It is not intended to derive the matrix elements for the transition probability W_{ij} $(= W_{ji})$. These can be found in the standard works on masers (e.g. Vuylsteke[1] and Siegman[3]).

$$W_{ij} = \left(\frac{g\beta\mu_o}{2\hbar}\right)^2 f(\nu) |\langle i|\underline{H}^*\underline{S}|j\rangle|^2$$

g is the spectroscopic splitting factor

β is the Bohr Magneton

$$\hbar = \frac{h}{2\pi}$$

$f(\nu)$ is the line shape function (usually taken to be Lorentzian).

It is in both cases desired that W_{ij} should be as large as possible and since all the other terms in the above expression are fixed, this means that $|\langle i|\underline{H}^*\underline{S}|j\rangle|^2$ must be made as large as possible. This is the square of the amplitude of the transition probability matrix element. When the states i and j are such that the spin change from one to the other is ± 1 then

the matrix elements are large and the transition is "allowed". When the spin change is ±2, in general, the matrix elements are small and the transitions are said to be "forbidden". As has been previously mentioned the [redacted] host lattices for the ion must be chosen so that there is suitable admixture of the states which leads to these elements becoming large. The size of these elements depends on θ (the angle between the d.c. magnetic field and the c-axis of the crystal) and ξ (the angle between the magnetic field vector of the applied microwave field and the c-axis). The variation of the matrix elements with θ has been treated fully by Chang and Siegman[16] and curves of σ_L^2 against θ are plotted for d.c. fields H_0 in 1 Kilogauss steps. Siegman defines σ_L^2 as the maximum value of σ^2 for a linearly polarised field (such as exists in microwave cavities) and σ^2 is a convenient way of expressing the tensor $\underline{\underline{\sigma\sigma}}^*$ for a given set of conditions.

$$\sigma^2 = \frac{(\underline{H}^* \, \underline{\underline{\sigma\sigma}}^* \, \underline{H})}{(\underline{H}^* . \underline{H})} = \frac{|\underline{H}^* \langle i | \underline{S} | j \rangle|^2}{(\underline{H}^* . \underline{H})}$$

and $\underline{H}^* \underline{H} = H_1^2$ the amplitude squared of the microwave field. Siegman's curves show that for the d.c. field of about 4 Kilogauss, the values of σ_L^2 for the pump transitions are approximately constant from $\theta = 40^\circ$ to $\theta = 90^\circ$. For the signal transition, however, σ_L^2 for $\theta = 90^\circ$ is approximately 1¼ times its value for $\theta = 55^\circ$ and thus operating at the double pump angle does not affect the transition probability for the pump transitions and only slightly decreases it from the maximum for the signal transition.

The above assumes the optimum angle ξ for each transition which, in practice, at least for the double pump transition, is impossible to achieve. In theory, with one pump and one signal transition, each microwave field may be applied with its plane of polarisation at the optimum angle although in practice an added constraint is usually imposed in that the microwave field vectors are made mutually perpendicular to reduce cross-coupling. This is particularly necessary at liquid nitrogen temperatures where the pump power required may be of the order of watts. In the case of four-level pumping, however, even if this constraint is not applied the polarisation of the microwave field cannot be optimised for both pump transitions. The pump power can, within reason, be increased to compensate for non-optimum ξ and therefore if only one transition probability can be maximised it should be that associated with the signal transition.

Most of the masers (including that with the best performance at 77°K) built to operate in the 4-level push-pull pumping mode had the crystals cut so that the crystal axis was at 54°44' to the shortest side of the crystal and it was therefore decided to conform to this practice. This has the added advantage that, it leads to the minimum pole gap for the magnet providing the d.c. field. In a practical application using a liquid nitrogen cooled maser whose size and weight are important this field would be provided by a permanent magnet inside the dewar. The weight and cost of such a magnet depends very much on the required pole gap and any unnecessary

increase of this is therefore to be avoided. The accepted "rule-of-thumb" approximation is that the weight is proportional to the cube of the pole gap.

Quite recently Genner and Plant[24] produced a report which describes the liquid-nitrogen-cooled masers built by a team at R.R.E. This team used the calculations of Howarth (unpublished) which apparently show the optimum angles ξ for each transition and optimised the signal transition probability. The crystal was cut accordingly but it is interesting to note that the performance of the maser was similar to those of the previous liquid nitrogen masers with their crystals cut at the $54^{\circ}44'$ angle.

Using the parameter σ^2 to replace the tensor quantity $\underline{\underline{\sigma\sigma}}^*$, (which, it must be stressed, can only be done for a specific set of conditions) W_{ij} may be expressed as follows.

$$W_{ij} = \left(\frac{g\beta\mu_o}{2}\right)^2 f(\nu)\ H_1^{\,2}\ \sigma^2$$

The only remaining variable is H_1 which is usually made as large as possible by placing the material in a structure which is resonant at the appropriate frequency. It will be shown that this is not always necessary at liquid helium temperatures but that at liquid nitrogen temperature it is essential for the signal field and almost essential for the pump field if the already large pump power requirements are not to be unnecessarily increased. Having done everything possible to optimise all other parameters, H_1 for the pump field must be increased as necessary to make W_{ij} for the corresponding

transitions large enough to maintain saturation.

3.2 Magnetic Q, Q_m

It is convenient to describe the signal frequency behaviour of the maser material by a parameter called the "magnetic Q", Q_m, defined as follows:

$$Q_m = -2\pi \frac{\text{energy stored}}{\text{energy emitted/cycle}}$$

The negative sign conforms with the normal definition of Q for which the denominator is "energy lost/cycle". Obviously for an emissive Q of this nature the lower the value of $|Q_m|$ the better the maser material. It can be shown (Siegman[3]) that

$$1/Q_m = \frac{g^2\beta^2\mu_0^2}{\pi} \cdot \frac{n_3 - n_2}{\Delta\nu_L} \cdot \frac{\int_{\text{crystal}} \underline{H}^* \cdot \underline{\underline{\sigma}}\underline{\sigma}^* \cdot \underline{H}\, dV}{\int_{\text{cavity}} \underline{H}^* \cdot \underline{H}\, dV}$$

$\Delta\nu_L$ is the 3 dB width of the resonance line which is assumed to have a Lorentzian shape.

n_2, n_3 are spin concentrations in the various levels i.e. n_2 is the no. of spins per unit volume in level 2.

An important feature of this expression is that Q_m is dependant only on the spin concentration in the material - not on the total number of spins present. Henceforth n_i will be used to denote the spin concentration in the ith level and n_t the total spin concentration.

Q_m is a property of the given material under the prevailing conditions and the only dependance on the containing

structure is in the ratio of the integrals. This ratio is usually defined in terms of a "filling factor" η

$$\eta = \frac{\int_{\text{crystal}} \underline{H}^* . \underline{\underline{\sigma\sigma}}^* . \underline{H} \, dV}{\sigma_L^2 \int_{\text{cavity}} \underline{H}^* . \underline{H} \, dV}$$

This has the maximum value of unity when the crystal fills the cavity and is so oriented in the cavity that the maximum transition probability is attained. Techniques in which the crystal itself is plated to form the cavity result in the first of these conditions being fulfilled but not necessarily the second. As explained in Section 3.1., for a given set of conditions the scalar σ^2 may replace the tensor $\underline{\underline{\sigma\sigma}}^*$ and then for a completely filled cavity the filling factor, η, is simply σ^2/σ_L^2 which is fixed by the angle at which the crystal is cut. Thus Q_m is given by:

$$1/Q_m = \frac{2g^2\beta^2\mu_0}{h} \cdot \left(\frac{n_3 - n_2}{\Delta\nu_L}\right) \cdot \sigma^2 \eta$$

or in terms of the inversion ratio, I, for a 4-level system

$$1/Q_m = \frac{2g^2\beta^2\mu_0}{h} \frac{n_t}{4} \frac{h\nu_s}{kT} \cdot \frac{I}{\Delta\nu_L} \cdot \sigma_L^2 \eta$$

With the constants evaluated this can be written

$$1/Q_m = 10^{-18} \left(\frac{h\nu_s}{kT}\right) \frac{n_t}{4} \frac{I\sigma^2\eta}{\Delta\nu_L}$$

(n is in spins cm^{-3} and $\Delta\nu_L$ is in Mc/s.)

The only remaining variable is $(n_3 - n_2)/\Delta\nu_L \propto n\, I/\Delta\nu_L$ and this must be made as large as possible.

3.3 Optimisation of $(n_3 - n_2)/\Delta\nu_L$

The first stage in increasing $(n_3 - n_2)/\Delta\nu_L$ is to make the inversion ratio, I, as large as possible. Having done this the remaining possibility is to increase n_t but this must be done with caution since it has two undesirable effects. Firstly increasing n_t increases the spin-spin interaction and hence increases $\Delta\nu_L$ and secondly increasing n_t beyond a certain stage leads to a decrease in the value of I due to cross-relaxation. $\Delta\nu_L$ does not increase as fast as n_t and therefore the concentration can be increased until the concentration-dependent relaxation processes start to affect I. Before considering this, however, it will be shown quantitatively how 3-level and 4-level pumping compare.

Kikuchi et al[19], following the work of Bloembergen[6], derived expressions for the population difference $(n_3 - n_2)$ in ruby.

Thermal interaction with the lattice is considered as stimulated emission and absorption of phonons and transition probabilities w_{ij} are used to denote the probability of a stimulated phonon transition from level i to level j. Unlike the processes of emission and absorption of electromagnetic radiation discussed in Chapter One, however, there is no phonon process analogous to spontaneous emission and therefore the number of stimulated transitions in each direction must be equal if the ions are in thermal equilibrium with the lattice. From the Boltzmann Distribution it is known that the populations of the levels j (upper) and i (lower) are in the ratio

$\exp\left(-\frac{h\nu_{ij}}{kT}\right)$. Consequently the downward transition probability w_{ji} and the upward transition probability w_{ij} must be in the inverse ratio $\exp\left(\frac{h\nu_{ij}}{kT}\right)$. However, as has been shown, $\exp\frac{h\nu_{ij}}{kT}$ for ν_{ij} of the order of 10 Gc/s at a temperature of 77°K, is approximately unity and thus it is permissible to write $w_{ij} \approx w_{ji}$.

The expressions for $n_3 - n_2$ are found by considering the rate equations:

$$\frac{dn_i}{dt} = \sum_{j=1}^{4} n_j \alpha_{ji} - n_i \alpha_{ij}$$

where the α_{ij} include the thermal relaxation times and, where applicable, the stimulated radiation transition probabilities. Steady state conditions in the presence of pump fields are found by equating the $\frac{dn_i}{dt}$ to zero.

Three different modes are available for the four levels of Cr^{3+} in Al_2O_3.

(a) Three-level Pumping - levels 1 and 3 saturated

The pump and signal transition probabilities are denoted by P and S respectively

$$\alpha_{13} = w_{13} + P_{13} \quad \text{and} \quad \alpha_{31} = w_{31} + P_{31}$$

$$\alpha_{23} = w_{23} + S_{23} \quad \text{and} \quad \alpha_{32} = w_{32} + S_{32}$$

and the other α_{ij} are simply w_{ij}

$P_{13} = P_{31}$ and $S_{23} = S_{32}$ from fundamental considerations

and, in practice, $w_{ij} \approx w_{ji}$. Thus the above equations reduce to

$$\alpha_{13} = w_{13} + P_{13} = \alpha_{31}$$

$$\text{and} \quad \alpha_{23} = w_{23} + P_{23} = \alpha_{23}$$

Equating the $\frac{dn_i}{dt}$ to zero and solving for $(n_3 - n_2)$:

$$(n_3-n_2) = \frac{n_t h}{4kT} \cdot \frac{w_{42}(w_{41}\nu_{21}-w_{43}\nu_{32})+(w_{41}+w_{42}+w_{43})(w_{21}\nu_{21}-w_{32}\nu_{32})}{w_{42}(w_{41}+w_{43})+(w_{41}+w_{42}+w_{43})(w_{21}+w_{32}+S_{32})}$$

P_{13} does not appear in this expression but it has been assumed that the pump power is such that $P_{13} \gg w_{13}$ which is the condition for saturation of levels 1 and 3.

(b) Three-level Pumping - levels 2 and 4 saturated

Similarly, for this case it can be shown that

$$(n_3-n_2) = \frac{n_t h}{4kT} \cdot \frac{w_{31}(w_{21}\nu_{32}-w_{41}\nu_{43})+(w_{12}+w_{13}+w_{14})(w_{32}\nu_{32}-w_{43}\nu_{43})}{w_{31}(w_{21}+w_{41})+(w_{12}+w_{13}+w_{14})(w_{23}+w_{34}+S_{23})}$$

For the present only the small-signal case will be considered and S_{23} which is, of course, dependent on the strength of the applied signal field, will be assumed to be small compared with the w_{ij}.

In general the thermal transition probabilities are not known with any accuracy. It is extremely difficult to measure the relaxation times $(\tau_1)_{ij} \sim \frac{1}{w_{ij}}$ for a multi-level system since measurement of the time constant associated with the decay of some non-equilibrium state between two levels is not the relaxation time for that transition but a function of the relaxation times for all possible transitions of the system. It is therefore necessary to make assumptions concerning the

relative magnitudes of these transition probabilities and the simplest and most plausible assumption is that they are all of the same order. This allows cancellation of the w_{ij} leaving

$$(n_3 - n_2) = \frac{n_t h}{4kT}\left(\frac{\nu_p}{2} - \nu_s\right) \text{ for both (a) and (b)}$$

($\nu_{13} = \nu_s$ in (a), $\nu_{24} = \nu_p$ in (b) and $\nu_{23} = \nu_s$ in both)
Optimum pumping results in (a) and (b) if w_{43} and w_{21} respectively are greater than all other w_{ij} when

$$(n_3 - n_2) = \frac{n_t h}{4kT}(\nu_p - \nu_s) \text{ in both cases.}$$

(c) Four-level Pumping: levels 1 and 3 and 2 and 4 saturated ($\theta = 54^\circ 44'$)

$$(n_3 - n_2) = \frac{n_t h}{4kT} \frac{w_{41}\nu_{41} + w_{43}\nu_{43} + w_{21}\nu_{21} - w_{32}\nu_{32}}{w_{12} + w_{43} + w_{14} + w_{23} + S_{32}}$$

$$= \frac{n_t h}{4kT}(\nu_p - \nu_s) \text{ for all } w_{ij} \text{ of the same order}$$

Here the optimum situation is $w_{14} \gg w_{43} \sim w_{21} \gg w_{32}$ in which case:

$$(n_3 - n_2) = \frac{n_t h}{4kT}(2\nu_p - \nu_s)$$

For a signal frequency of approximately 10 Gc/s, the pump frequency for 4-level pumping is about 24 Gc/s and the values of the inversion ratios for the above cases compare as follows:

Relation between w_{ij}	Inversion Ratio, I	
	3-level	4-level
all w_{ij} of same order	$\frac{\nu_p - 2\nu_s}{2\nu_s} = 0{\cdot}2$	$\frac{\nu_p - \nu_s}{\nu_s} = 1{\cdot}4$
Optimum Ratio of w_{ij}	$\frac{\nu_p - \nu_s}{\nu_s} = 1{\cdot}4$	$\frac{2\nu_p - \nu_s}{\nu_s} = 3{\cdot}8$

This predicts an improvement of 7 times using 4-level pumping if the relaxation times are all of the same order and about 2½ times if the relative magnitudes of the relaxation times are optimal. It is seen that in either case a worthwhile improvement is obtained if 4-level pumping is used. It is also apparent that the 4-level mode is less sensitive to variation of the relative magnitudes of the relaxation times. At liquid helium temperatures Kikuchi et al. measured an improvement of about 4 times using the 4-level push-pull mode.

The population difference is proportional to the total concentration n_t and inversely proportional to T in all cases and therefore increasing the temperature from 4·2°K to 77°K decreases $(n_3 - n_2)$ by a factor of about 18 for a given sample. Obviously the 4-level pumping scheme should be used at liquid nitrogen temperature to obtain maximum performance. There is no published record of a 3-level maser operating at 77°K.

The only remaining way of increasing $(n_3 - n_2)/\Delta\nu_L$ is to increase n_t. This can be done only until I starts to decrease due to cross-relaxation effects but Maiman[25] has shown that n_t can be increased by at least a factor of 2 within this limitation and more recent reports suggest that greater increases may be possible. Discussion of the limiting processes is aided by definition of the relaxation mechanisms involved.

3.3.1 Spin-spin Relaxation Time, τ_2

This is mainly encountered in the function, $f(\nu)$, describing the line shape which is normally taken to be

Lorentzian

$$f(\nu) = \frac{2\tau_2}{1 + 4\pi^2\tau_2^2(\nu - \nu_0)^2} \qquad (\nu_0 = \text{resonant frequency})$$

This time constant τ_2 describing the line shape is only the true spin-spin relaxation time when there is no cause of line broadening except spin-spin interaction. Since even the best crystals have defects and inhomogeneities this will seldom be true and τ_2 is therefore difficult to measure accurately.

In a two-level system of identical ions coupled by spin-spin interaction, if some of them could be perturbed to a non-equilibrium condition without perturbing the others, the time constant associated with the perturbed ions coming into equilibrium with the unperturbed ones is τ_2. In the case to be considered, however, this situation does not arise and τ_2 is only of interest for its effect on the line-width $\Delta\nu_L$. For maser materials of the concentrations used at liquid nitrogen temperature the τ_2 are short (typically ~ a few nanoseconds).

3.3.2 Spin Lattice Relaxation Time, τ_1

This has already been mentioned and is the strongest and hence the predominant relaxation mechanism for very dilute salts of the type used at liquid helium temperatures. When the system relaxes by this mechanism the energy is exchanged with the lattice phonons. The strong crystalline electric field is modulated by thermal vibrations of the lattice but is unable to interact directly with electron spins since the latter have no electric moment. (There must, however, be a second order effect allowing direct coupling since any oscillating electric

field must have associated with it an oscillating magnetic field.) The primary coupling mechanism is through the electron orbits which have both electric and magnetic dipole moments. The crystal field couples to the electric dipole moment of the orbit and thence to the spin by spin-orbit coupling. Kronig[26] and Van-Vleck[27] developed a theory of spin-lattice relaxation based on the above argument. For very low temperatures i.e. liquid helium temperatures this theory predicts an inverse variation of τ_1 with temperature T corresponding to processes where one phonon is exchanged directly for one quantum of spin energy. This leads to τ_1's which can be of the order of seconds for a material with small orbital angular momentum or small spin-orbit coupling. At higher temperatures and hence higher phonon energies the Kronig-Van-Vleck theory predicts $\tau_1 \alpha {}^1/_{T^7}$ which involves so called "Raman" scattering of phonons by spins. In this type of scattering the phonon energy is increased or decreased by the amount of the spin transition energy but the process does not involve the direct emission or absorption of a phonon.

Experiment agrees partially with this theory in that the low temperature variation of τ_1 does appear to be inversely with T. Pace et al.[28] found this agreement but for temperatures in the region of 77°K they found $\tau_1 \alpha {}^1/_{T^5}$ rather than the predicted ${}^1/_{T^7}$. The chief discrepancy between the Kronig-Van-Vleck theory and experiment is in the observed concentration-dependence of τ_1. The theory considers the coupling between each spin and the lattice and therefore

predicts complete concentration-independence of T_1. This concentration-dependence of T_1 has yet to be satisfactorily explained but it is believed that it may be due to "cross-relaxation" effects involving "impurities".

3.3.3 Cross-Relaxation

Cross-relaxation is a type of spin-spin or dipolar interaction process. The mechanism is the same as for spin-spin relaxation but the term cross-relaxation denotes relaxation by dipolar coupling between spin transitions which are not the same, for example between two different but intermingled systems or between different transitions in a multilevel system. This mechanism in its simplest form involves an upward transition in one system (Fig. 3.1 (a)) accompanied by a downward transition in the other (Fig. 3.1 (b)).

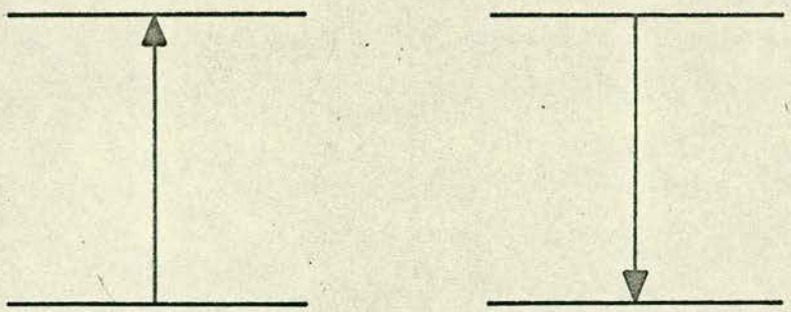

Fig.3.1

This process occurs with highest probability where energy can be conserved, i.e. where the lines overlap.

An example of the use of this process to good advantage is the Ce^{3+} doping of the gadolinium (lanthanum) ethyl sulphate used by Scovil et al.[10] and shown in Fig. 2.2. The orientation of the crystal in the d.c. magnetic field is such that the transition of Ce^{3+} ions coincides with the "idler" transition of the 3-level maser system in the Gd^{3+} ion. This allows appreciable cross-relaxation to take place and, since the spin-lattice relaxation time of the Ce^{3+} ions is very short (due to strong spin-orbit coupling), this two-stage process via the Ce^{3+} ions affords a faster relaxation path for the idler transition than by direct spin-lattice relaxation. This shortening of the idler relaxation time enhances the pumping - indeed, in this case since $\nu_p - \nu_s < \nu_s$, maser action is impossible without it.

It is obvious that cross-relaxation may take place when energy is conserved but, at increased concentrations, strong cross-relaxation is observed when the frequencies differ by amounts corresponding to several line widths. This has to be explained by consideration of the dipolar energy of the system as a whole as a "reservoir" of energy which can absorb or make up the difference.

Cross-relaxation in ruby has been investigated experimentally by Mims and McGee[29], Geusic[30], Manenkov and Prokhorov[31] and Roberts et al.[32]. A cross-relaxation time τ_{21} is defined which is the time constant associated with attaining

equilibrium between two spin systems in the absence of spin-lattice relaxation. At low concentrations (as used in liquid-helium-cooled masers) $\tau_{21} \gg \tau_1$ and each system (if disturbed from equilibrium) relaxes to the lattice independently. As the concentration is increased, however, transitions begin to couple by cross-relaxation at first only where energy is conserved but this becomes increasingly less important. Mims and McGee showed that at 4·2°K, if the concentration is increased to 0·3% Cr^{3+}/Al_2O_3 cross-relaxation becomes so strong that, regardless of energy conservation, line widths, etc., all transitions couple to all other transitions so that no difference of spin temperature between transitions can be set up. In the intermediate stage where $\tau_2 < \tau_{21} < \tau_1$, τ_{21} is found to be independent of T and to vary as $n_0^{2.4}$ for the range of concentrations 0·02% to 0·3% Cr^{3+}/Al_2O_3.

Geusic showed that the expected process of "harmonic cross-relaxation" also occurs (Fig. 3.2) e.g. τ_{21} becomes shorter when $\nu_{14} = n\,\nu_{23}$ where n is an integer. Various combinations of multiple spin and harmonic cross-relaxation have been observed.

The relevant feature governing the choice of concentration of a maser material is the onset of the first cross-relaxation process which appreciably affects the inversion. For ruby at $\theta = 54°44'$ it is immediately apparent that the processes shown in Fig. 3.3 should occur strongly in all but the very weakest concentrations. These processes leave the population difference $(n_3 - n_2)$ unchanged, however, and the fact that the corresponding cross-relaxation time can be expected to be

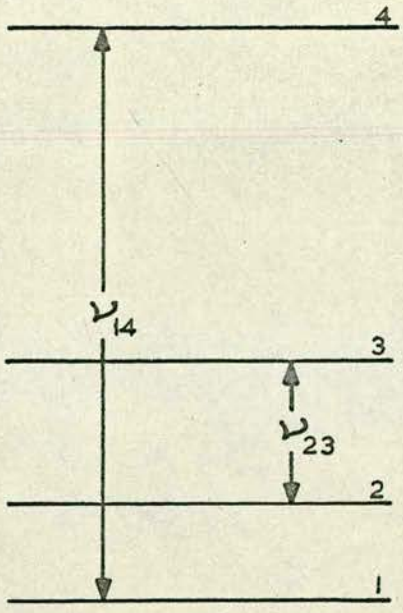

$$\nu_{14} = n\nu_{23}$$

Harmonic Cross-relaxation

Fig.3.2

shortened to of the order of the spin-spin relaxation time, τ_2, is of no consequence. Roberts et al.[32] have shown that the first processes to become appreciable at this double pump orientation are the 5-spin processes shown in Fig 3.4.

For each process there is also a reciprocal process (i.e. all arrows reversed).

It is a general rule that, for a given concentration, the greater the number of simultaneous spin transitions required

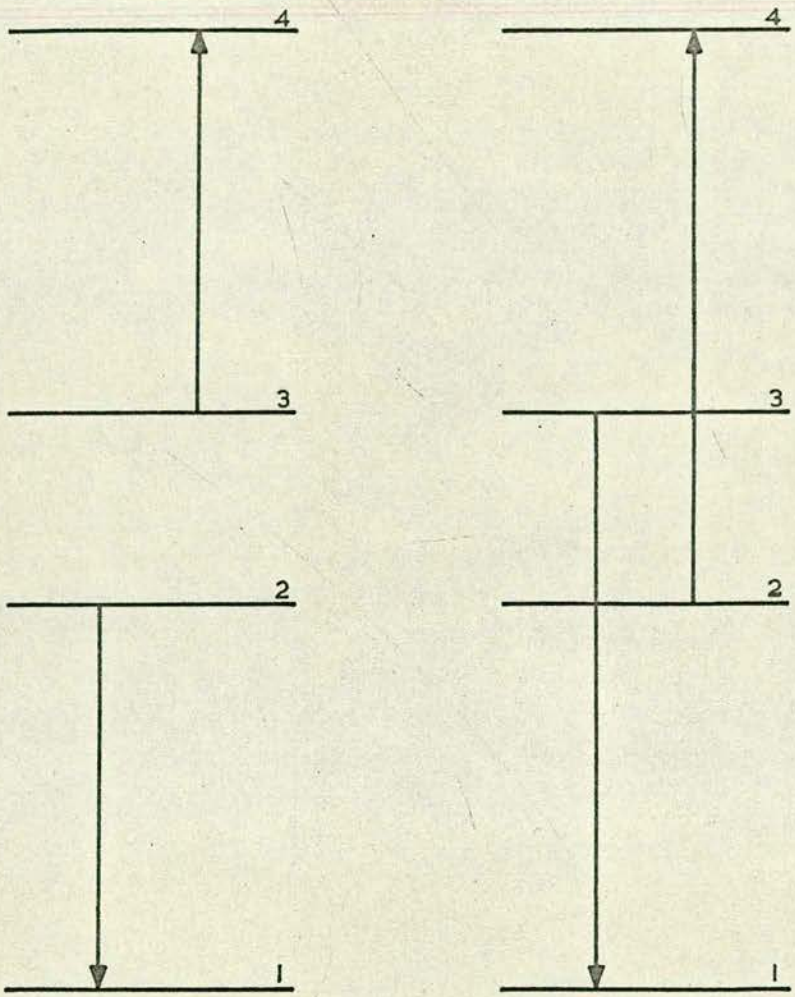

2-spin Cross-relaxation

Fig.3.3

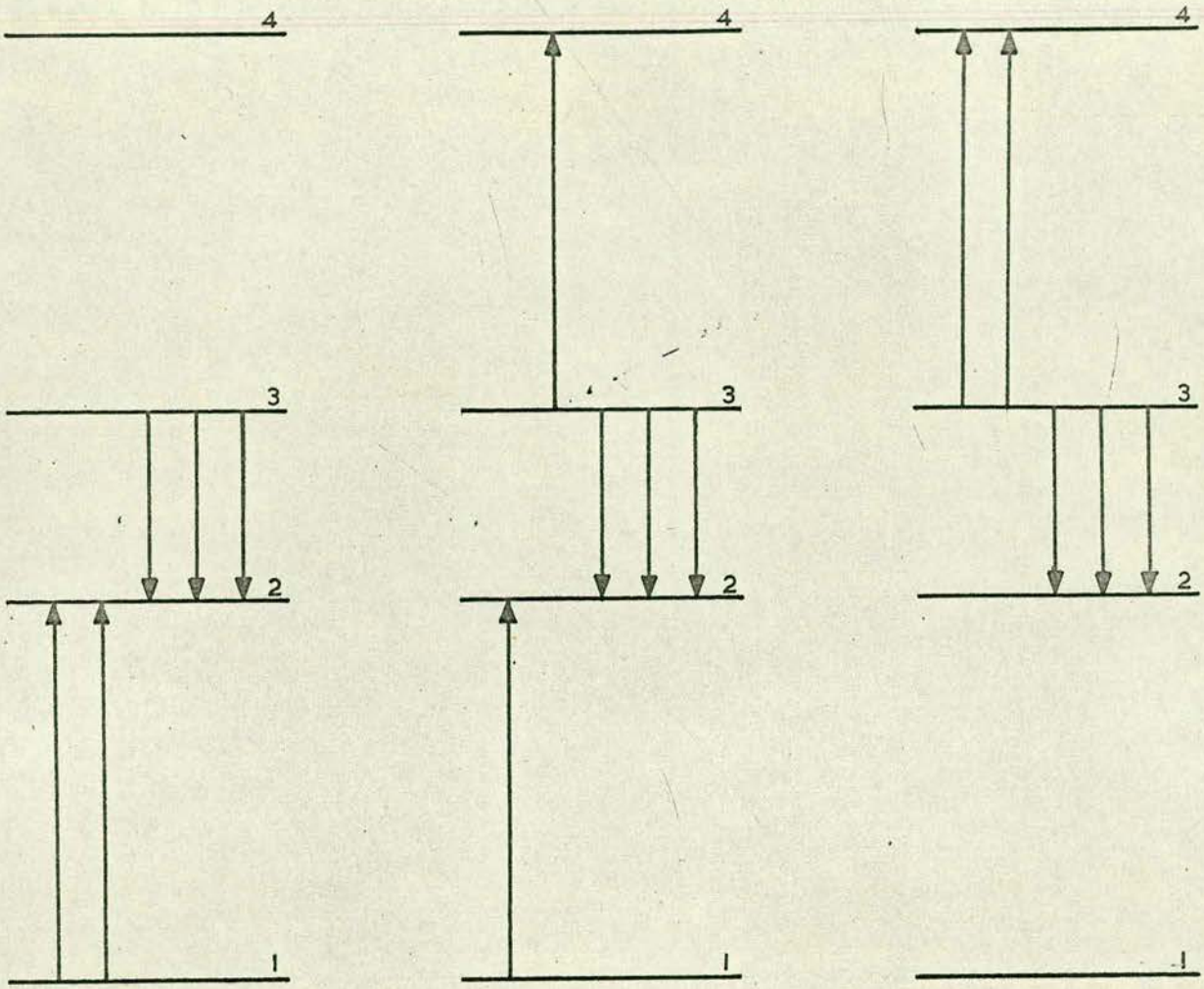

5-spin Cross-relaxation

Fig.3.4

for a cross-relaxation process the lower is its probability. However, it is also true to say that the higher the order the greater the concentration dependence. This means that since the first significant cross-relaxation process is of a relatively high order (5 spin) it is to be expected that the resultant limitation on maser action will not occur at such low concentration as it would if the limiting process was a 3- or 4-spin one. Once deterioration of maser action starts to occur, however, it is to be expected that it will vary more sharply with concentration than it would if a cross-relaxation process of lower order was the limiting process. This tendency will be further increased by the simultaneous onset of the three different relaxation mechanisms discussed above.

From the foregoing it is apparent that the optimisation of $(n_3 - n_2)/\Delta\nu_L$ is governed either by cross-relaxation between transitions of the Cr^{3+} ions or by τ_1 shortening so much that available powers are no longer adequate to saturate the pump transitions. This concentration-dependence of τ_1 may be attributable to cross-relaxation between Cr^{3+} ions and some "fast-relaxing" impurity and this is currently being investigated elsewhere. The limited amount of experimental data available indicates that it is the cross-relaxation between transitions of the Cr^{3+} ions which limits the extent to which the concentration can be increased.

Maiman was the first to suggest that the best concentration for use in a liquid nitrogen temperature maser would be higher than that for a liquid helium one. Maiman[25] showed, by

extending Bloembergen's results that the dependence of inversion on cross-relaxation in a 4-level system has the form

$$(n_3 - n_2) \alpha n_t \frac{\nu_p - \nu_s(1 + \tau_1/4\tau_{21})}{(1 + \tau_1/4\tau_{21})}$$

This again assumes that the pump power is sufficient to maintain saturation of the pump transitions and, if this condition is fulfilled, the population difference is not directly dependent on τ_1 and depends only on the ratio τ_1/τ_{21}. All the τ_1's are assumed to be of the same order and for good inversion $4\tau_{21}$ must be very much greater than τ_1. τ_{21} is the cross-relaxation time for the dominant cross-relaxation process. Maiman thought that this was coupling between the pump (1-3 and 2-4) and idler (1-2 and 3-4) transitions which involves a very considerable frequency difference. From the more recent work of Roberts et al.[32] it is much more likely that the 5-spin processes described in Section 3.3.3 are the dominant cross-relaxation processes. It was reasoned that since raising the temperature from 4·2°K to 77°K would shorten τ_1 (by a factor of about 500) the condition $\tau_1 \ll 4\tau_{21}$ would be more than adequately satisfied for a crystal of low concentration. The system should therefore tolerate an increase in concentration, with an attendant decrease in τ_{21}, before the inversion ratio I begins to decrease

$$I = \frac{\nu_p/\nu_s - (1 + \tau_1/4\tau_{21})}{(1 + \tau_1/4\tau_{21})}$$

Maiman did not discuss the concentration-dependence of τ_1 which would help to keep I at the value for low concentration by shortening τ_1 as τ_{21} shortened. If τ_1 was more concentration-dependent than τ_{21} the limiting factor would be the available pump power. Experimental results indicate, however, that the variation of τ_{21} with concentration is faster than the variation of τ_1 which seems reasonable in view of the conclusions about the cross-relaxation processes reached in Section 3.3.3.

Maiman showed, in agreement with his predictions, that a crystal of concentration 0·6% Cr_2O_3/Al_2O_3 showed maser amplification and oscillation at 77°K but at 4·2°K no degree of inversion could be produced in this crystal at all. In a less concentrated crystal of 0·2% Cr_2O_3/Al_2O_3 a negative spin temperature of 150°K was produced at 4·2°K and this improved to 51°K at 77°K. Maiman's paper did not make it clear why the 0·2% crystal had been chosen in preference to the 0·6% one for building the actual maser; presumably despite the fact that maser action was observed in the higher concentration crystal, the very short τ_{21} ($\sim \mu$ sec.) was limiting the performance to a value less than that of the 0·2% crystal. The pump power used for this maser was not given in the same paper but is believed to have been about one watt with the cavity resonant at the pump frequency. The crystal size in this maser was 7 × 7 × 3·5 mm.

Reitbock and Redhardt[33] built a liquid-oxygen-cooled maser (T = 90°K) with a voltage-gain-bandwidth product ($\sqrt{GB}$) of 21·5 Mc/s. which constitutes a 50% improvement over that of

Maiman and is the best reported to date. They also had conducted a series of preliminary experiments to determine the best concentration for use at this temperature and quoted a value of 0·6% Cr_2O_3/Al_2O_3. However, a private communication from Reitbock in answer to an enquiry about this seemingly high value states that this was the starting power concentration and that the concentration of the actual crystal was thought to be about 0·4%. Reitbock recommended that the optimum value for 77°K should be of this order. From discussion with other people in this field, however, it seems unlikely that at such a high concentration ⅔ of the starting powder concentration would be retained in the final crystal and that, in the absence of an analysis, the figure quoted should be regarded as an upper limit.

The most encouraging feature of Reitbock's maser was that the pump power used was only 80 mW and in view of the high reported performance it was assumed that the pump transitions were saturated. The explanation of this was revealed when Reitbock's thesis was printed in full and it was found that this was not the case. This is most interesting since it seems to indicate that more has been gained by increased concentration than has been lost by the failure of the pump power to produce saturation. This principle is easy to accept but the 50% improvement in performance with the very much reduced pump power does seem incredible since even without relaxation effects reducing the inversion ratio a more concentrated crystal would require proportionately more pump power for saturation. The

crystal size, on which the required pump power also depends, was the same for this maser as it was for Maiman's and in fact the similarity of these two masers in all respects other than crystal concentration and pump power should allow a direct comparison.

In support of his choice of concentration Reitbock cites a paper by Wiederhold[34] in which a series of experiments is described indicating that the best maser action at liquid nitrogen temperatures would be obtained with a concentration of the order of 0·4% Cr_2O_3/Al_2O_3.

Work done in this country on liquid nitrogen masers by Ditchfield, Genner and Plant[35,24] at the Royal Radar Establishment in conjunction with Fruin, Ahern and Paxman[36,37] at Mullard produced performances similar to those obtained by Maiman i.e. $\sqrt{GB}$ products of up to 14-16 Mc/s. Genner and Plant used a material of concentration ·27% Cr_2O_3/Al_2O_3 but they stated that insufficient information was available to determine whether or not this was the optimum concentration. Paxman did a series of experiments showing that the optimum concentration was about 0·23% Cr_2O_3/Al_2O_3 which gave a value of $|Q_m|$ of about 680-700 which is the best measured to date. These masers required several watts to pump them although this is partially accounted for by the fact that the crystals were much larger (19 x 13·5 x 4·2 mm) than those of Maiman and Reitbock.

It therefore appeared that the optimum concentration was about 0·20-0·27% Cr_2O_3/Al_2O_3. The rather larger value

recommended by the Germans was not supported by analysis as were the British values. Theoretical discussion cannot define accurately the optimum concentration because the processes governing variation of maser action with concentration have not been investigated quantitatively in sufficient detail. The main reason why this has not been done is that it is impossible to obtain completely homogeneous, defect-free crystals. With the advent of electron probe microanalysis techniques, Dils et al.[38] investigated the concentration variation across various high quality ruby crystals grown by Linde and Adolf Meller. The resolution was about 10 μ, the crystals were mostly about 0·1% Cr^{3+}/Al_2O_3 and the standard deviations of the measured percentage varied typically from 15 to 25% and in one case was as high as 45%. In view of the larger size of the Cr^{3+} ions compared with Al^{3+} introducing Cr^{3+} into Al_2O_3 even in small quantities produces strains and defects in the lattice and this limits the quality of the crystals which can be grown. The more concentrated the crystal is, the more difficult it is to achieve high quality. It is further believed that on a smaller scale "clustering" of Cr^{3+} ions may occur since the large Cr^{3+} ions tend to take up sites of low energy, which occur near defects and this clustering would then create more defects. This process would be aided by the high diffusion rates of Cr^{3+} at the temperature of crystallisation (~ 2,000°C). Apart from its adverse effect on the lattice, this tendency to cluster either on a large or small scale is undesirable since it increases the

cross-relaxation which imposes on the system the limitations of a more concentrated crystal without the advantage of the larger number of participating ions.

In view of the unpredictability of the properties of even the best crystals, therefore, it was decided that the most advisable course of action would be to order 3 or 4 crystals of the highest available quality with concentrations ranging from about 0·15% to 0·4% Cr_2O_3/Al_2O_3 from which the crystal exhibiting the best maser action could be chosen.

After these decisions had been taken a thesis by Ammann[39] became available containing measurements of $|Q_m|$ and I for various concentrations. Instead of specifying the concentration by the more usual method of Cr_2O_3/Al_2O_3 by weight, as in all the above figures, Ammann quoted Cr^{3+}/Al_2O_3 by weight and, to allow direct comparison, equivalent values on the Cr_2O_3/Al_2O_3 scale have been added.

Concentration		$\|Q_m\|$	I	$\Delta\nu_L$(Mc/s)
% Cr^{3+}/Al_2O_3	% Cr_2O_3/Al_2O_3			
0·021	0·03	4770	1·16	70
0·046	0·07	2530	1·17	82
0·077	0·12	1700	1·11	99
0.14	0·21	1250	1·02	127
0·34	0·50	3630	0·33	222
0·40	0·60	4970	0·25	250

There is nothing in these results which contradicts the preceeding discussion and it is inferred from Ammann's results that the optimum concentration should be not less than 0·2% Cr_2O_3/Al_2O_3 and rather less than 0·45% Cr_2O_3/Al_2O_3. It is unfortunate that there is such a large gap (0·2% to 0·45%) over the most interesting region. The values of I show that, as discussed in connection with Reitbock's maser, the smallest $|Q_m|$ is obtained with a concentration at which the value of I has already started to decrease due to cross-relaxation. However, the extent to which this occurs is rather more credible in this case.

The smallest $|Q_m|$ obtained by Ammann (1250) seems rather large in view of the fact that Paxman observed a $|Q_m|$ of about 700 with a crystal of similar concentration. This endorses the above contention that the performance may vary quite widely even for samples of the same average concentration.

3.4 Signal Saturation

Signal saturation is the decrease in maser gain with increasing signal input power and its onset determines the upper limit of the linear operating range of the amplifier.

In Section 3.2 the following expression was quoted for the population difference $(n_3 - n_2)$:

$$(n_3 - n_2) = \frac{n_t h}{4kT} \frac{w_{41}\nu_{41} + w_{43}\nu_{43} + w_{21}\nu_{21} - w_{32}\nu_{32}}{w_{12} + w_{43} + w_{14} + w_{23} + S_{32}}$$

It was assumed that S_{32}, the stimulated transition probability, was negligible in comparison with the w_{ij} in the denominator.

This is true for small signal powers but, since S_{32} is proportional to the signal power, a point is reached for which this power becomes large enough to make S_{32} of the same order as the w_{ij}. Again assuming all w_{ij} of the same order:

$$(n_3 - n_2) = \frac{n_t h}{4kT} \quad \frac{\nu_p - \nu_s}{1 + \frac{1}{4} S_{32}/w}$$

and $$w \sim \frac{1}{\tau_1}$$

Therefore, $$(n_3 - n_2) = \frac{n_t h}{4kT} \quad \frac{\nu_p - \nu_s}{1 + \frac{1}{4} S_{32}\tau_1}$$

For the gain to be independent of the signal power $\frac{1}{4} S_{32}\tau_1$ must be very much less than unity.

Without evaluating the absolute power for which signal saturation starts to affect the gain it is possible to compare the liquid helium and liquid nitrogen cases. The power for which saturation starts to become apparent is inversely proportional to τ_1 and hence, from the measured relaxation times at both temperatures and the measured value of saturation onset at 4·2°K, the upper limit of signal power at 77°K can be estimated.

For suitable concentrations Pace et al.[28] observed a decrease in τ_1 from 22 millisec. at 4·2°K to 44 μsec. at 77°K - a reduction of 500 times. Describing one of the best liquid helium masers to date - that used in the Telstar and Early Bird projects - Tabor and Sibilia[40] state that the onset of signal saturation occurs at about 10^{-11} watts. It is therefore to be expected that the onset of signal saturation should

occur in a liquid nitrogen maser at input signal powers of the order of 10^{-9} to 10^{-8} watts. Reitbock[18] has observed the onset of signal saturation to occur at about 4×10^{-8} watts for a maser operating at 90°K which is in fair agreement with the above. The above analysis does not apply directly in this case since the pump transitions were not saturated in Reitbock's maser but it is expected that this would lower rather than raise the power at which signal saturation occurs.

This increased signal saturation power is the only respect in which masers operating at 77°K show an improvement over those operating at 4·2°K. Although the satellite communication systems in which liquid helium masers have been used employ powers which extend into the region of signal saturation the systems have been designed to tolerate this. Sky-beamed (or space) radar systems could not be so readily designed to accommodate this, however, since a further consequence of the long relaxation times is that if the maser gain is saturated the recovery time is of the order of τ_1. This means that, if the amplifier is "blanked off" by a near reflection, the recovery time would be of the order of milliseconds for a liquid-helium-cooled maser.

From the expression for $(n_3 - n_2)$ above it is seen that pumping harder than is required for saturation of the pump transitions does not improve the position with regard to signal saturation. What could be done to raise the signal saturation level of the liquid helium maser is to reduce τ_1 by some means (e.g. by doping with a fast relaxing ion) and

increase the pump power to maintain saturation. Since T determines the population difference independently of τ_1, the high performance of the liquid helium maser would be maintained and at the same time the signal saturation level would be raised. In practice, however, the extent to which the pump power would have to be increased to appreciably raise the signal saturation power might lead to difficulty in keeping the maser material at 4·2°K. Also as has been discussed above, it is difficult enough to achieve high quality in ruby material with only the chromium doping without the added complication of trying to ensure even distribution of a further impurity.

Thus the liquid nitrogen maser does offer the possibility of a preamplifier of equivalent noise temperature of 75-100°K (Maiman[25]) with an upper limit of signal power of the order of 27dB higher than the liquid-helium-cooled maser.

CHAPTER FOUR

Cavities and Travelling-Wave Structures for Masers

The structure in which the maser material is placed must allow "suitable" interaction of the material with the pump and signal fields. This term "suitable" implies that the microwave fields must remain in the material for sufficient time to stimulate enough transitions to achieve pumping and the required degree of amplification. For a "fast-wave" structure, such as a waveguide loaded with the active material, the length required for usable amplification of the signal would necessitate impracticably large crystals and pump powers. To provide the signal field with suitable interaction it is necessary to set up a standing wave (cavity maser) or a slowly propagating wave (travelling-wave maser) in the pumped active material. It is not quite so important to make similar provision for the pump field since this is controlled locally and can, if necessary, be increased. Liquid-helium-cooled masers have been operated in which the pump field did propagate through a fast-wave structure loaded with crystal. At liquid nitrogen temperature, however, pump powers are much larger and it is necessary to consider how the most efficient coupling between the field and the material may be achieved.

4.1 Cavity Masers

The theory of the single cavity maser has been developed fully by several authors including Butcher[4] and Siegman[3] and therefore the results will be quoted here with only a brief explanation of how they are obtained.

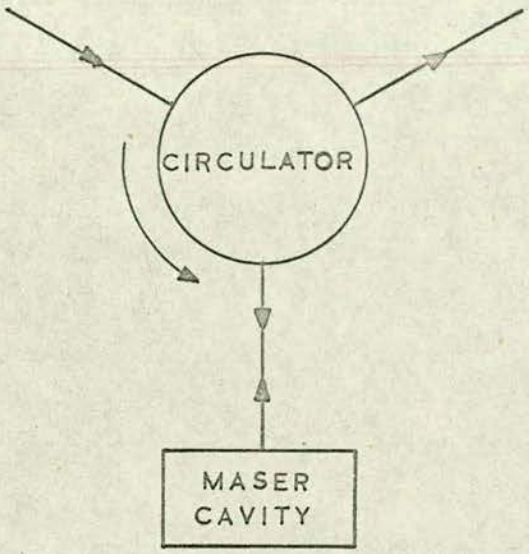

Reflection (One-port) Cavity Maser

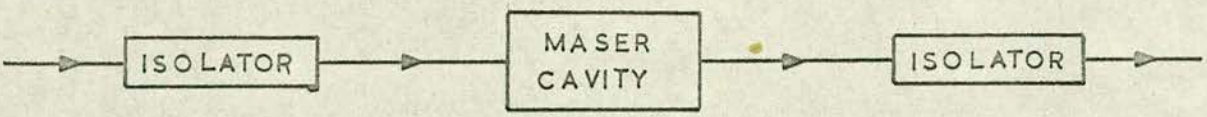

Transmission (Two-port) Cavity Maser

Fig. 4.1

There are two possible configurations for a single cavity maser. These are the "one-port" or "reflection" cavity maser and the "two-port" or "transmission" cavity maser. These are shown in Fig. 4.1. The gain in a cavity maser is bi-directional and consequently the performance of the transmission cavity maser is only half that of the reflection type since in the former half the available output power passes through the input coupling slot and is absorbed in the isolator. This is shown by Butcher by direct analysis of both types from first principles. Further discussion will therefore be confined to the reflection cavity maser.

The expression for Q_m quoted in Section 3.2 contains a function $f(\nu)$ which has the maximum value unity when $\nu = \nu_s$ the frequency of the paramagnetic resonance. The form of $f(\nu)$ is taken to be Lorentzian. Typical line-widths are 50-100 Mc/s for the lower (liquid helium) concentrations and 100-200 Mc/s for the higher (liquid nitrogen) concentrations. A good cavity has a bandwidth of about 1-2 Mc/s at liquid helium temperature increasing perhaps to 2-3 Mc/s at liquid nitrogen temperature. The analysis of the single cavity maser is greatly simplified by assuming frequency independence of Q_m over the bandwidth of the maser cavity. Since the line-width of the material is so much larger than the cavity bandwidth this is a reasonable approximation. Account of the frequency dependence of Q_m will be taken when the two-cavity maser is considered in the next chapter.

The single cavity maser is considered as an L-C-R circuit with an extra, negative resistance, element representing the

effect of the pumped maser material. This is shown in Fig. 4.2.

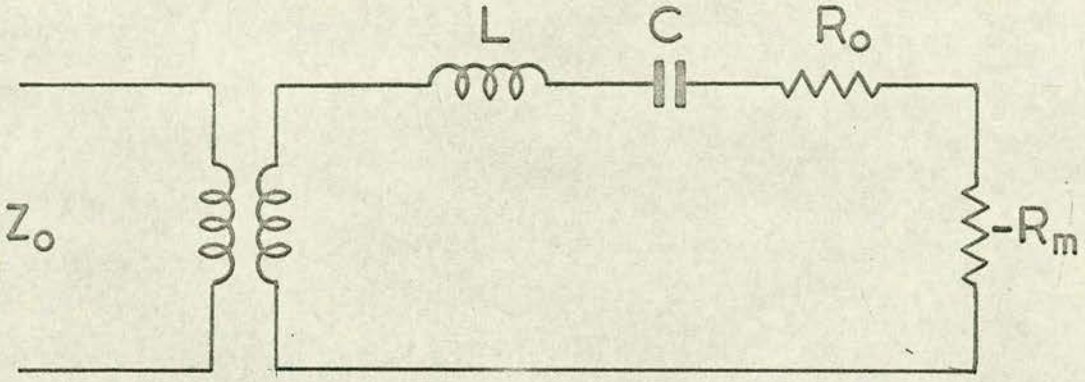

Fig.4.2

The transformer represents the effect of the slot coupling the cavity to the input waveguide. It is customary to describe the action of this coupling slot between the input waveguide and the cavity by an "external Q", Q_e, defined:

$$Q_e = 2\pi \frac{\text{energy stored in cavity}}{\text{power radiated through coupling slot/cycle}}$$

The normalised impedance of the cavity terminating the line is:

$$Z/Z_o = \frac{1/Q_e}{-\frac{1}{|Q_m|} + \frac{1}{Q_o} + 2j\left(\frac{\nu - \nu_s}{\nu_s}\right)}$$

Q_o is the unloaded Q of the cavity. This includes both the wall losses and the dielectric losses.

ν is the applied frequency and ν_s is the signal frequency for paramagnetic resonance.

The power reflection coefficient is the gain, G,

$$G = \left| \frac{1 - Z/Z_o}{1 + Z/Z_o} \right|^2$$

and at resonance this is a maximum

$$G_o = \frac{\left\{ 1/Q_e + \left(\left| \frac{1}{Q_m} \right| - \frac{1}{Q_o} \right) \right\}^2}{\left\{ 1/Q_e - \left(\left| \frac{1}{Q_m} \right| - \frac{1}{Q_o} \right) \right\}}$$

For amplification to occur, $\left| \frac{1}{Q_m} \right|$ must be greater than $\frac{1}{Q_o}$.

This states the obvious requirement that the power emitted by the maser material must be greater than the power absorbed by the wall and dielectric losses of the cavity. To prevent oscillation the external loading must be adjusted so that

$$\left| \frac{1}{Q_m} \right| - \frac{1}{Q_o} < \frac{1}{Q_e}$$

From the expression for G_o it is seen that high gains are obtained when this condition is just satisfied i.e. to obtain a high gain the maser must be operated on the verge of instability. The circulator prevents variations in impedance from the aerial or the receiver being "seen" by the maser but, it is possible for variations to occur between the circulator and the maser. When the maser is operating at a high gain even quite small variations in loading can take it into oscillation and this is a serious disadvantage of the cavity maser.

Assuming constant $|Q_m|$, the frequency dependence of the cavity maser is determined solely by the cavity and it can be shown that, for high gains, the 3 dB bandwidth is

$$B = \nu_s\left(\frac{1}{Q_e} - \left|\frac{1}{Q_m}\right| + \frac{1}{Q_o}\right)$$

from which it is seen that

$$(\sqrt{G_o} - 1)B = 2\nu_s\left(\left|\frac{1}{Q_m}\right| - \frac{1}{Q_o}\right)$$

and, since G is high, this may be written

$$\sqrt{G_o}B = 2\nu_s\left(\left|\frac{1}{Q_m}\right| - \frac{1}{Q_o}\right)$$

Thus the voltage-gain-bandwidth product is constant for a single cavity maser. When discussing performances the subscript o is dropped and, in the expression $\sqrt{G}B$, G is understood to be the maximum gain.

If the frequency variation is taken into account the $\sqrt{G}B$ product is still a constant but then

$$\sqrt{G}B = \frac{2\nu_s\left(\left|\frac{1}{Q_m}\right| - \frac{1}{Q_o}\right)}{\left(1 + \left|\frac{Q_p}{Q_m}\right|\right)}$$

Q_p is the Q of the paramagnetic resonance line, $\frac{\nu_s}{\Delta\nu_L}$ which is of the order of 5-10 for a material of the higher concentrations used at 77°K.

$|Q_m|$ is in the range 700-1000 so it is seen that the assumption of $|Q_m|$ constant is a justifiable approximation.

Taking the best value of $|Q_m| \sim 700$ and a good $Q_o \sim 5{,}000$ $\sqrt{G}B$ is about 24 Gc/s at 77°K. This is larger than most

observed values, which are in the range 14-16 Mc/s. The best value so far reported is a $\sqrt{GB}$ product of 21·5 Mc/s with a Q_o of only 3,000 (Reitbock[18]). The noise temperature of a liquid-nitrogen-cooled maser should be of the order of 75-100°K and to derive the benefit from this the gain would, in general, have to be of the order of 17-20 dB. This assumes that the maser is operating directly into a conventional balanced mixer followed by a good I.F. amplifier (noise figure about 7-8 dB) and a gain of 17-20 dB is sufficient to make the noise contribution of the stages after the maser considerably less than that of the maser itself. It is quite conceivable that the maser could be followed by a tunnel diode amplifier (noise temperature ~600°K) which would require a much lower maser gain. However, the figure of 17-20 dB will be taken as a suitable gain for a liquid nitrogen maser. For a gain of 20 dB the bandwidth is limited to about 2½ Mc/s at the most. Because the frequency response is governed by a single tuned circuit the gain is not approximately constant even over a fraction of the 3 dB bandwidth.

Thus the chief disadvantages of the single cavity maser are that the bandwidth is limited and the shape of the response curve is far from ideal. The advantage of the cavity maser is that the performance is not proportional to cavity volume and therefore small crystals can be used and the cavity can be made resonant at both pump and signal frequencies.

4.2 Travelling-Wave Masers

Since it will be shown from a brief and fairly elementary consideration of the travelling-wave maser that it is not suitable for operation at liquid nitrogen temperature it is not relevant either to extol the advantages or to expound the intricacies of this device at great length. This section will therefore set out briefly the formulae for the main features of the travelling-wave maser and by inserting the "best values" of the various parameters at 77°K the impracticability of the device at this temperature will be demonstrated.

The first travelling-wave maser was built at Bell Labs. in 1958[12] very shortly after the first cavity maser and since then, for liquid helium operation where broad bandwidth was required, they have been used almost universally. The chief advantage of the travelling-wave maser over the cavity maser is the greatly increased bandwidth. Since slow wave structures can be designed with bandwidths much greater than the maser material line width it is the latter which limits the bandwidth of the maser. (As will be shown this does not, however, mean that the bandwidth of the maser is equal to the linewidth of the material.) This might at first sight make the prospect of a liquid-nitrogen-cooled travelling-wave maser appear attractive since optimum maser action at 77°K has been shown above to occur in materials of higher concentration, and hence greater bandwidth, than are used at liquid helium temperature. This would indeed produce larger potential bandwidths but since the maser action at 77°K is much weaker, the gain per unit length is so small that impracticably long

structures would be required.

4.2.1 Gain and Bandwidth in Travelling-Wave Masers

The simplest analysis of the travelling-wave maser assumes a length of guide completely filled with maser material down which the signal propagates with a certain group velocity v_g. In most practical cases, in order to achieve the desired slowing factors, some sort of periodic structure has to be used which complicates the analysis but this does not affect the form of the final result and attention will be confined to the simple case.

It has been shown[4.1,3] that the amplification is governed by a parameter α_m which depends on $|Q_m|$ and the group velocity v_g as follows:

$$\alpha_m = \frac{\pi \nu_s}{|Q_m| \cdot v_g}$$

so that power dP added to signal in length $d\ell = 2.\alpha_m.P.d\ell$. and hence for a length ℓ the gain G is

$$G = e^{2.\alpha_m.\ell.}$$

It is customary to describe the length ℓ as a number, N, of free space wavelengths λ_o ($N = \ell/\lambda_o$). A "slowing factor", S, $= c/v_g$ is defined and the gain, expressed in dB, is

$$G_{dB} = 27{\cdot}3 \left|\frac{SN}{Q_m}\right|$$

This is called the "electronic gain" since it is the theoretical gain of the amplifier, taking no account of the losses in the structure. It is seen that α_m is proportional

to $1/|Q_m|$ and hence the 3 dB bandwidth of α_m is the linewidth of the material. However, the bandwidth, B, of the maser is the 3 dB width not of α_m but of $e^{2.\alpha_m.\ell}$ and this can be shown to be

$$B = \Delta\nu_L\left(\frac{3}{G_{dB} - 3}\right)^{\frac{1}{2}}$$

which is only equal to $\Delta\nu_L$ for a gain of 6 dB and which decreases as G increases as is to be expected.

The other main advantage of the travelling-wave maser is that isolation can be incorporated so that the maser is a two-port unidirectional amplifier. Such a device is stable even when faced with a bad mismatch at either end. In general the response of a maser material to a circularly polarised microwave field is different for the two directions of polarisation. Since many slow wave structures have symmetrically situated regions in which the propagating wave has circularly polarised components of opposite senses it is possible, by placing the maser material in the appropriate region, to obtain a greater gain in one direction than in the other. Generally, however, this effect of non-reciprocity is exploited further by placing non-reciprocal ferrite components so as to absorb relatively in the reverse direction while causing minimum attenuation in the forward direction. Typical figures for recent liquid-helium-cooled TWMs are: (Tabor and Sibilia[40]) greater than 120 dB reverse isolation with a forward loss of 4 dB which is quite tolerable since it is more than recouped by the much higher gains for which the maser can be made stable than would

be possible without the isolation.

However, at liquid nitrogen temperature the losses would be greater - not only because of the higher inherent forward loss of the ferrite elements but also because of the longer structures which would be required.

For high gain in a TWM, S and N should be as large as possible and, as is general for all masers, $|Q_m|$ should be small. The first step seems, as before, to find the material with the best $|Q_m|$ but this is not completely divorced from the other considerations in the case of TWM's since a material like rutile which has $\epsilon_r \sim 100\text{-}250$ provides a slowing factor $\sqrt{\epsilon_r} \sim 10\text{-}15$ from the material itself and a Cr^{3+} doped form of this material has been used to good advantage at $4{\cdot}2^{\circ}K$ by Sabisky and Gerritsen[42]. In view of their success it seems surprising that no one has used iron-doped rutile which would combine the advantages of the zero field maser of King and Terhune[21] with this "self-slowing" characteristic associated with its very high dielectric constant. At liquid nitrogen temperature, however, where the best reported $|Q_m|$'s (with ruby, $\epsilon_r \sim 10$) are about 700, to achieve an electronic gain of 17 dB would require SN to be about 440. A typical value for S is (Haddad and Paxman[43]) of the order of 100 which would require the structure length to be $4\frac{1}{2}\ \lambda_0$. At 10 Gc/s $\lambda_0 = 3$ cm which would require the structure length to be about 14 cms. If S could be increased to 150 the required length could reduce to 10 cms. Even assuming that good maser crystals of this length could be obtained, the magnetic field requirements would be

difficult to meet and so far no losses in the structure have been considered.

Paxman[37] has considered the feasibility of a liquid-nitrogen-cooled travelling-wave maser and concluded that the construction of such a maser was impracticable. He investigated various concentrations of ruby and obtained one of the best quoted values of $|Q_m|$ (~ 680). Several slow wave structures were made of types ranging from ladder lines of the type used by Haddad and Rowe[44] through meander lines to the more usual comb structures. Eventually it was deemed best to use the comb structure, mainly, it seems, due to considerable local experience in frabicating this type of structure. The structure tested was loaded on one side with a ruby block 3·1 mm. × 1 mm. and about 1 cm. long and no ferrite isolation material was incorporated. The measured losses were 1 dB/cm. at 290°K (S = 75) and 0·88 dB/cm. at 77°K (S = 81). Paxman states that from other work done on slow wave structures at Mullard, losses for this type of structure generally are in the 0·5 to 1 dB/cm. range. Paxman concluded that even if the slowing factor could be increased to 150 and the structure losses kept at the lower limit of 0·5 dB/cm the maser would need to be about 24 cm. long. In view of Paxman's measurements it seems unlikely that this could be done since it is a general rule with slow wave structures that increasing S increases the losses and also, some isolation material with associated losses would have to be included. However, even if it is assumed that these "best value" figures could be

achieved and that suitably large single crystals could be purchased, there are still two major difficulties.

The first is the provision of a homogeneous field of about 4 Kgauss over the length of the structure using a magnet of reasonable size. This would involve a large permanent magnet and although this would be very heavy and expensive this difficulty is not insurmountable if adequate funds are available. If the maser is to reap the advantage of freedom from helium liquefiers in order to permit small packaging, for, say, airborne use, then from this standpoint the use of such a bulky and heavy magnet would be prohibited. The losses involved in folding a slow-wave structure even once are too large to make reduction of the required volume of magnetic field by this means an attractive prospect.

The second remaining difficulty and, it is felt, the most serious drawback of all is that the very large ruby crystals would probably require more pump power than even a high power 12TFK2 could provide. It is significant that although Paxman built several travelling-wave structures he used cavity methods to measure the $|Q_m|$'s because (even with a 12TFK2) he could not saturate the pump transitions despite structure lengths of the order of only one centimetre.

For the above reasons it was decided that Paxman's conclusion that liquid-nitrogen-cooled travelling-wave masers are not a feasible proposition was justified and it was therefore decided to concentrate attention on the best way of optimising the performance of the cavity maser.

CHAPTER FIVE

Reactance Compensation in Cavity Masers

The susceptibility, μ_s, of a paramagnetic material near resonance is given by the expression:

$$\mu = \mu_0\left(1 - \frac{j.\chi_m''}{1 + j.2\pi.T_2.\Delta\nu}\right)$$

where χ_m'' = peak value of the absorptive component of the complex susceptibility. $\chi_m'' = \frac{1}{Q_p}$

$\Delta\nu$ = frequency deviation from resonance $(\nu - \nu_s)$

T_2 = spin-spin relaxation time.

This applies to a Lorentzian line shape of the type exhibited by the higher concentration materials used at liquid nitrogen temperature where the line width and shape are determined by spin-spin interaction. It is normally accepted as a good approximation for the lower concentration material used at liquid helium temperature although here the line shape is

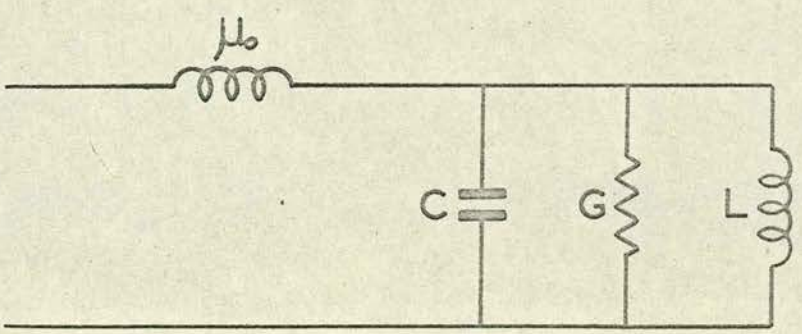

Fig. 5.1

beleived to tend more to the Gaussian since it is determined by lattice defects rather than spin concentration. It is convenient to represent this by the network shown in Fig. 5.1. where

$$G = \frac{1}{\mu_0 \cdot \chi_m'' \cdot 2\pi \cdot \nu_s} = \frac{Q_n}{\mu_0 \cdot 2\pi \cdot \nu_s}$$

and there is also a reactance

$$jX = \frac{j \cdot T_2 \cdot \Delta\nu}{\mu_0 \cdot \chi_m'' \cdot \nu_s} = \frac{j \cdot T_2 \cdot \Delta\nu \cdot Q_n}{\mu_0 \cdot \nu_s}$$

Inversion of the resonance gives

$$\mu = \mu_0\left(1 + \frac{j \cdot \chi_m''}{1 + j \cdot T_2 \cdot \Delta\nu}\right) \qquad \left(\text{Here } \chi_m'' = \left|\frac{1}{Q_m}\right| \text{ for unity filling factor}\right)$$

This is represented by the above network with signs of G, L and C reversed (Fig. 5.2)

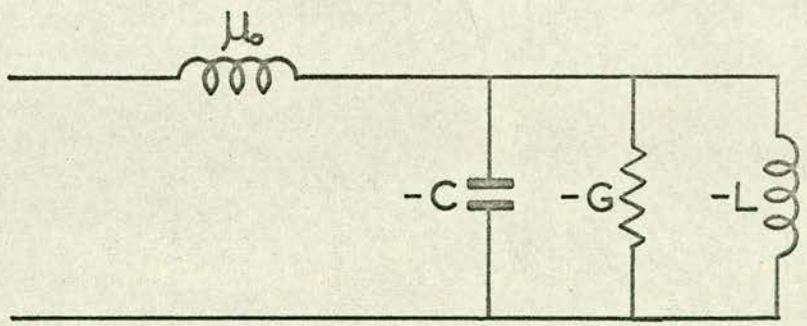

Fig. 5.2

Kyhl[45] in 1960 first suggested that it should be possible to exploit the negative L and C which occur in addition to the negative G in order to improve the bandwidth of the cavity maser. He suggested that this might be done by interposing a

passive coupling cavity between the input waveguide and the maser cavity itself.

Cook et al.[46] used this principle in an X-band ruby maser for a radiometer. The coupling in this case consisted of a $\frac{1}{8}$ inch brass plate with a rectangular hole cut in it. (The dimensions of the hole were determined empirically.) The front of the coupling plate was open to the guide which resulted in the desired strong overcoupling. The back of the coupling cavity was formed by the silver plated maser cavity with a small coupling slot cut in it to provide the smaller degree of coupling required between the two cavities. The coupling cavity contained a probe of adjustable penetration which caused the cavity to resonate in what the authors describe as a "semi-coaxial" mode and adjustment of the penetration of this probe tuned the cavity. Using this system at 4·2°K $\sqrt{G}B$ products of from 200-500 Mc/s. were obtained. For a system of this type $\sqrt{G}B = KG^{1/4}$ and the results were found to agree with this.

Nagy and Friedman[47] later extended this work by building a maser with two active cavities side-by-side across the "a" dimension of the waveguide each coupled to the waveguide by a resonant coupling very similar to those of Cook's maser. The active cavities were stagger-tuned 20-30 Mc/s. This maser produced $\sqrt{G}B$ products as high as 1700 Mc/s at 4·2°K. Nagy and Friedman suggested a rule for systems with n resonant elements:

$$G^{\frac{1}{2n}}B = K$$

This gives for n = 1 the familiar rule $G^{\frac{1}{2}}B = K$. For the system of Cook with n = 2 this gives $G^{1/4}B = K$ which is in agreement with the results obtained. If the system of Nagy and Friedman is taken to have n = 3 this predicts $G^{\frac{1}{2}}B = KG^{1/3}$ and the "best fit" to the experimental data was the exponent 0·305 which was claimed to be in good agreement. It is not immediately obvious which resonant elements constitute the three since at first sight there appear to be four (two active and two passive cavities). In answer to an enquiry about this, Nagy (private communication) agreed that it does appear that there are four rather than three resonances but stated that the experimental results agree more closely with the figures for a three-element system. He said also that they had observed the two-peaked response degenerating into a three-peaked response at lower mid-band gains. From his remarks it is apparent that it is very difficult to predict the performance and shape of the response curve for a system with two active cavities. Nagy commended the work of Kyhl et al.[48] since the cavities in their maser were restricted to a single mode which made analysis of the system much easier.

The paper of Kyhl et al. includes a theoretical and practical account of a maser with one active maser cavity and one passive coupling cavity. In this case, the coupling cavity was loaded with undoped polycrystalline sapphire and was very similar to the maser cavity itself. Operating at liquid helium temperatures Kyhl obtained bandwidths of about 70 Mc/s at 14 db. gain (4·2°K), 100 Mc/s at 14 db gain (1·5°K)

and 140 Mc/s at 10 db (4·2°K). The paramagnetic line width of the material was 67 Mc/s and thus the bandwidths of the maser were of the same order as the linewidth. The mid-band gain of 14 db was no doubt chosen to show the extent to which this principle could be applied to increase the bandwidth. For any practical application designed to take full advantage of the extremely low noise temperature of the liquid-helium-cooled maser a more realistic gain would be in the range 25-35 dB. Nevertheless the improvement in bandwidth over other cavity masers even at higher gains would be considerable and the most salient feature of this paper is the remarkable degree of agreement between theory and experiment which extends not only to the bandwidth but also to the detailed shape of the response curves.

In designing the liquid-nitrogen-cooled maser it was decided to follow the single active cavity approach of Kyhl et al. for two main reasons. Firstly, the detailed analysis which is possible with only one cavity exhibiting maser action would allow an assessment to be made of the performance which could be expected from such a maser. Secondly, the question of available pump power dictates that the size and number of active cavities be kept to a minimum. As has been stated earlier it is marginal whether or not a cavity maser using a small crystal of suitable concentration can be pumped using a conventional low-power reflex klystron rather than the high-power floating-drift-velocity tube. It was considered most unlikely that a maser with two such cavities could be effectively pumped with the low-power tube.

The analysis which follows is based on the analysis of Kyhl except that it has been necessary to extend Kyhl's treatment to include cavity losses. Kyhl neglected cavity losses completely since the values of $|Q_m|$ were 155 (1·5°K) and 240 (4·2°K). The relevant parameter is the ratio of $|Q_m|$ to Q_o, the unloaded cavity Q. No values of Q_o are available for Kyhl's maser but from similar masers operating at these temperatures it is reasonable to assume a Q_o of about 5,000. The worse of the two cases with $|Q_m| = 240$ therefore yields a value of $|Q_m|/Q_o$ of the order of 0·05 which can legitimately be neglected in relation to -1. However, at liquid nitrogen temperature $|Q_m|$ is much higher and Q_o is lower and allowance must be made for this. The system is represented by the network shown in Fig. 5.3.

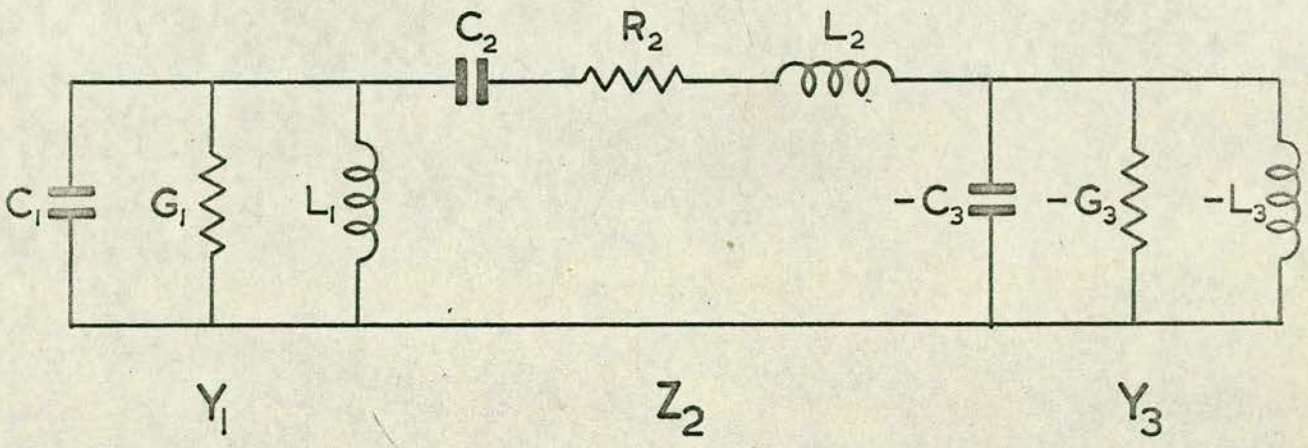

Fig. 5.3

Near resonance

$$Y_1 = G_1 - 4\pi j(\nu - \nu_s)C_1$$

$$Z_2 = R_2 - 4\pi j(\nu - \nu_s)L_2$$

$$Y_3 = -G_3 - 4\pi j(\nu - \nu_s)C_3$$

The width of the paramagnetic line, $\Delta\nu_L$, is

$$\Delta\nu_L = \frac{\frac{1}{2\pi}G_3}{C_3}$$

and the Q-factor of the paramagnetic resonance line, Q_p, is

$$Q_p = \frac{\nu_s}{\Delta\nu_L} = 2\pi\nu_s\frac{C_3}{G_3}$$

The magnetic Q, Q_m, is defined as before:-

$$Q_m = -\frac{2\pi \text{ energy stored}}{\text{energy emitted/cycle}} = -2\pi\nu_s L_2 G_3$$

The coupling between the two cavities produces a split in resonant frequencies in the absence of paramagnetic resonance

$$\nu_B - \nu_A = \frac{1}{2\pi\sqrt{L_1 C_2}}$$

and this is normalised to the line width thus:

$$\text{Coupling parameter } k = \frac{\nu_B - \nu_A}{\Delta\nu_L} = \frac{C_3}{G_3\sqrt{L_1 C_2}}$$

The extent to which reactance compensation may be applied is determined by the parameter 'a' which is the ratio of the energy stored in the cavity to the energy stored in the line. It is desirable that this parameter be as small as possible.

$$a = \frac{L_2 G_3{}^2}{C_3} = |Q_m|/Q_p$$

The parameter which describes how much of the emitted power will be lost in the cavities is $b = |Q_m|/Q_o$ and this should also be as small as possible. For a system like that of Kyhl where the coupling cavity and the maser cavity are very similar it is reasonable to take b as the same for each. (In a system where this is not so a different value of b for

each cavity must be used which complicates the algebra but does not affect the form of the analysis.)

The mid-band gain is determined by the coupling between the waveguide and the coupling cavity and this is conveniently represented by an ideal transformer of turns ratio n:1. Thus near resonance the circuit of fig. 5.3 becomes 5.4.

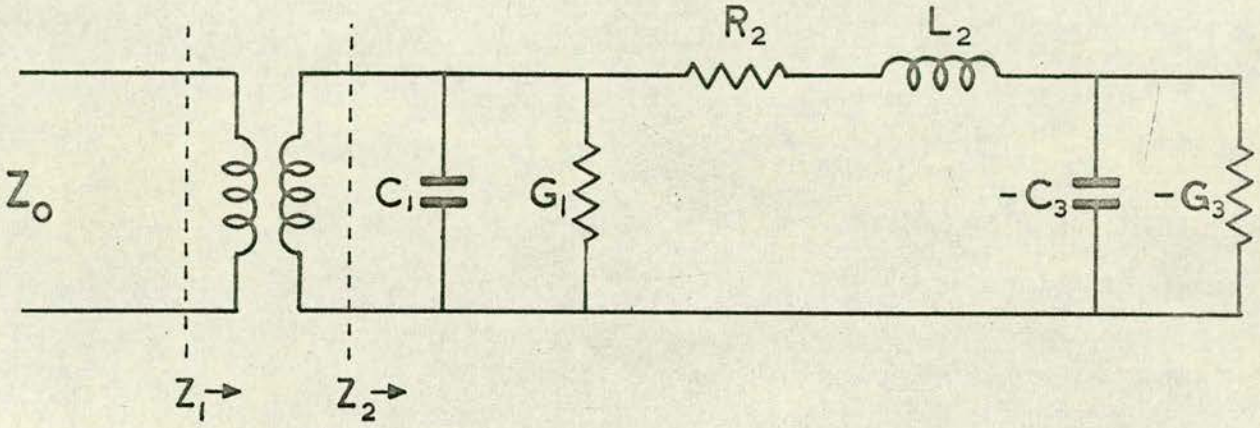

Fig.5.4

In terms of a normalised frequency variable $x = \frac{\nu - \nu_s}{\frac{1}{2}\Delta\nu_L}$, the values of the normalised impedances associated with the circuit elements are:

$$C_1 = \frac{b}{Z_o}$$

$$C_1 = \frac{j}{aZ_o}\frac{1}{k^2}x$$

$$R_2 = bZ_o$$

$$L_2 = jaZ_o x$$

$$G_3 = -\frac{1}{Z_o}$$

$$C_3 = -\frac{jx}{Z_o}$$

The turns-ratio of the ideal transformer is such that

$Z_1 = n^2 Z_2$.

The choice of G_3 equal to $-\frac{1}{Z_0}$ is abitrary. This is convenient because then the condition with n = 1 and b = 0 is a perfect "anti-match". This corresponds to the limiting case of infinite gain. Since the impedance of the waveguide is not in general equal to $-\frac{1}{G_3}$ it is necessary to transform to this from the actual impedance of the waveguide. In theory this merely requires suitable adjustment of the turns-ratio of the ideal transformer. The difficulties involved in achieving this in practice particularly where the crystal size is small will be discussed in the next chapter.

For x = 0 the mid-band gain G_0 is given by

$$G_0^{\frac{1}{2}} = \frac{(1 + n^2) + \frac{b^2}{(1 - b)}}{(1 - n^2) + \frac{b^2}{(1 - b)}}$$

Hence from the reciprocal expression:

$$n^2 = \frac{G_0^{\frac{1}{2}} - 1}{G_0^{\frac{1}{2}} + 1}\left(1 + \frac{b^2}{1 - b}\right)$$

the required value of n^2 for any desired G_0 may be calculated allowing for b. For the chosen mid-band gain and the available a and b values variation of gain with x and k can be computed. This was done for gains of 50 (17 db) and 100 (20 db). The values of b used ranged from 0 to 0·20. b = 0 is the ideal case of lossless broadbanding elements used by Kyhl. The value of 'a' used for the initial computations was taken as 6·0. This was arrived at in the following way. The

best values quoted for $|Q_m|$ were about 680 (calculated from data given by Paxman[37] and Reitbock's[18]). In neither case was the linewidth of the material measured but from information on line widths provided by J. C. Gill (private communication) it was estimated that the linewidths of these materials would be in the region of 100-150 Mc/s. This would give a best value for 'a' of about 7 but since it was subsequently established that in Reitbock's maser the pump transitions were not saturated completely a slightly lower value was used in anticipation of an improvement when a crystal of concentration similar to his could be adequately pumped.

Figures for single cavity masers with the same parameters a and b and the same mid-band gain were also computed using the following network;

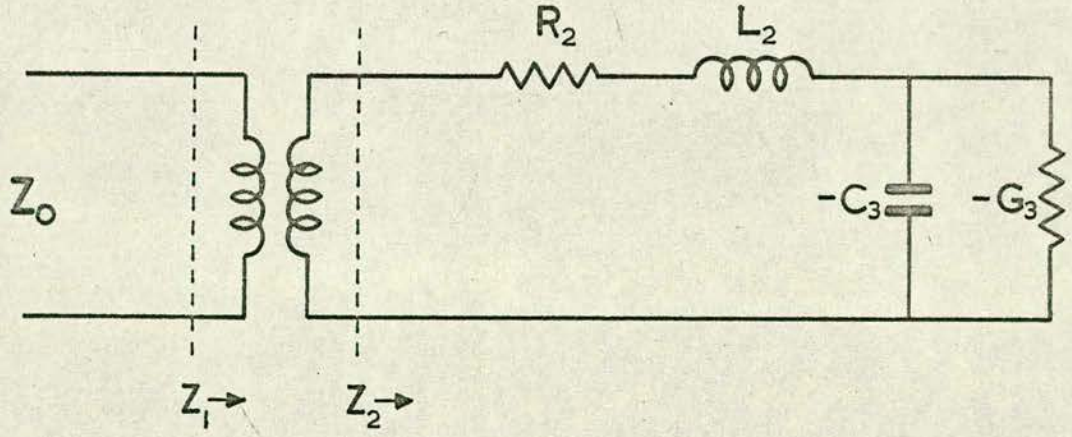

Fig. 5.5

where all the component values are the same as for the two-cavity maser except for n which becomes n'. This is because calculation of the mid-band gain now only involves the loss

due to one cavity.

Hence $$G_0^{\frac{1}{2}} = \frac{1 + n^2(1 - b)}{1 - n^2(1 - b)}$$

or, for a given G_0 and b

$$n'^2 = \frac{G_0^{\frac{1}{2}} - 1}{G_0^{\frac{1}{2}} + 1} \cdot \frac{1}{1 - b}$$

Fig. 5.6 shows the response curves for G = 100 with k values selected to give the best characteristics. Curves are drawn for b = 0, 0·10 and 0·20.

Fig. 5.7 shows similar curves for G = 50.

It can be seen that the improvement of the double cavity over the single cavity maser is appreciable even for the relatively poor b value of 0·20. This value would correspond to $|Q_m| = 1{,}000$ and $Q_0 = 5{,}000$ which should be readily attainable.

Fig. 5.8 shows the variation of response curve with the parameter k. It is striking how sensitive the shape of the response curve is to this parameter. It became apparent at this point that, in a system with no means of adjusting k other than by adjusting the size of the coupling slot, this would be the most critical adjustment involved in the construction of the maser.

It is important to note not only the improvement in the 3 db bandwidth but also the improvement in the shape of the response curve. For the single cavity maser with its Lorentzian response shape there is zero bandwidth which is effectively flat. In the case of the double cavity maser the flat region of the response curve, though small in extent at

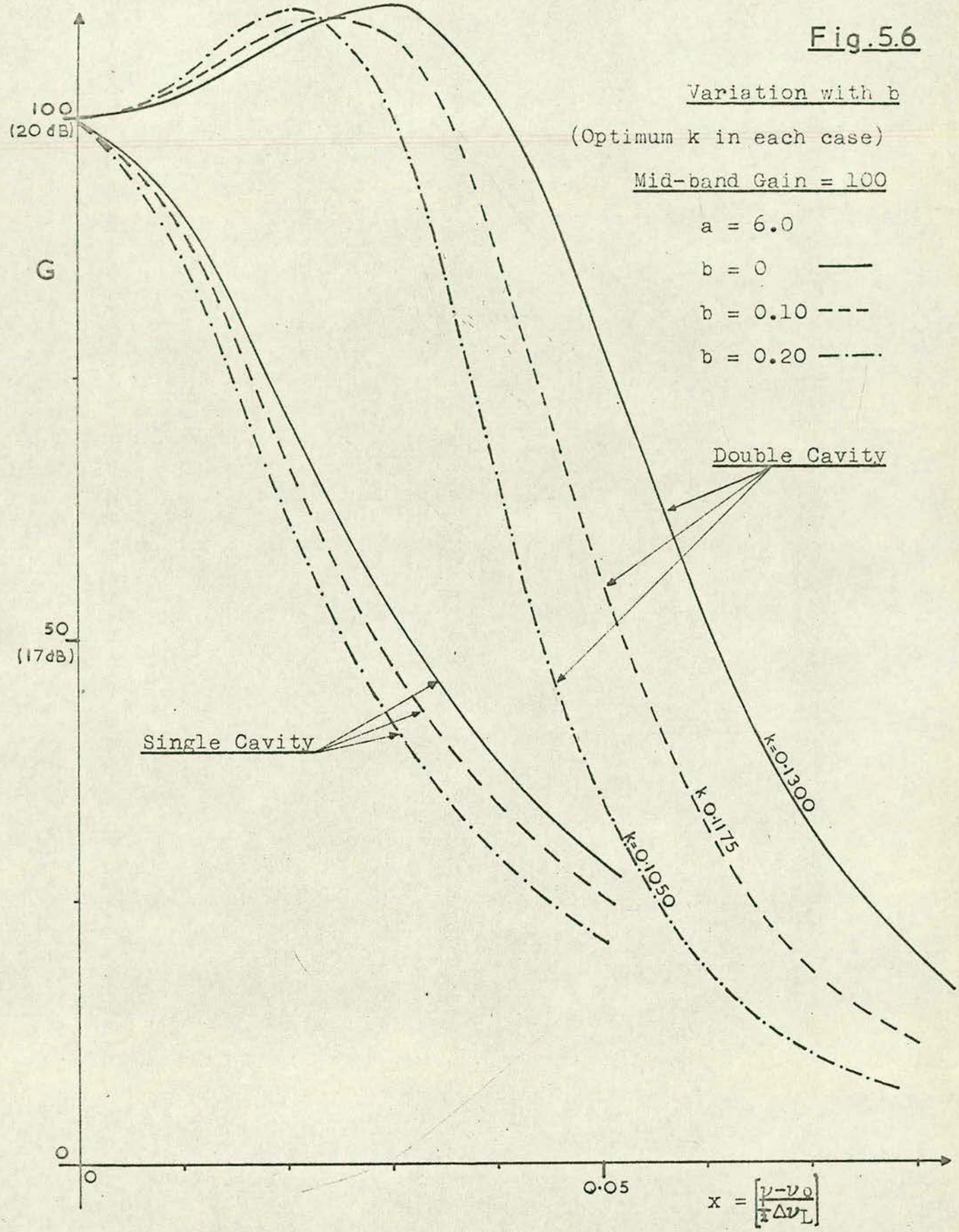
Fig.5.6
Variation with b
(Optimum k in each case)
Mid-band Gain = 100
a = 6.0
b = 0
b = 0.10
b = 0.20
100
(20 dB)
G
50
(17dB)
0
Double Cavity
Single Cavity
k=0·1300
k=0·1175
k=0·1050
0
0·05
$x = \left[\frac{\nu-\nu_0}{\frac{1}{2}\Delta\nu_L}\right]$

Fig.5.6

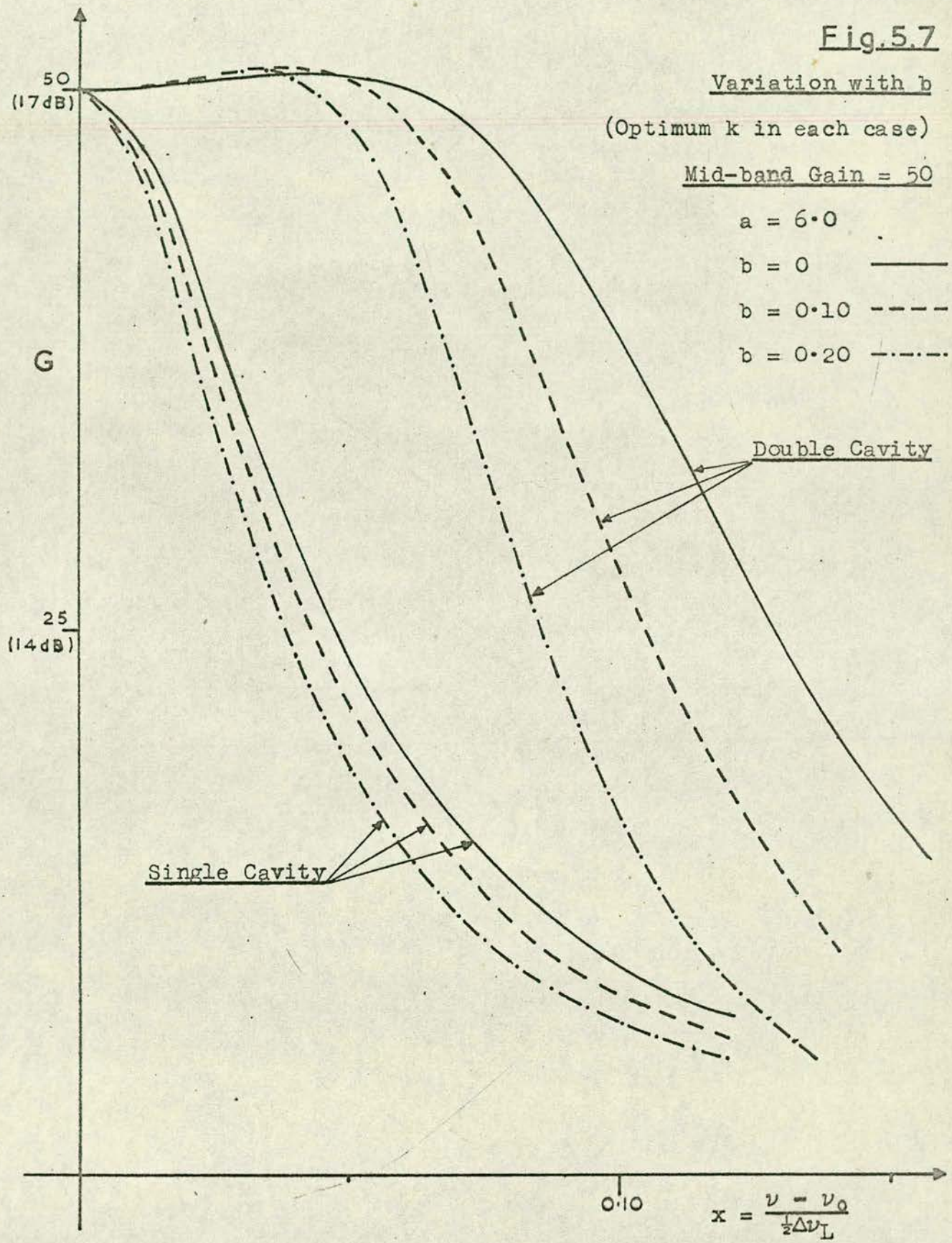
Fig.5.7
Variation with b
(Optimum k in each case)
Mid-band Gain = 50
a = 6·0
b = 0
b = 0·10
b = 0·20
50
(17dB)
25
(14dB)
G
Double Cavity
Single Cavity
0·10
$x = \frac{\nu - \nu_0}{\frac{1}{2}\Delta\nu_L}$

Fig.5.7

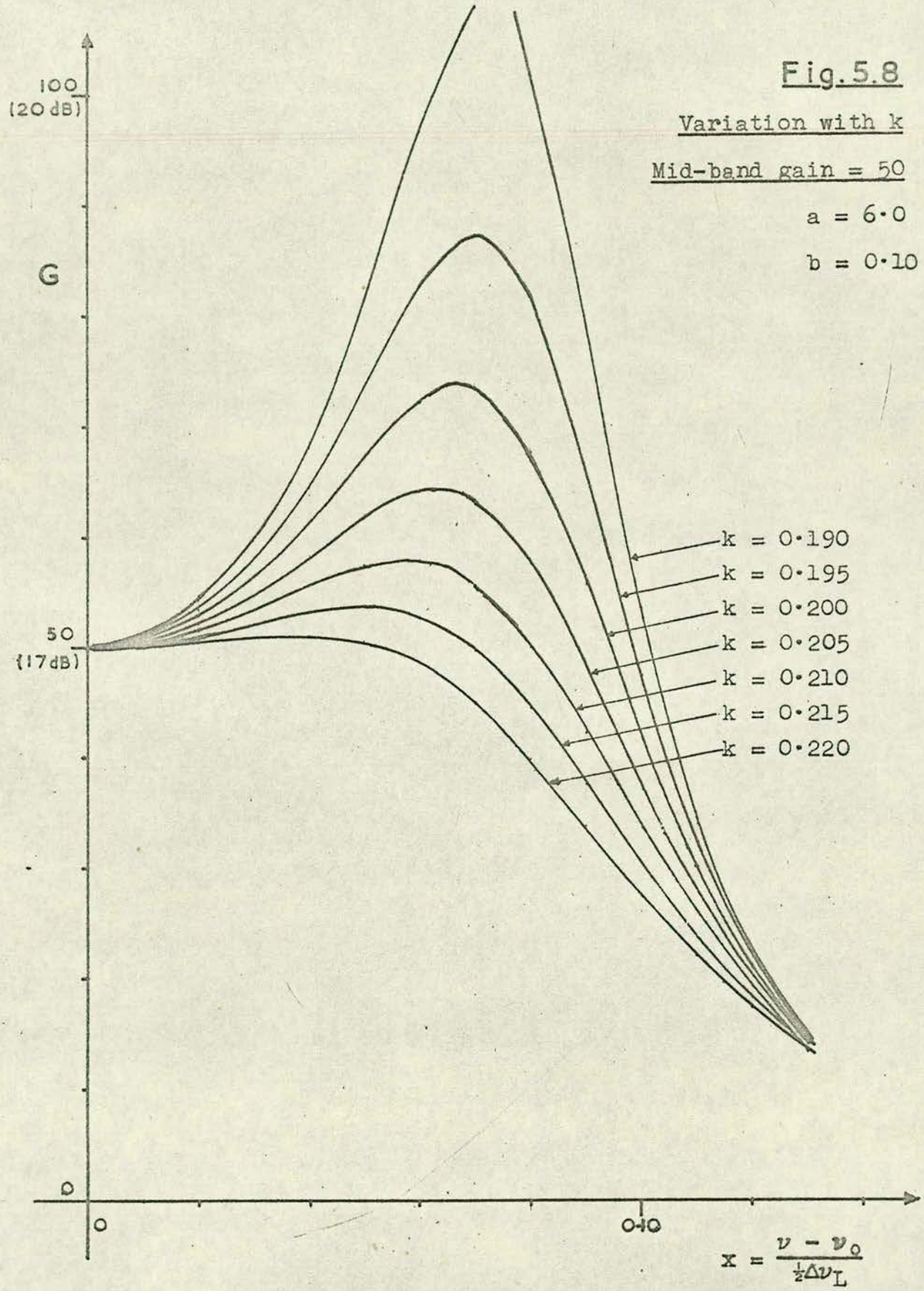

Fig.5.8

Variation with k

Mid-band gain = 50

a = 6·0

b = 0·10

Fig.5.8

liquid nitrogen temperature, does exist and the 1 db and ½ db bandwidths are very much improved over those of the single cavity maser.

Some idea of the expected performance can be obtained by inserting estimated values for the various parameters. Line widths of maser materials vary quite widely but, for the concentrations to be used, $\Delta\nu_L$ is of the order of 150 Mc/s. The parameter "b" cannot be expected to be any smaller than 0·10 at best. Using these values in conjunction with Figs. 5.6 and 5.7 it is found that the best expected bandwiths are:

7·5 Mc/s for 20 dB gain

and 15 Mc/s for 17 dB gain.

From the above calculations it was concluded that at liquid nitrogen temperature a two cavity maser of the Kyhl type would provide a significant improvement over the single cavity masers previously used at this temperature.

CHAPTER SIX

Design and Construction of a Two-Cavity Maser

6.1 Methods of Cavity Construction

It was necessary to decide at an early stage how the cavities were to be made and to what extent (if any) they were to be tunable. The first tunable cavity maser was built by Morris, Kyhl and Strandberg[20] in 1958. It involved a 1 x 1 x ½ cm ruby crystal across the shorted end of a length of 1 cm x 1 cm waveguide and the remaining wall of the cavity was a non-contacting plunger. Since the volume of the guide not occupied by the high dielectric constant of the ruby was beyond cut off the TE_{10} mode was evanescent in this region which meant that the field intensity in this region was low. This had two important effects; the filling factor η remained high despite the comparatively large volume change required to tune the maser over its signal tuning range from 8·4 to 9·7 Gc/s and the Q_0 even with the non-contacting plunger was adequate (2,000).

Even with a single cavity maser, however, tunability is a doubtful asset since, to follow the signal tuning, the pump frequency and d.c. magnetic field must be tuned accordingly. Theoretically it would be possible to calibrate adjustments for these so that they could be adjusted to any desired operating point but in practice it would be necessary to have test equipment on site to check this from time to time. This adjustment which is complex for a single cavity maser would

be totally impracticable for the two-cavity maser in view of the sensitivity of the latter to the parameter k. In view of these difficulties and also the consideration that in many possible applications of the liquid nitrogen maser e.g. airborne radar, satellite communication and EPR spectrometers, tunability would not be particularly advantageous and, in most cases, adjustable parameters might be a decided disadvantage since steps would have to be taken to ensure that they did not drift off the proper settings during operation. Thus it was felt that efforts to make the maser tunable would have little prospect of success without very cumbersome and possibly unreliable adjustments and even if this success was achieved the increased losses necessarily introduced by providing these adjustments would considerably inhibit the performance. It was therefore decided that it would be preferable to concentrate on broadbanding the maser as much as possible rather than to sacrifice some of the bandwidth in an endeavour to achieve tunability.

Tunability of the coupling cavity would, however, be a most useful feature since, adjusting the slot between the two cavities to vary k changes their resonant frequencies by different amounts. This is because the common slot is the only slot in the maser cavity whereas it is the smaller of two slots in the coupling cavity. It would therefore be advantageous to be able to re-adjust the resonant frequency of the coupling cavity to coincide with that of the maser cavity.

The choice here is between the resonant coupling plate of Cook et al. and a proper tunable cavity. The Cook type of

cavity has several disadvantages apart from those pointed out by Nagy (private communication) regarding uncertainty as to which mode or modes the coupling plate oscillates in. To retain the tunability feature, the cavity formed by the hole in the plate could not be loaded with dielectric which means that the maser crystals would have to be large and even then the coupling hole between the crystal-filled maser cavity and the air-filled coupling cavity might have to be larger than is desirable. This is incompatible with the decision to keep the maser crystals as small as possible from considerations of available pump power, crystal quality and cost. Furthermore the Q_o of such a resonant coupling plate could not be expected to be high. Some very brief preliminary experiments were carried out using a cavity of this type but no results were obtained.

The highest Q's are obtained with air-filled cylindrical cavities operating in the TE_{110} mode. This is the type of cavity normally used for wavemeters since the wall currents are everywhere azimuthal and therefore the Q is not affected by the contact between the sliding plunger and the wall. An air-filled cavity of this type is subject to the same objection concerning difficulty in coupling to a small crystal as the coupling plate since it would have to be so much larger than the maser cavity. A further objection to the air-filled cavity, also because of its size, is the large volume which would require to be refrigerated and the large pole gap of the d.c. magnet required if the coupling cavity is to be adjacent to the maser cavity. In principle there is no reason why the

coupling cavity cannot be placed a whole number of wavelengths away from the maser cavity and remain at room temperature. Since the use of small maser crystals dictates that tapered wave-guide sections be used to connect the maser cavity and the guide, determination of the correct coupling would, in practice, be extremely difficult unless the characteristics of the taper are near-ideal.

The simplest and, it was felt the best, approach, therefore, seems to be to have the coupling and the maser cavities as similar as possible and in immediate juxtaposition to one another. To achieve this using the desired small maser crystals, the coupling cavity must be loaded with a low-loss material of dielectric constant similar to that of the ruby itself, such as undoped Al_2O_3. To retain the feature of tunability of the coupling cavity it would then be necessary to use a cavity of the type used by Morris et al. but terminating one end of the cavity in a length of guide beyond cut-off does not appear to permit a large enough Q_0 for use at liquid nitrogen temperature. The Q_0 obtained by Morris et al. was 2,000 at 4·2°K. which was acceptable since the value of $|Q_m|$ was about 350. Even assuming that the Q_0 would not be any lower at 77°K, this value is too low since the estimated best value of $|Q_m|$ at this temperature is about 650 and this would lead to a value for the parameter b of about 0·3 which is rather high for an extra broadbanding element. It was therefore reluctantly decided not to make the coupling cavity tunable. This was only done after careful consideration since

it was realised from the results of Chapter 5 that, owing to the extreme sensitivity of the maser to the parameter k it would be difficult to align the maser without any means of tuning the coupling cavity other than by altering the dimensions of the cavity or the sizes of the coupling slots.

Having accepted that fixed tuned cavities would be used it was decided to make the cavities by cutting the ruby material (or Al_2O_3 for the coupling cavity) to a suitable size for resonance and plating the material itself to form the cavity. This method was first suggested by Cross[49] and has been widely used both at liquid helium and liquid nitrogen temperatures. Although masers have been built with machined cavities and good results obtained at liquid helium temperature, the performance of masers at liquid nitrogen temperature has been better with plated cavities. The following table shows values for various liquid nitrogen masers.

Mode	Crystal Size (mm)	Construction	Q_o	Authors
TE_{101}	7·1 x 3·5 x 7·1	Silver Plated Crystal	4,000	Maiman[25]
TE_{101}	7·1 x 3·5 x 7·1	Silver Plated Crystal	3,000	Reitbock[18]
TE_{101}	7·7 x 3·5 x 7·1	Machined Cavity	1,915	Fruin and Ahern[36]
TE_{202}	19 x 4·1 x 13·6	Hobbed	3,670	Genner and Plant[24]
TE_{202}	19 x 4·1 x 13·6	Copper Plated	11,600	

It should be noted that, other things being equal, the TE_{202} mode has a Q_0 about 35% higher than the TE_{101} mode. From the table it is seen that the plated cavities gave much better results than the machined cavities.

The best results quoted were obtained with the copper plated cavity of Genner and Plant. In order to make the copper adhere to the ruby a layer of aluminium about 100 Å thick was first evaporated on to the crystal and then about 3,000 Å of copper was deposited. The thickness of copper was then built up to the required extent by electroplating. In a discussion with Plant it was suggested that the vacuum was degraded from 10^{-5} or 5×10^{-6} torr to about 5×10^{-4} torr while evaporating the aluminium in order to allow the aluminium to oxidise slightly and hence act as an adhesive bond between the Al_2O_3 crystal and the copper which will not adhere to one another. Genner and Plant stated that the chief advantage of this method apart from the high Q_0 was the very strong bond which withstands repeated recycling to 77°K and can also (once the thickness has been built up) withstand the temperatures necessary for soft-soldering.

The two chief problems in coating crystals by this method are the prevention of contamination and the related difficulty of manipulating the crystals in the vacuum chamber. In an effort to reproduce the results of Genner and Plant a rotary drive was built so that four sides of the crystal could be coated without removing the crystal from the vacuum. Absolute cleanliness is essential and a typical cleaning process is:

12 hours in hot caustic soda, 6 hours in aqua regia, followed by washing in double (or preferably triple) distilled water. After the first 4 sides have been coated the crystal must then be removed from the chamber and turned around in the mount so that the other 2 sides may be coated. It is obvious that this is crucial since there can be no question of the cleaning process being repeated at this stage without removing the coatings already applied. The original team at R.R.E. had considerable trouble with this process and despite information kindly supplied by Plant (private communication) the results obtained with this method here were not satisfactory and it was eventually abandoned in favour of the simpler and more reliable method of fired silver coatings. In retrospect, even if the evaporation process had been successful, the time taken to adjust the slots would have been prohibitive since this method requires that all six faces be plated if any reduction in the size of coupling slots is required. The silver coating method involves painting the crystal with a colloidal suspension of silver in an organic base and then baking it at 750°C to remove the base, leaving a coating of silver. This method was first suggested by Cross[49] who used a paint called Hanovia 32-A but better results have been obtained here using Degussa 178L recommended by Reitbock.

The crystals are first cut oversize from the boule using a diamond saw (e.g. Burger and Meyer Quartz Cutting Machine QS2). Grinding excess ruby off can be done fairly rapidly with 120 or 240 grit carborundum and water on a cast iron lap.

The crystal must then be polished with diamond lapping paste of decreasing particle size. This material is expensive and a convenient and satisfactory approach was found to be to use a fairly large particle size (14 micron) for the initial polishing out of the carborundum scratches and then to polish with the same particle size on a special paper pad (Hyprocel) which effectively reduces the particle size. After polishing the crystals are washed in acetone or carbon tetrachloride and coated with silver. 3 or 4 coats of silver are required to achieve maximum Q_o and this yields a coating of silver about 1-2 thousandths of an inch in thickness. Each coat must be taken up to 750°C slowly (about 3 hours), held at that temperature for 30 minutes and allowed to cool very slowly (4-5 hours). Alternative silver suspensions requiring to be heated to only about 300°C were tried but these did not give as good Q_o's as those fired at 750°C and furthermore the bond between the silver and the crystal was not strong enough to permit repeated recycling between room temperature and 77°K. Even with the Degussa silver some trouble was encountered with this differential cooling problem but, following a suggestion by Reitbock that the corners of the crystals should be rounded off, this problem was overcome. Reitbock recommended rounding off the corners to a radius of about 0·5 mm. but is has been found unnecessary to round off quite as much as this. The radius of curvature is difficult to measure but can be reasonably estimated using a microscope with a traversing stage. The stages of construction from boule to finished cavity are shown in Fig. 6.1.

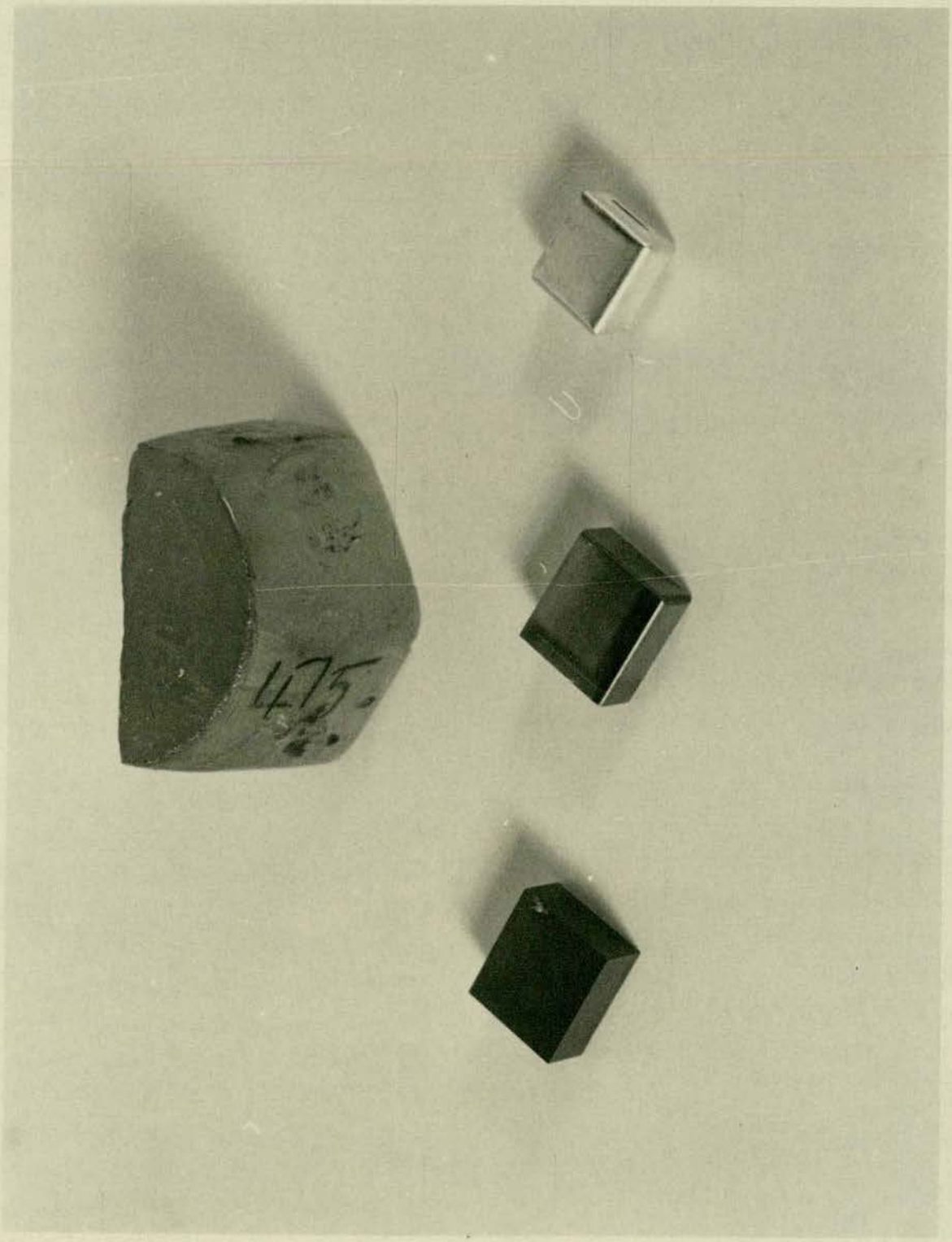

Fig.6.1

Values of Q_o in the range 3,500 to 4,000 were recorded for cavities made in this way. Since the method of measuring Q_o involves measuring the apparent Q_o at critical coupling and doubling this, Q_o cannot be measured for the finally adjusted cavities but it was assumed that these would have Q_o's of the same order.

6.2 Maser Cavity

The maser crystal dimensions were originally designed to be similar to those of Maiman and Reitbock as shown on p.104 referring to Fig. 6.2. With the crystal cut at the angle shown these are the minimum dimensions which will support resonances at the required pump and signal frequencies. The modes are TE_{101} at X-band for the signal frequency and TE_{103} at K-band for the pump. The appropriate value of the dielectric constant, ϵ_θ, for an E vector at angle θ to the c-axis is given by the following equation (which is derived from the tensor ellipsoid of ϵ):

$$\frac{1}{\epsilon_\theta^2} = \frac{\cos^2\theta}{\epsilon_{||}^2} + \frac{\sin^2\theta}{\epsilon_\perp^2}$$

$\epsilon_{||}$ and $\epsilon_\perp$ are the values of ϵ parallel and perpendicular to the c-axis. For the configuration shown in Fig. 6.2 the dielectric constant for the signal mode is ϵ_θ and that for the pump mode is simply $\epsilon_\perp$. Using the accepted values of 11·53 and 9·53 for $\epsilon_{||}$ and $\epsilon_\perp$ respectively gives $\epsilon_{54044} = 10{\cdot}1$.

$$\nu_s = \frac{c_o}{2\sqrt{\epsilon_\theta}}\left(\frac{1}{a^2} + \frac{1}{c^2}\right) \quad (c_o = \text{velocity of light in vacuum})$$

and for the pump,

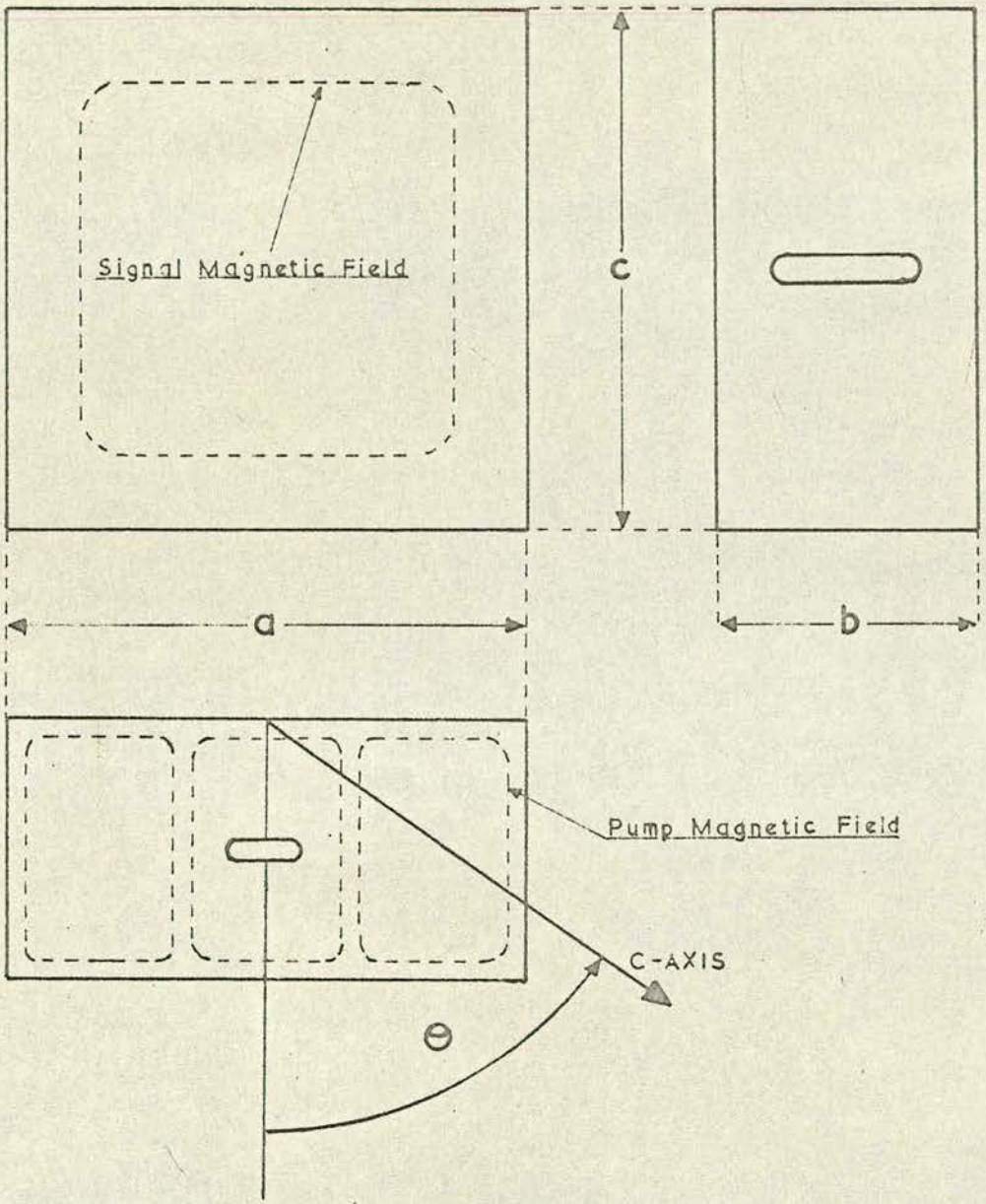

Maser Cavity Configuration

Fig.6.2

$$\nu_p = \frac{c_0}{2\sqrt{\epsilon_\perp}}\left(\frac{1}{b^2} + \frac{3^2}{c^2}\right)$$

It will be seen that each of the modes is labelled as if the corresponding coupling slot was parallel to the direction corresponding to the first index in the expression $TE_{\ell mn}$. These modes are chosen with their E-vectors at right angles to one another to prevent coupling of the pump power into the signal waveguide. In view of the small size of the crystals the pump power is introduced through a side face of the crystal.

The above expressions for ν_s and ν_p leave one dimension arbitrary and it is convenient to make a = c which also maximises the Q_0 for the TE_{101} mode.

The original design was for a signal frequency of 9·375 Gc/s with the corresponding pump frequency at 23·57 Gc/s. With the configuration shown in Fig. 6.2 and $\theta = 54^\circ 44'$, the dimensions as calculated are

a = 7·13 mm.

b = 0·41 mm.

c = 7·13 mm.

Calculation of the values to the above number of figures is misleading since there are three separate effects which cannot be calculated.

1. The "rounding-off" at the edges of the crystal required to provide adhesion of the silver coating causes an increase in frequency of from 1% to 3%.

2. The coupling slots lower the frequency by an amount which can be as large as 2% for a cavity which is over-coupled to the input guide.

3. Obviously the cavity must be adjusted for resonance at the correct frequencies at 77°K. Unfortunately the percentage increase in resonant frequency on cooling from room temperature to 77°K is not constant but depends on the size of the coupling slots. It is in the region of 1%.

Adjustment of the cavities can, in the final stages, therefore only be achieved by "cut-and-try" methods.

It was decided to order 4 crystals of concentrations varying from about 0·15% to about 0·6% Cr_2O_3/Al_2O_3. Despite the fact that it was expected that the size could be calculated to within a few percent, it was deemed advisable to order the crystals considerably oversize. A further precaution was to order the crystals rectangular to avoid the risk of confusion of axis direction if two of the dimensions were the same. The specification was as follows:

9·0 x 8·0 x 4·0 mm. c-axis at angle of 55° to the normal to the 9·0 x 8·0 mm. face and in the plane of the 9·0 x 4·0 mm. face.

The crystals were ordered cut because, although experience in cutting crystals from the boule had been obtained, it was felt that the resources of a large concern would produce better results. This assumption proved to be incorrect. The first crystals which were delivered were cut correctly but contained inclusions so large that they could be seen with the naked eye and the promised analyses of chromium content were not supplied. These crystals were replaced but this took about 5 months and

after some difficulty had been experienced in obtaining even approximate agreement with the theoretical calculations it was concluded that the crystals were wrongly cut. It was verified by optical and X-ray analysis and by EPR that the crystals were cut with the c-axis at 55° to the plane of the 9·0 x 8·0 mm. face, not the normal to this plane as specified. It was unthinkable, however, to wait a further 5 months to have these crystals replaced. Fortuitously the effective dielectric constant in the relevant direction is greater and hence the crystals were too large rather than too small. It was therefore decided to change the cavity dimensions to make use of these crystals. It was impossible to retain the feature of equal a and c dimensions because the c dimension also affects the K-band resonance. Since the c-axis is in the correct plane (perpendicular to the E-vector for the pump resonance) the dimensions for the pump resonance are unchanged. The value of ϵ_θ corresponding to $\theta = 35°6'$ is 10·55 and, putting this into the expression for ν_s, it is found that, with a = 7·15, c should be reduced to 6·84 mm.

The analyses provided with the crystals showed that the concentrations were 0·15, 0·20, 0·26 and 0·46% Cr_2O_3 in Al_2O_3. It is unfortunate that such a large gap should exist between the 0·26 and 0·46 concentrations. This could not have been avoided without considerable expense since the crystals cannot be grown with exactly specified concentration and the only method of obtaining crystals of closely specified concentration is by growing them with approximately the desired concentration

until one close enough to the required specification is obtained. Since the 4 which were obtained by specifying approximately the concentration cost £150 each it was impracticable to demand closer tolerances on the concentration.

Had the crystals arrived to specification and within the originally quoted order time the approach would have been to cut the crystal of lowest concentration to exact size first and thus to determine fairly accurately the required size for the other three. The intention was to have eventually four maser cavities each operating as a single cavity maser, from which the parameter $|Q_m|$ could be measured for each and the crystal exhibiting the strongest maser action chosen. The line width would then have been measured for this crystal after which the crystal would have been replated with smaller coupling slots and adjusted for two-cavity operation. This would permit calculation of all the parameters involved and allow detailed comparison of the experimental results and the theory. It is an unfortunate consequence of the weaker maser action at 77°K that the optimum value of the coupling parameter "k" is very much smaller ($\sim 0{\cdot}2$) than at 4·2°K (~ 2). This means that the slot between the maser cavity and the coupling cavity must be so small that if the guide is terminated by the maser cavity alone, the maser is undercoupled to such an extent that it can only be operated as an oscillator. As a result of this the operating frequency of the two-cavity maser would have to be higher than that of the single cavity maser. This leads to the further complication that the cavity would have to be lapped

to bring the K-band pump resonance to the corresponding frequency. Due to the delay caused by the wrong orientation of the crystals, however, it was necessary to confine attention to one crystal only and the 0·26% crystal was chosen. Furthermore with the alteration in signal frequency dimension "c" while endeavouring to keep the K-band resonant frequency constant the signal frequency was higher than originally intended before suitable resonances corresponding to the same d.c. magnetic field were obtained and it was decided to proceed directly to two-cavity operation. The mode configuration of the maser cavity is as shown in Fig. 6.2 but θ is now $35^{\circ}6'$ which makes the relevant value of the dielectric constant $\epsilon_{35^{\circ}6'} = 10{\cdot}55$. The dimensions are as follows:

$$a = 0{\cdot}28" = 7{\cdot}11 \text{ mm.}$$

$$b = 0{\cdot}154" = 3{\cdot}91 \text{ mm.}$$

$$c = 0{\cdot}253" = 6{\cdot}43 \text{ mm.}$$

The values of the resonant frequencies calculated from these dimensions and the values observed experimentally are:

	calculated	observed (room temperature)	observed ($77^{\circ}K$)
ν_s (Gc/s)	9·68	-	9·70
ν_{fl} (Gc/s)	23·97	23·98	24·14

The X-band coupling slot is so small that it is difficult to observe the resonance at room temperature.

The size of the K-band coupling slot is 2 mm × 0·4 mm.

6.3 Coupling Cavity

It was originally intended to use polycrystalline alumina for the coupling cavity since this material is isotropic and has a dielectric constant of the same order as the ruby itself. This was the material used by Kyhl et al.[48] in the two-cavity reactance compensated maser discussed in Chapter 5. Such samples of polycrystalline alumina as were tested however, were not suitable for plating in the manner used for the ruby crystals. These samples could only be polished to a limited extent, beyond which the finish could not be improved. Kyhl et al. used fabricated cavities and therefore the Q_o was not dependent on the surface finish of the dielectric material. It would thus appear that for this application the best material would be single crystal undoped Al_2O_3. This material, however, is expensive and since several ruby crystals were available which were unsuitable for use in the active cavity (for a variety of reasons) it was decided to use one of these for the passive coupling cavity. Care must obviously be taken to ensure that the crystal is not so oriented relative to the d.c. magnetic field that an absorptive paramagnetic resonance occurs which would constitute a source of loss in the maser. Since the angular spread of the absorption lines present in ruby of the concentration being used is limited this condition can be readily satisfied.

As decided previously the coupling cavity is operated in the same mode as the signal resonance of the maser cavity, i.e. TE_{101}. For the orientation used, $\theta = 79^\circ$ and $\epsilon_\theta = 9{\cdot}58$. The

final dimensions are as follows:

"a" = 0·266" = 6·75 mm.

"b" = 0·156" = 3·96 mm.

"c" = 0·287" = 7·29 mm.

The front coupling slot which represents the ideal transformer in the lumped circuit representation has dimensions 3·5 mm x 0·3 mm. The resonant frequencies of this cavity at room temperature and 77°K are recorded below but it should be noted that neither of the two cases quoted corresponds directly to the loading effect of the maser cavity.

	calculated	observed (room temperature)	observed (77°K)
second slot open	9·72	9·615	9·704
second slot covered		9·611	9·698

For this cavity the observed frequencies are in all cases less than the calculated one due to the large coupling slot. This predominates over the effect of rounding off the crystal corners and the cooling to 77°K both of which tend to increase the resonant frequency.

6.4 Adjustment of Coupling Slots

The final adjustment of the resonant frequencies of the two cavities is effected by slight variations in the coupling slot sizes. This also affects the gain and the bandwidth of

the maser. The coupling between the passive coupling cavity and the input waveguide governs the gain (in conjunction with $|Q_m|$) and the coupling between the two cavities (described by the coupling parameter k) determines the bandwidth and the shape of the response curve.

At first, attempts were made to photo-etch the slots but this proved to be extremely difficult since available photo-resists do not protect against etchants strong enough for silver. These attempts were abandoned at a fairly early stage when it was realised that even if perfected, photo-etching is a rather cumbersome method since the desired size of the slot is not known and this method does not lend itself well to adjustment of the slots.

Eventually it was found that satisfactory results could be obtained simply by painting the silver round the slots with a fine brush. Small reductions in slot size can readily be made under a low power microscope but enlarging the slot size has to be done by scraping the silver away with a sharp scriber and then etching very carefully with nitric acid to remove any silver remaining. This frequently resulted in rather too much coming off and the slot size having to be reduced again. This was avoided as much as possible by endeavouring always to be adjusting down in size rather than up.

The most troublesome feature in the adjustment of the parameter k is that altering the size of the common slot does not have the same effect on the resonant frequency of both cavities. This slot is the only X-band slot in the maser

cavity and therefore even small changes in the slot size shift the frequency by an amount large compared with the small shift in the frequency of the coupling cavity which is already heavily loaded by the large slot coupling it to the guide.

6.5 The Tapered Waveguide Sections

In order to couple efficiently into these small cavities it is necessary to reduce the dimensions of the input waveguides to such an extent that they are beyond cut-off unless they are dielectric-loaded. The most suitable material for this loading is polycrystalline sapphire or alumina (Al_2O_3) and the load is tapered so that the effective width of the guide is approximately constant. For low VSWR, tapered transitions in waveguides should, if possible, be "long" i.e. about 10 guide wavelengths. This would require, however, that the X-band "a" dimension taper be at least 20 cm long and the "b" dimension taper longer still, resulting in an X-band transition more than 50 cms long. This is impracticably long and thus a "short" transition must be used.

For a short taper the best dimensions must be determined empirically which is extremely difficult to do since to assess accurately the VSWR of the taper a matched load in the reduced guide section would be required. This would, of course, also have to be dielectric-loaded to keep it above cut-off. Furthermore, to determine the VSWR of this load would require a slotted line in the reduced (and hence dielectric-loaded) section. It was therefore decided to accept the dimensions of Reitbock for the short tapers he used of which he was kind

enough to supply detailed drawings. The dimensions used are the same as Reitbock's but the mechanical construction has been altered to allow the X and K-band guides to slide relative to one another in order that the position of the K-band coupling slot relative to the end of the X-band guide could be altered to permit use of one or two cavities.

The waveguide material in Reitbock's case was cupro-nickel which was used to cut down the heat flow from the room temperature end of the guide. The use of this material for cryogenic work is standard practice but it was not expedient to have these rather awkward guide sections made in this material and so they were made from brass. This would have one of two possible effects: either the guide is cooled satisfactorily but the refrigerant boils off more rapidly or the guide simply does not attain the temperature of the refrigerant. For the laboratory system under consideration the first of these is acceptable since the refrigerant may readily be topped up. To verify that the first occurred a thermocouple was placed inside the X-band waveguide as near the cavity position as possible and it was verified that the reading on this was the same as that of the thermocouple itself immersed in the liquid nitrogen.

The broad wall of the K-band guide must be as thin as possible since the coupling slot for the pump power is in this wall. Since the coupling slot is between a dielectric-loaded guide and a ruby-filled cavity it is undesirable that the wall containing the slot should be any thicker than is absolutely

necessary. It was found possible to reduce the thickness of this wall from 40 thousandths of an inch (standard WG20) to about 20 thousandths.

The inside dimensions of the (tapered) waveguide sections are as shown in Fig. 6.3 and the complete maser assembly is shown in Figs. 6.4, 6.5 and 6.6.

In order to facilitate removal for adjustment the crystals are clamped to the end of the X-band waveguide and located by the mount of the brass coupling shim as shown. The aluminium clamp was not part of the original design but was added later to ensure that there is no air-gap between the maser cavity and the K-band guide.

Scale 2:1 (Dimensions in mm.)

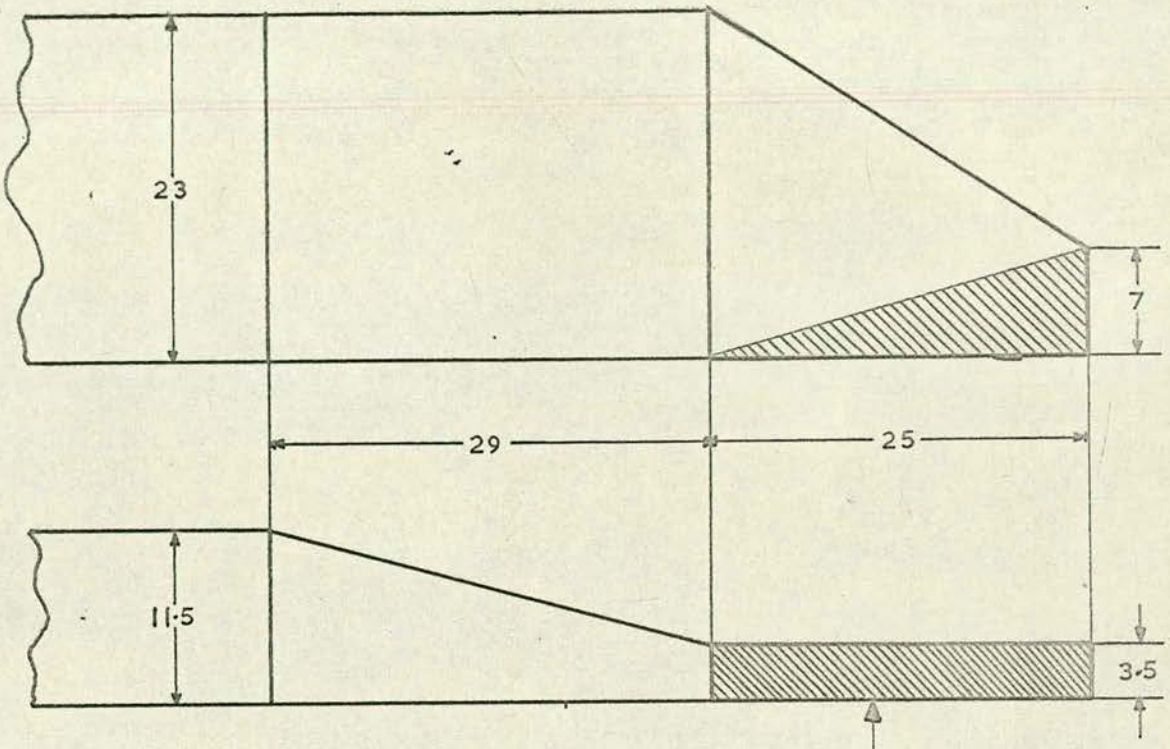

X-band taper (ALUMINA)

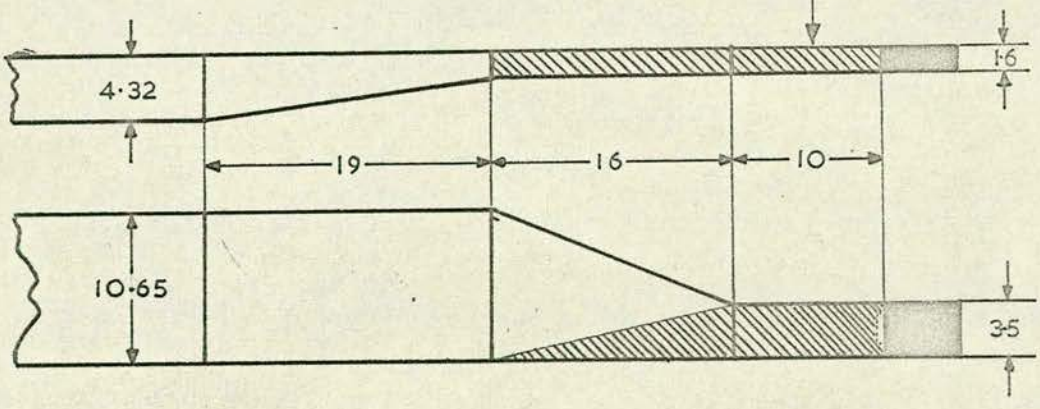

K-band taper

Fig. 6.3

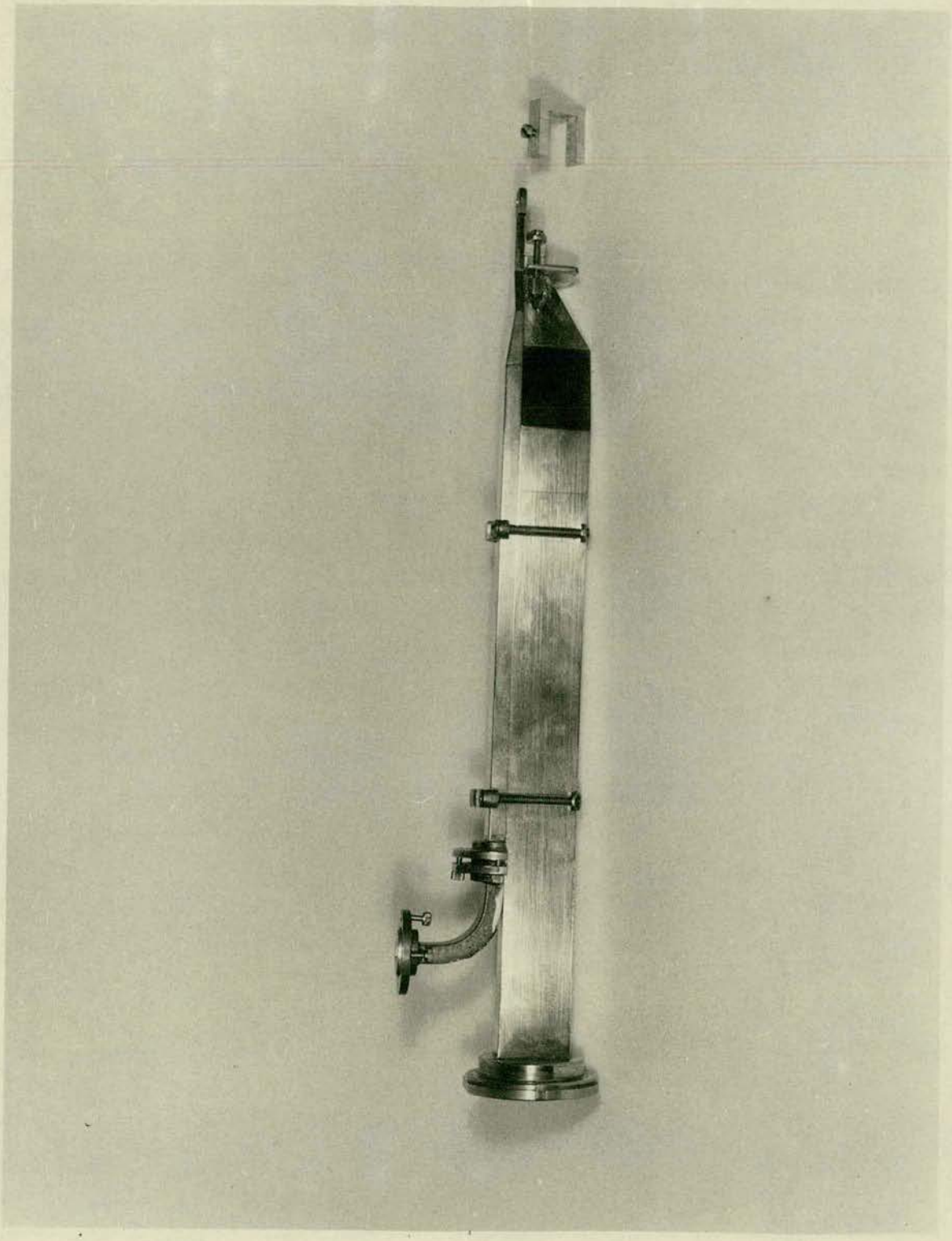

Fig.6.4

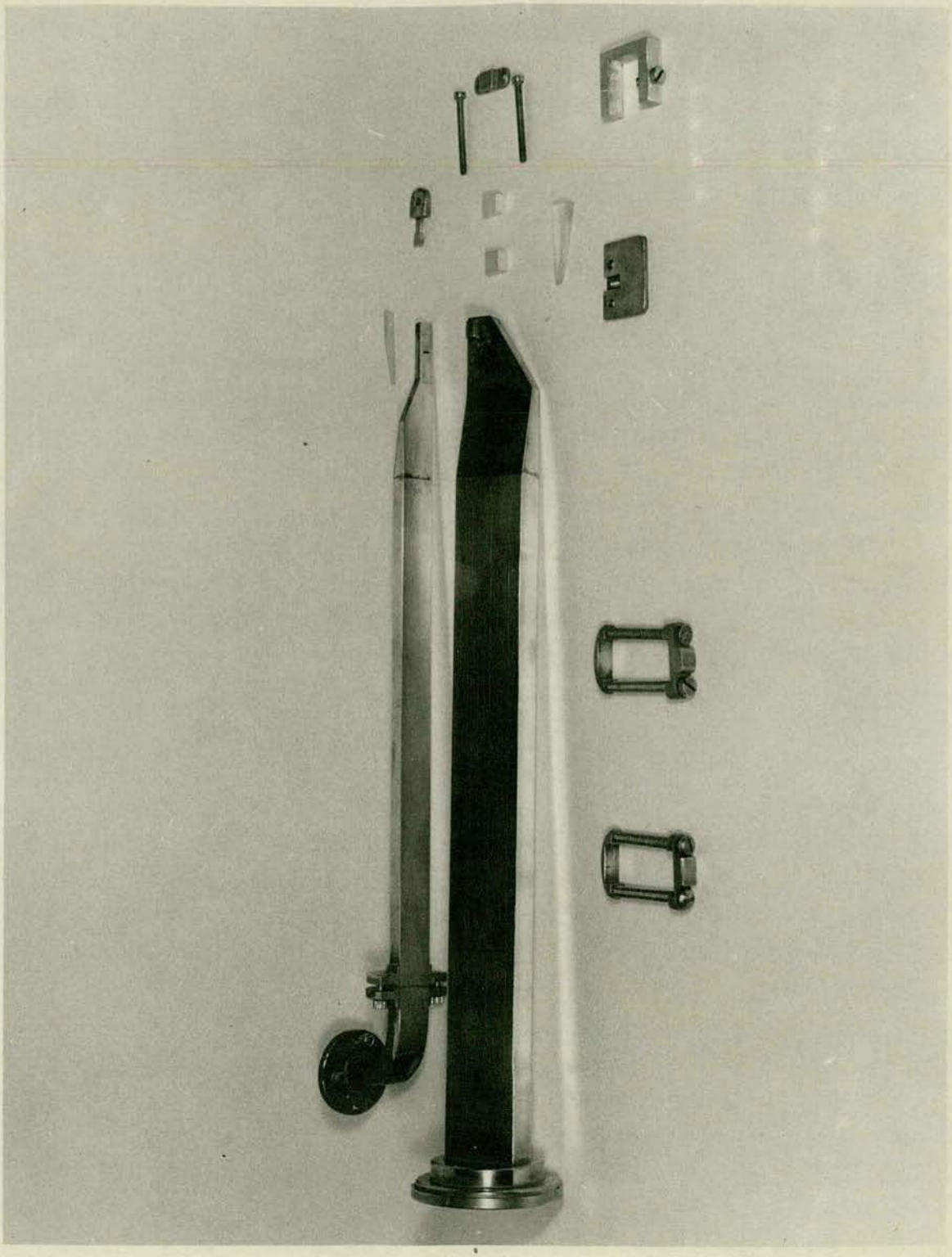

Fig.6.5

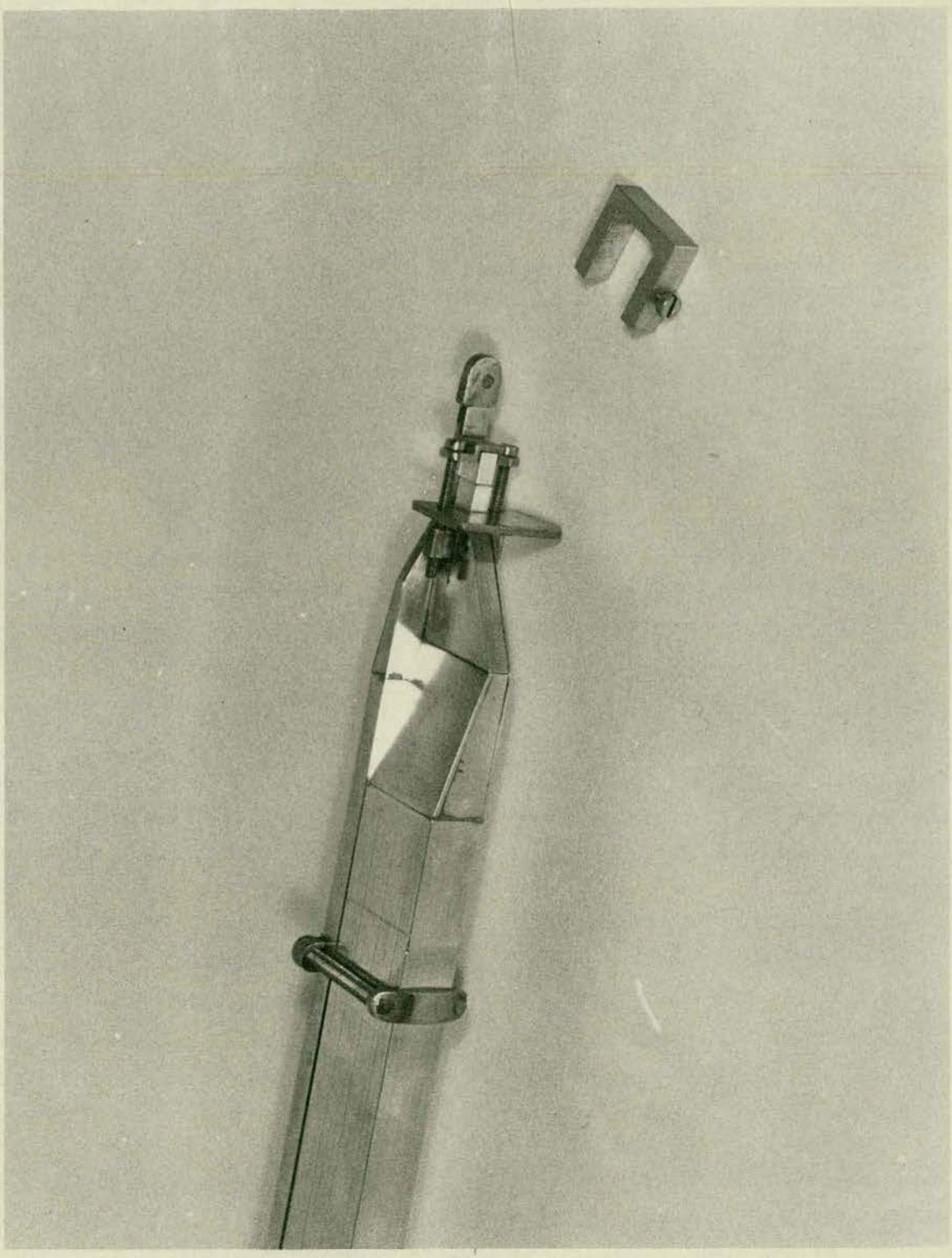

Fig.6.6

CHAPTER SEVEN

Ancillary Equipment

7.1 The d.c. Magnetic Field

It is highly probable that in any "packaged" maser system designed to exploit fully the practical advantages of freedom from helium liquefiers would incorporate a small permanent magnet immersed in the refrigerant. Such magnets can be made to provide the required degree of field homogeneity for small crystals but, as has already been mentioned, with the larger gaps required for larger crystals the weight and cost of the magnet increase rapidly. For the construction of the maser, however, an electromagnet greatly facilitates matters since the field can be readily adjusted.

In order to determine the required degree of homogeneity it is necessary to consider the variation of the signal frequency ν_s with the d.c. field H_0. From the solution of the secular equation quoted in Chapter 3, it follows that

$$\nu_s = 2(\nu_D^2 + \tfrac{5}{4}\nu_0^2 - \nu_0\sqrt{3\nu_D^2 + \nu_0^2})^{\frac{1}{2}}$$

where, as before, ν_D is a constant = 5·79 Gc/s.

and $\nu_0 = \frac{2\beta}{h} H_0 = 11{\cdot}55$ for $H_0 = 4{\cdot}13$ (corresponding to $\nu_s = 9{\cdot}7$ Gc/s).

Differentiating this expression, for ν_s,

$$\frac{d\nu_s}{d\nu_0} = \frac{2}{\nu_s}\left(\tfrac{5}{2}\nu_0 - \frac{3\nu_D^2 + 2\nu_0^2}{\sqrt{3\nu_D^2 + \nu_0^2}}\right)$$

For the values of ν_D and ν_o given above, which are those relevant to the maser under discussion, this expression is very close to unity.

From this, therefore,

$$\frac{d\nu_s}{dH_o} \approx \frac{2\beta}{h}$$

and $$\Delta\nu_s = \frac{2\beta}{h}(\Delta H_o) = 3 \times 10^6 (\Delta H_o)$$

It is required to ensure that the broadening of the maser line due to the inhomogeneity of the magnetic field over the volume of the crystal is negligible compared with the line width due to other effects present. Since the line width of the maser material is expected to be of the order of 150 Mc/s, variation of ν_s by about 1·5 Mc/s corresponds to a line broadening effect due to field inhomogeneity of about 1% of that due to other causes. From the above it is seen that this would be produced by a field variation of the order of 0·5 gauss over the volume of the crystal. With $H_o \sim 4$ Kgauss this means that the homogeneity required would be 1 part in 10^4. The size of magnet required to produce this homogeneity is, of course, increased by the necessity to produce it at the centre of a gap large enough to accommodate the dewar flask containing the maser.

To accommodate the waveguide system described in the previous chapter a dewar with an outside diameter of just under 2½ inches was required. The magnet used was a Newport Instruments 7" Type E Electromagnet fitted with special shims. This magnet, with a gap of 2½ inches, provides a volume

¾ in. × ¾ in. × ¾ in. over which the homogeneity is better than 1 part in 10^5. This volume amply accommodates the maser crystal and this homogeneity corresponds to only about 0·1% of the line width of the material. The power supply (Type C155) has a stability of 1 part in 10^5 which ensures that the stability of H_0 is of the same order.

This magnet specification ensures that it may be confidently assumed that the maser performance is not, in practice, affected by the inhomogeneity of the magnetic field H_0.

7.2 Pump Frequency Equipment (K-band)

At various stages in the alignment and operation of the maser, three different K-band circuits were used. Fig. 7.1 shows a simple EPR bridge circuit, Fig. 7.2 shows a low-power swept frequency circuit and Fig. 7.3 shows the high power maser pump circuit.

7.2.1 K-band Bridge Circuit

To investigate the paramagnetic resonance spectrum at K-band the circuit of Fig. 7.1 was used. This is a simple form of the standard bridge circuits used in EPR spectrometers. The low power klystron (EMI:9602A) is used at a fixed frequency and the d.c. magnetic field has a low amplitude 50 c/s modulation applied to it by means of a pair of Helmholtz coils. The 3-stub tuner is adjusted for minimum output from the crystal detector with no applied field. The change in absorption caused by the paramagnetic resonance produces a signal which is detected and displayed on the oscilloscope.

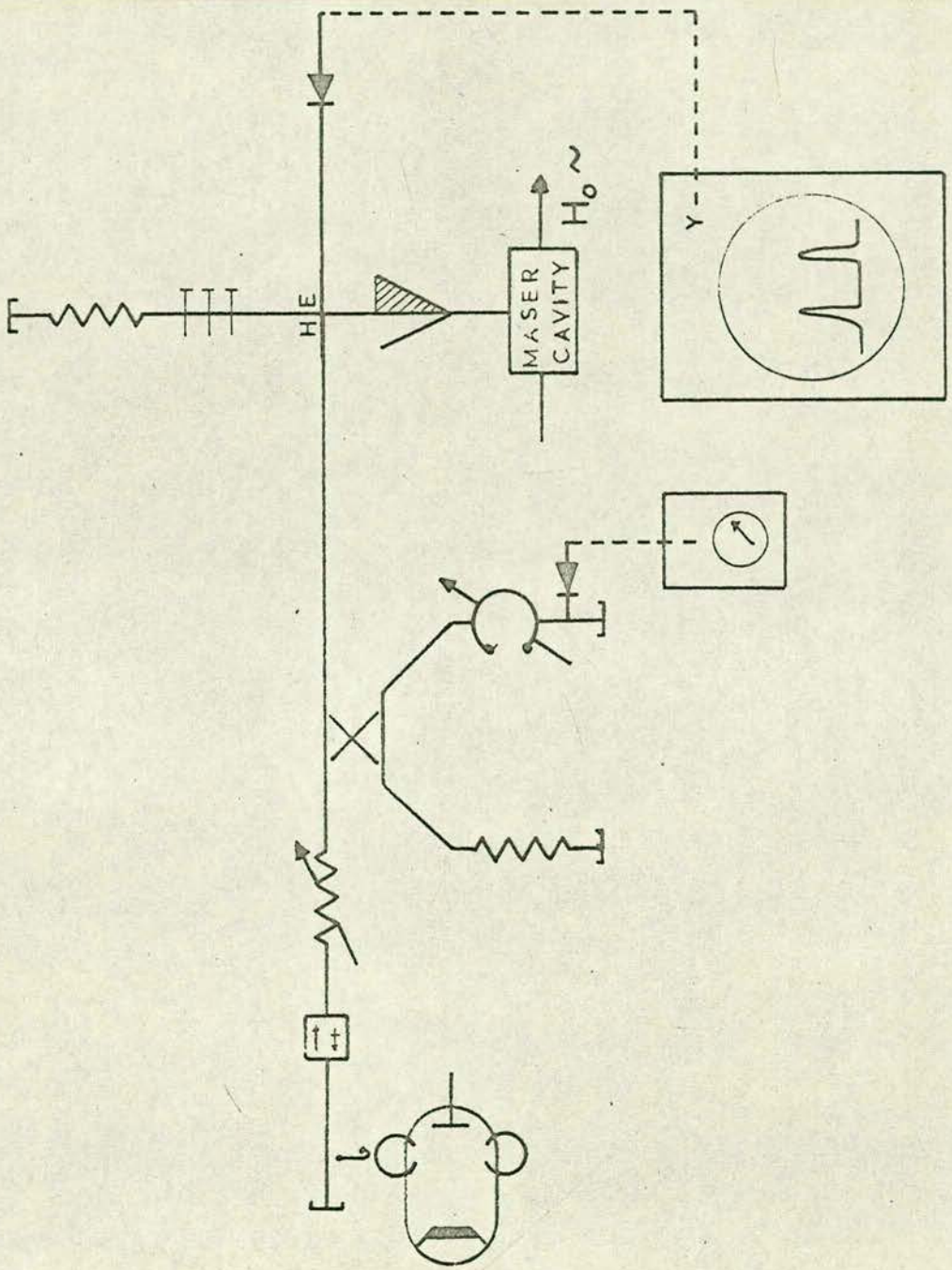

Fig.7.1 K-band Bridge Circuit

Fig. 7.1

The most sensitive bridges are actually operated slightly unbalanced for maximum sensitivity but the balanced bridge proved quite adequate for this application. The bridge circuit was useful for checking the orientation of the crystals particularly when this was necessary to verify the suspicion that they were wrongly cut. This display is also ideal for setting the magnetic field to the $\theta = 54^{\circ}44'$ double pump angle since the resonance peaks corresponding to the 1-3 and 2-4 transitions can be seen to move into coincidence as the magnet is rotated to the correct angle.

7.2.2 Low-Power Swept-Frequency K-band Circuit

The low-power circuit shown in Fig. 7.2 uses a conventional reflex klystron (EMI:R9602A) which is frequency-swept by applying the time-base voltage of an oscilloscope to the reflector. The power reflected from the cavity is rectified by the crystal detector and the output applied to the oscilloscope. This gives a display of amplitude v. frequency which enables investigation of cavity resonances. Once the cavity resonance has been adjusted for critical coupling at the required frequency the high power pump circuit may be applied. To assist in the final stages of this adjustment a 3 stub tuner is included.

The adjustment of the cavity for critical coupling assumes that the available pump power is sufficient to saturate the pump transitions. With the magnetic field on and a low pump power applied, paramagnetic absorption causes a loss in the cavity which becomes undercoupled as a result. As the power

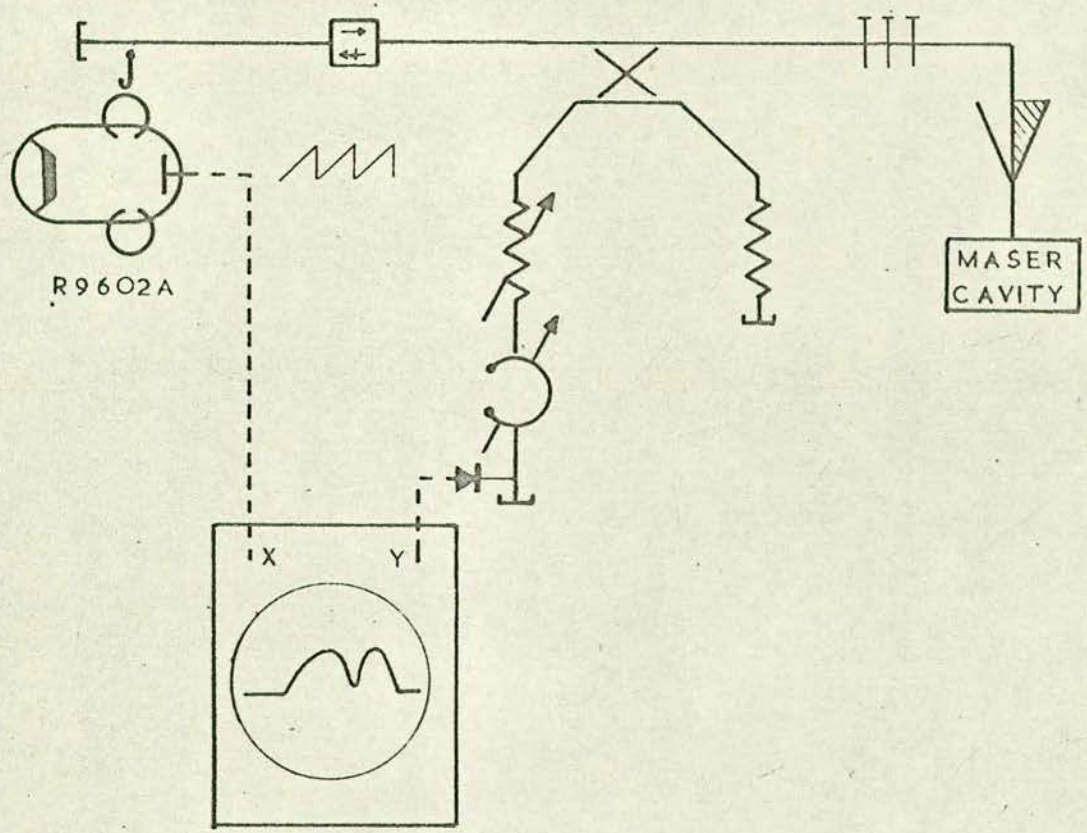

Fig.7.2: K-band Swept-Frequency Circuit

Fig.7.2

is increased, however, the populations of the upper and lower levels of the pump transitions approach one another, the amount of the extra absorptive loss decreases and the degree of undercoupling is reduced. Finally, when the applied power is sufficient to produce saturation, the maser material becomes "transparent" at the pump frequency and the cavity returns to its critically-coupled condition. Obviously, this is the required situation for maximum performance.

If a maser has to be operated with insufficient pump power to produce saturation, however, then to make the most efficient use of the available power the cavity should be adjusted so as to be overcoupled (with the magnetic field off) to the extent that when the paramagnetic absorption is present the effect of the associated loss and the cavity together produce a perfect match. This ensures that none of the power is reflected. Clearly the adjustment for optimum operation is more difficult in this case than it is when the pump power is adequate for saturation.

7.2.3 High-Power K-band Pump Circuit

The actual circuit used to pump the maser is shown in Fig. 7.3.

The main pump source for this maser is an Elliott 12TFK2 floating-drift-velocity klystron with a rated output of 10 watts C.W. Actually both tubes of this type which were used were capable of producing 15 watts. This tube was chosen to ensure that ample pump power would be available. The 12TFK2 is rather heavy (11 lbs.) and its power requirements are high

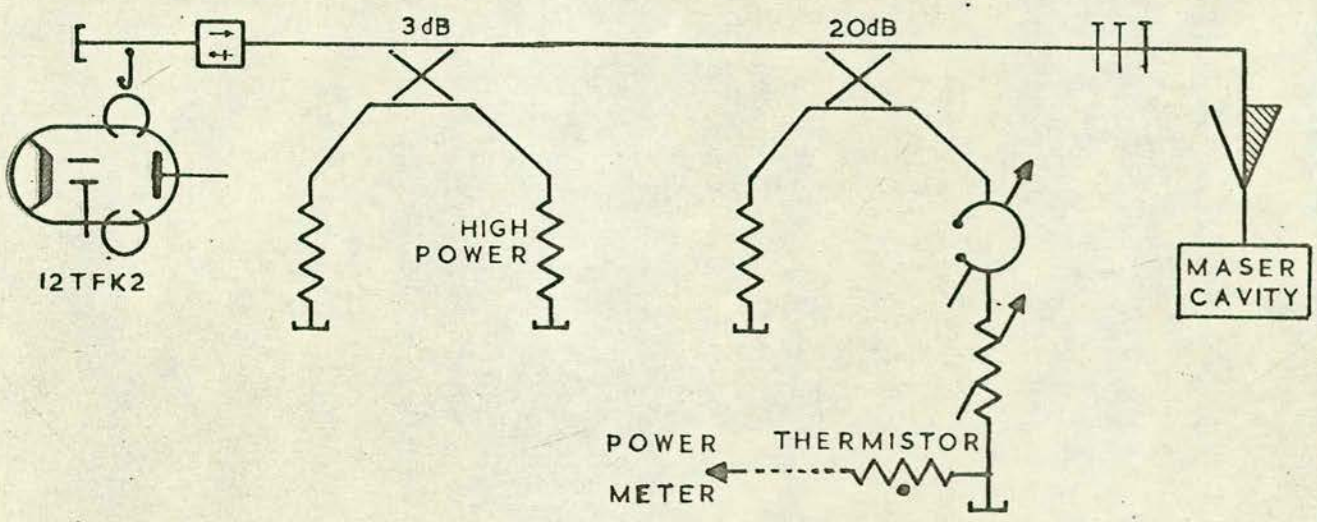

Fig.7.3 High-Power Pump Circuit

(4 kV, ~100 mA). It also requires water cooling at the rate of 1 litre/min.

It is important that this tube never looks into a mismatch greater than 1·2:1. The isolator (FXR type K157A) shown is of the conventional E-plane ferrite slab type. The manufacturer's specification states that the maximum power for this component is 10 watts CW with a load VSWR of 5. This means that the ferrite should be able to absorb up to about 8 watts. This seemed rather a high power density and since the full power of the tube was never required it was always operated into a 3 dB coupler with a high-power load on one output arm. Even if the guide is short circuited completely this should be amply sufficient to ensure that both the klystron and the isolator are protected.

It was originally intended that this circuit should include a variable attenuator to allow continuous control of the incident pump power. Such a component rated at 10 watts was purchased but when this was examined it proved to be simply a conventional low-power attenuator which the manufacturer had uprated. Attempts were made to use this component after the original vane had been replaced by one of cement and asbestos. This material was kindly provided by the Royal Radar Establishment and it was recommended because it retains its attenuating properties even when heated to several hundred degrees centigrade. The disadvantage of this material is that it is very brittle and cannot be drilled readily. Sticking the vane to the mounting rods with araldite allowed

the attenuator to be used but only over a limited range since the araldite would not withstand the heat if too much power was absorbed by the vane.

Eventually, however, this attenuator was abandoned in favour of varying the power output of the tube by adjustment of the voltage on the focus electrode. This had not been done earlier firstly because it was felt that this might damage the tube and secondly because it was thought that this might tend to alter the frequency as the output power was varied. Since being assured by the manufacturer, however, that this was a proper method of varying the power output it has been used and it has been found that the frequency remains constant.

The pump power input to the maser is monitored with a thermistor in the side arm of a 20 dB coupler.

7.3 Signal-Frequency (X-band) Equipment

A bridge circuit and method similar to those described in Section 7.2.1 were used for EPR investigation of the crystal axis orientation at X-band.

The main X-band circuit is shown in Fig. 7.4.

As a preamplifier for inclusion in a system the "maser amplifier" would have to include the cavities, the waveguide transitions, the circulator and the low pass filter. The remainder of the equipment is associated with measurement of the gain and bandwidth. ~~This component~~ The filter (Hewlett Packard: 362A) has an insertion loss of less than 1 dB over the pass-band (8·2-12·4 Gc/s) and provides at least 40 dB rejection over the stop band (16-37·5 Gc/s). The detection system is the simplest

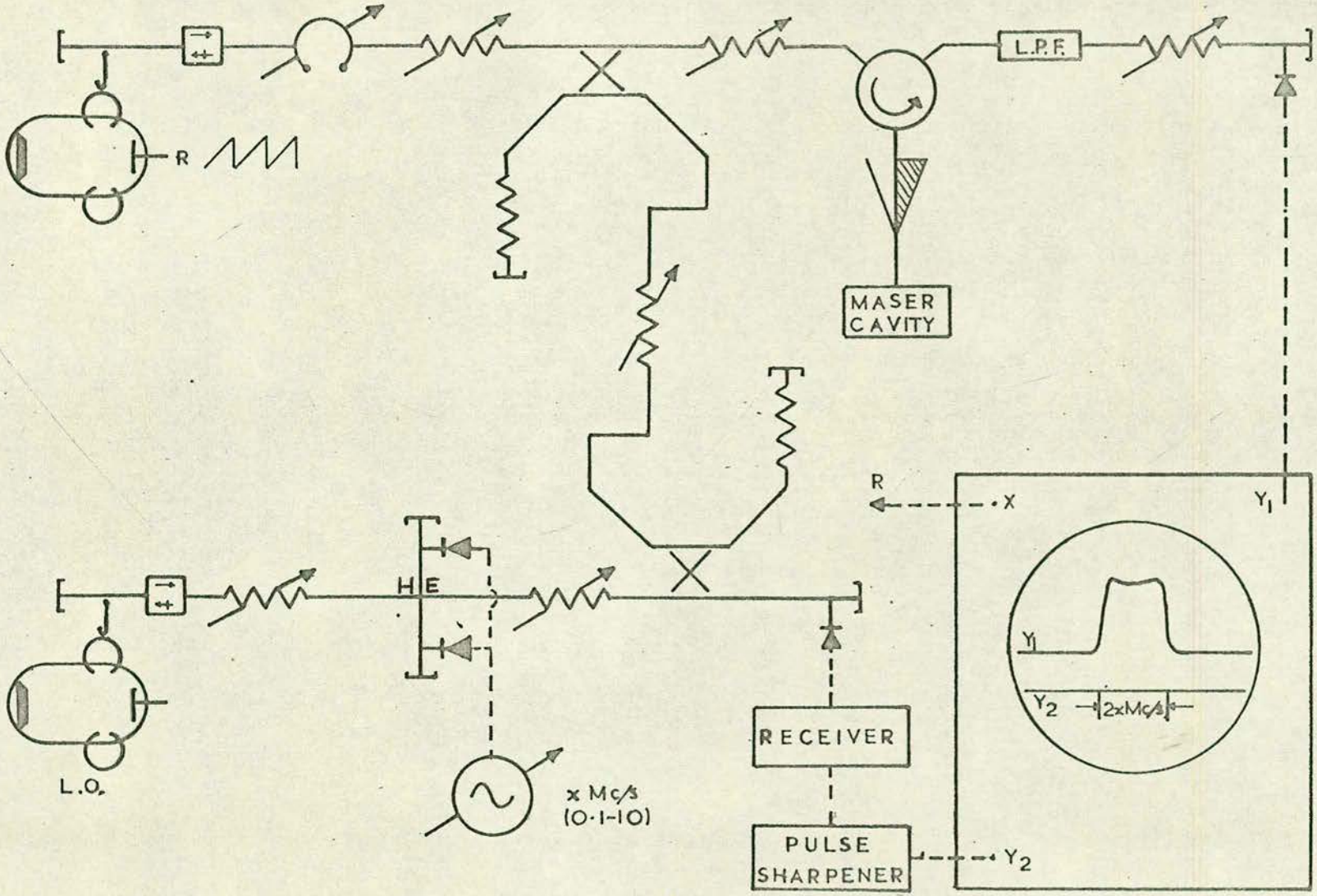

Fig.7.4 X-band Circuit

possible (i.e. crystal-video) as is essential for setting up the maser. The klystron frequency is swept by the time-base of the oscilloscope as described in Section 7.2.2 above. Unfortunately, applying a linear time-base voltage to the reflector of a reflex klystron does not produce a linear frequency sweep. It is therefore necessary to provide "markers" on this sweep between which there is a known and variable frequency interval. This is done by coupling off a fraction of the swept signal which is to be applied to the maser and mixing it with a fixed local oscillator (L.O.) signal (frequency ν_{LO}) which differs from the mid-band frequency of the maser by the frequency of the receiver. This signal has first been mixed with the signal from a variable frequency oscillator covering the range 0·1-10 Mc/s (frequency ν_{HF}). This mixing is done in a balanced mixer to suppress the L.O. frequency and provide two components, $\nu_{LO} \pm \nu_{HF}$. The difference frequency between the swept signal and each component passes along the co-axial line to the receiver where, at the point in the sweep where the difference frequency is that to which the receiver is tuned a signal is produced. This results in two signals at times on the frequency sweep which are separated by an amount corresponding to $2\nu_{HF}$. These signals are passed through a simple pulse-sharpener and applied to the Y_2 input of the oscilloscope. This provides a display of the type shown in Fig. 7.4 where the position of the markers relative to the upper trace may be altered by varying either the frequency of the L.O. (coarse control) or of the receiver

(fine control) and their spacing may be altered by varying ν_{HF}. This provides a method of measuring bandwidth which does not depend on any assumptions regarding the frequency vs. reflector voltage characteristic of the swept-frequency klystron.

7.3.1 Maser Gain Measurement

The gain of the maser is determined by measuring the amount of attenuation it is necessary to insert after the maser to bring the signal level back to where it would be if the maser amplifier was replaced by a short circuit. It seems to be accepted to measure the maser gain, even of a single cavity device, by taking the signal level in the "pump off-magnetic field off" condition as that which represents the effect of replacing the maser by a short circuit (e.g. Genner and Plant This, however, shows the gain to be apparently higher than it really is because what is being taken as the input signal level to the maser is actually less than this by an amount corresponding to the losses in the maser cavity. The error which would be introduced by using this assumption with a two-cavity maser is fairly small because, as is shown in Fig. 7.5, the signal (at the mid-band frequency) which is reflected from the maser in the "pump off-magnetic field off" condition is not far below the true input signal level. This error is dependent on how close the cavity resonances are - the closer they are the larger the error. To avoid this error the gain was measured from what was estimated from the shape of the swept klystron mode on either side of the cavity resonances ("pump off-field off" condition). This can be estimated fairly accurately since the

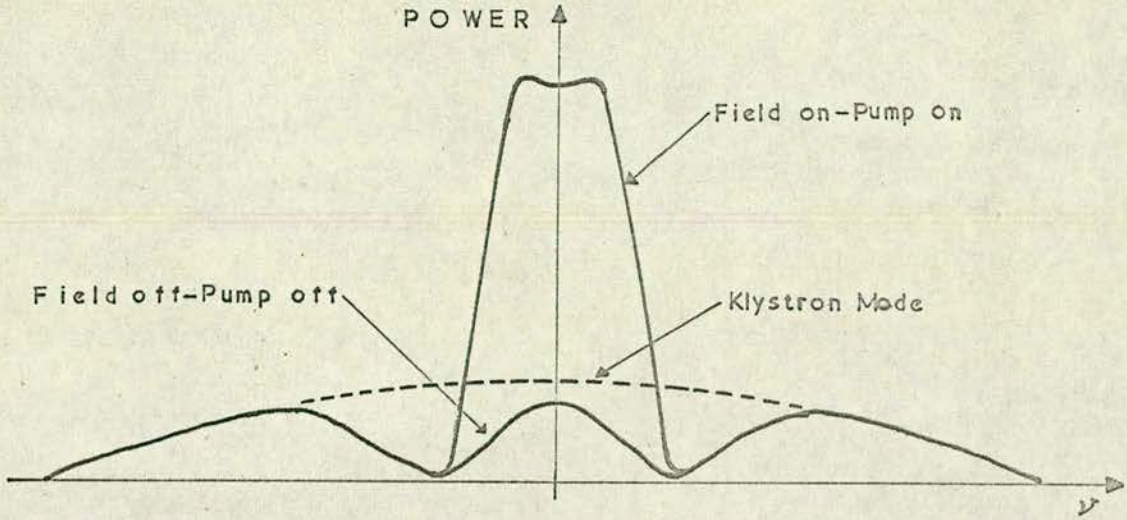

Fig.7.5

klystron mode shape is reasonably flat at the centre. In retrospect, however, it would have been simple and effective to use a waveguide switch between the circulator and the maser to switch between the latter and a short-circuited length of guide. This would permit a more accurate determination of the input signal level.

7.3.2 Maser Bandwidth Measurement

The bandwidth is measured by centering the marker pips and adjusting their separation until they lie on the trace from the maser output at the 3 dB points. The bandwidth is then simply twice the frequency to which the variable frequency oscillator is set. The 3 dB level is first determined by inserting 3 dB between the maser and the detector and positioning the Y_2 trace level with the top of the maser output trace. The 3 dB attenuator is then removed.

Fig. 7.6 is a photograph of the X-band and K-band microwave equipment and Fig. 7.7 is a general photograph of the experimental set-up.

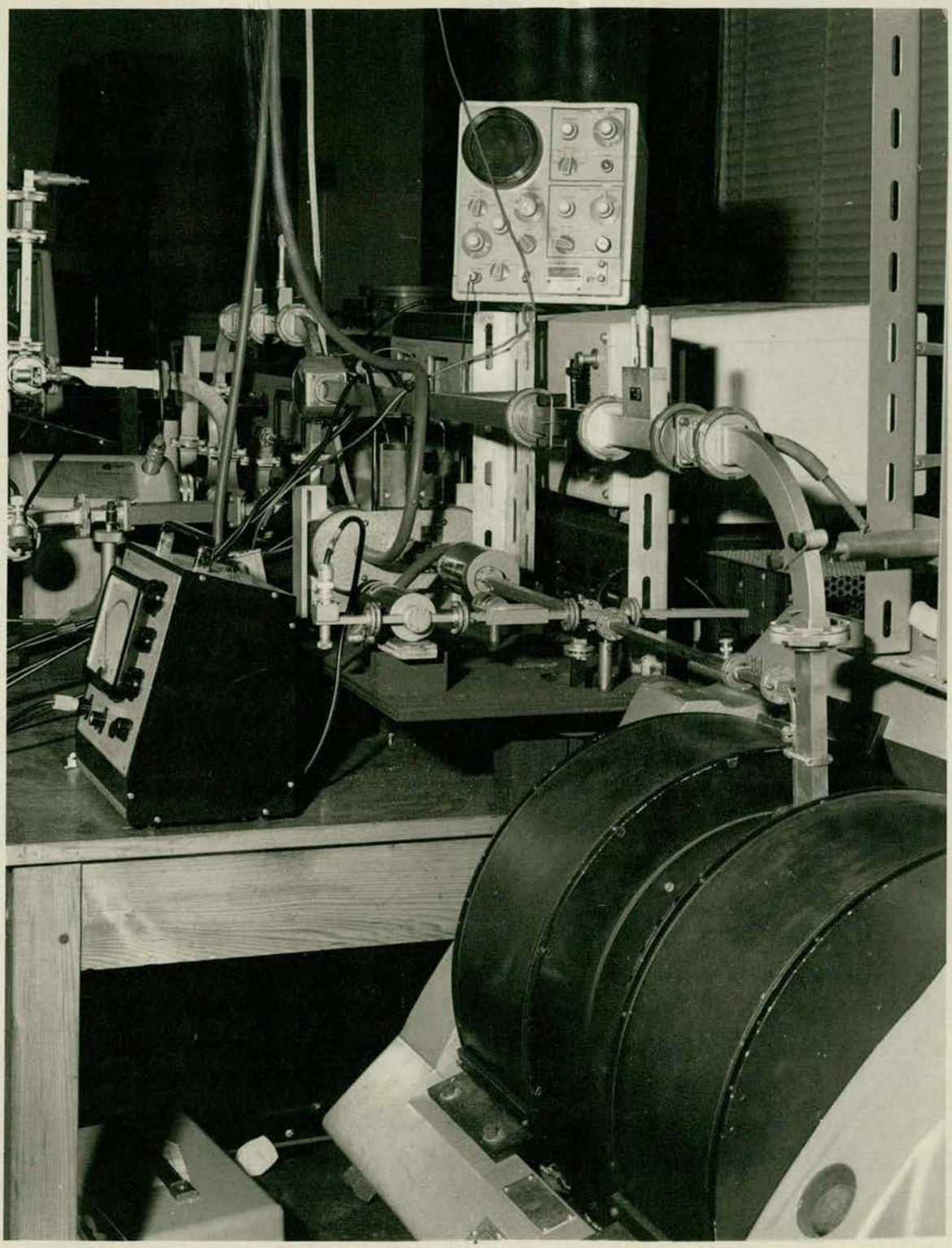

Fig.7.6

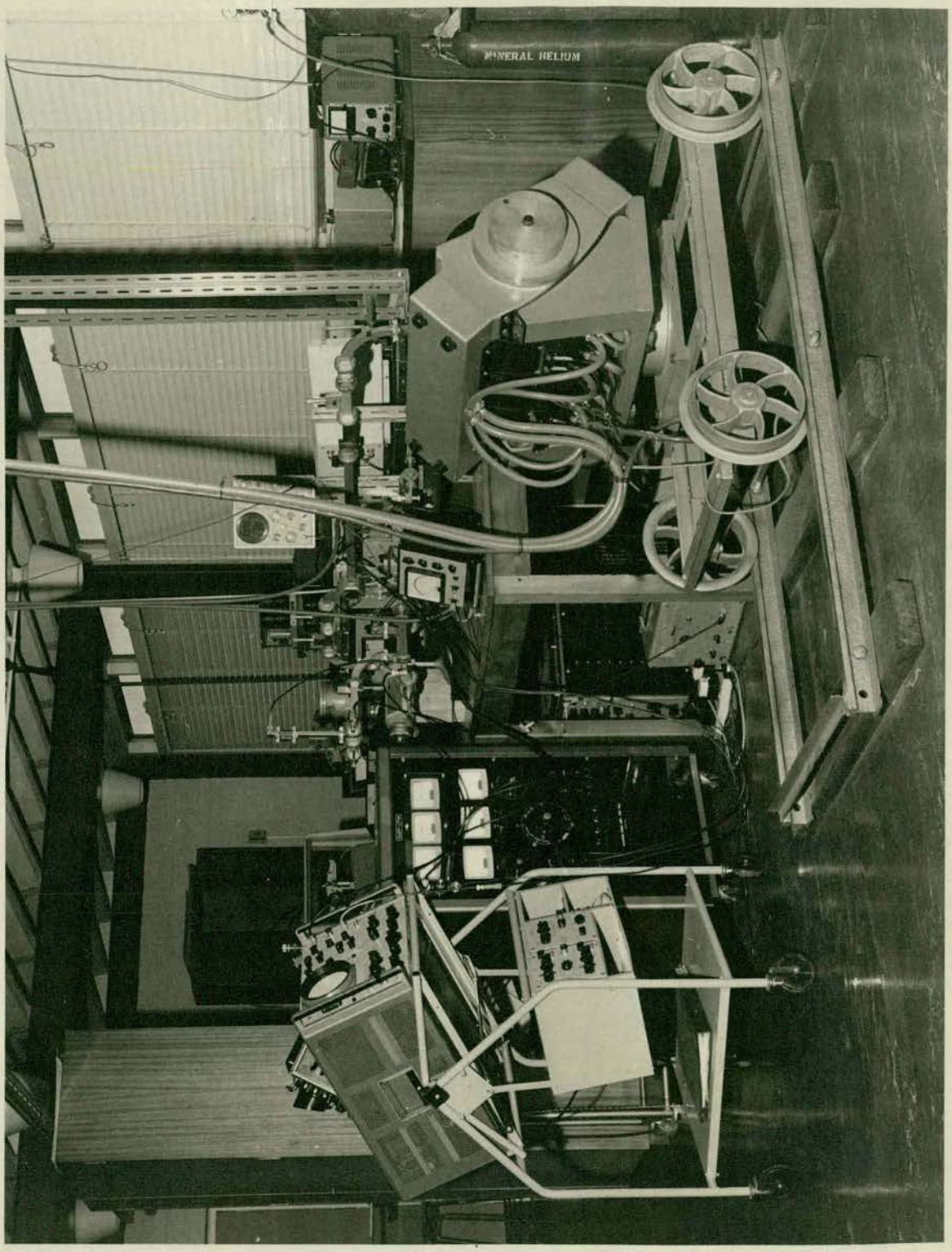

Fig.7.7

CHAPTER EIGHT

Results and Conclusions

8.1 Pump Power

As has been mentioned in the earlier discussion Reitbock and Redhardt[33] reported maser action in ruby at 90°K with only 80 mW of pump power. It was subsequently made clear in Reitbock's thesis[18] that the pump transitions were not saturated but a gain of 13 dB was achieved despite this. It was hoped that in the course of this work it would be possible to determine the optimum chromium concentration and exactly how much pump power was required to pump the minimum size cavity filled with this material. Unfortunately due to the delays involving the crystals it has only been possible to achieve two-cavity maser action with one of the 4 crystals ordered so the intended comparison between the concentrations cannot be made. The crystal concentration chosen was that which, in the light of the careful study made of the available information seemed likely to be the best of those available but it is disappointing that time did not permit experimental comparison of the crystals which had been obtained.

While awaiting the arrival of the replacement crystals one of the earlier samples was used in a single cavity maser and this exhibited gains ~ 10-15 dB with pump powers limited to 250 mW. This power was obtained from the selected EMI R9602 A tube (rated at 60 mW nominal) but at that time it was not possible to change over to the 12TFK2 to investigate how

far from saturation the maser was with the 250 mW. As far as pump power is concerned this was the best result obtained since all the work done on the double cavity maser has required the 12TFK2 supplying powers ~ 4 watts. As has already been explained in Chapter 6 some trouble was experienced in aligning the crystals for X and K-band resonances at the same d.c. magnetic field and, although the cavity is resonant at the pump frequency, the Q of this resonance appears to be low.

From the results on the single cavity maser it would seem that 4 watts is higher than one would expect to be necessary. At the outset of the project it was hoped that it could be shown that saturation could be achieved with a conventional reflex klystron. From the fact that it was not possible to saturate the single cavity maser with 250 mW it seems unlikely that this is so since from a tube of this type an output of 250 mW is as high as can be expected. However, since this project was started, new tubes operating on the same principle as ordinary reflex klystrons but with a design which allows outputs of the order of ½-1 watt have been produced and it would seem that these would be the most suitable tubes for the pumping of a practical liquid-nitrogen-cooled maser. Their power requirements are modest and they are air-cooled. This latter feature is important because, apart from laboratory applications (e.g. low noise EPR work), it is unlikely that in any application for a compact maser it would be convenient to have cooling water supplied. It is felt that if the cavity could be made to resonate at the pump frequency with a good Q,

this should be adequate for saturation but, even if this is not so, it would be possible to operate the device with this power.

8.2 Maser Performance

Before considering the photographs of the various stages in the alignment of the maser the method of aligning the cavities will be briefly considered.

8.2.1 Alignment of the Cavities

The desired effect is to have the two cavities resonant at exactly the same frequency and the splitting of the two resonances of the two-cavity assembly due only to the coupling between them. If the two cavities are resonant at different frequencies, there is very little coupling between them and, the two resonances are observed separately. How close the cavity resonances have to be before they couple is obviously dependent on the size of the mutual coupling slot. If they are far enough apart not to couple appreciably then the maser cavity couples to the guide through the coupling cavity but does not couple to the coupling cavity. Since there is no way of simulating the loading effect of each cavity on the other the alignment can only be done with the two cavities together. With the coupling slots in the cavities so different in size the state of no coupling at all is obvious because one cavity is very much more strongly coupled to the guide than the other. When they begin to couple to any appreciable extent, however, the two resonances begin to look more alike and it is necessary to use the EPR absorption to determine whether or not they are

resonant at exactly the same frequency. As will be shown in the photographs which follow, the EPR absorption will only occur equally in both resonances if the splitting is due entirely to the mutual coupling.

Determination of the starting point was rather difficult since it had not been possible to measure the line width of the material. From the computed data in Chapter 5 it seems that the parameter k may be expected to be of the order of 0·1 for a mid-band gain of 20 dB and 0·2 for a mid-band gain of 17 dB. For the crystal concentration used $\Delta\nu_L$ is expected to be of the order of 150 Mc/s and thus for the 17 dB case it was estimated that the cavity resonance splitting should be about 30 Mc/s. This was therefore taken as the starting point but it was found that the splitting had to be reduced considerably before any appreciable gain could be produced. This may indicate that the line width, $\Delta\nu_L$, is not as large as believed but it is most unlikely that it is less than 100 Mc/s.

8.2.2 Feedback and Probe Coupling to the Maser

In the early stages of alignment when the cavities are resonant at different frequencies, the maser cavity is very weakly coupled to the guide which causes oscillation. It was found that this could be prevented by using a stub mounted at the centre of the broad face of the input waveguide and a phase-shifter between this and the maser. This provides a reflection variable in amplitude and phase which feeds back the output signal to the maser. Obviously besides feeding back the output signal to the maser this stub will feed back

the input signal to the circulator and raise the effective noise temperature of the device. It is interesting to note, however, that with a small probe penetration in many cases the undercoupled maser could be adjusted from oscillation into the region of stable gain.

With much larger probe penetrations (~ half the "b" dimension of the guide) the phase-shifter could be used to tune the resonance associated with the probe across the klystron mode. This produced effects on the bandwidth similar to those expected from the second cavity. Unfortunately the effect on the gain was rather drastic. This will be recognised as being very similar to the resonant coupling plate method used by Cook et al. which was described in Chapter 5. Had time permitted it would have been interesting to make a quantitative comparison between this "tuned probe" method and that based on the addition of the extra cavity. This tuned probe method seems to be rather lossy but there is no doubt that it makes adjustment easier than it is where the size of the mutual coupling slot between the two cavities must be varied.

In view of the limited time available, however, it was necessary to proceed as quickly as possible to the operation of the two-cavity maser. The photographs in the following section are of the maser at various stages in the alignment process. However, the probe and phase-shifter were not required to produce these results.

8.2.3 Photographs Showing the Alignment of the Two-Cavity Maser

Figs. 8.1 to 8.16 show various features of the alignment of the maser. The explanations are interleaved with the photographs and precede the photographs to which they refer. In all photographs the frequency increases from right to left. The mid-band frequency of the two-cavity maser is 9·695 Gc/s ± 5 Mc/s in all cases.

Fig. 8.1 Shows the maser in oscillation. The resonant frequencies of the two cavities are so far apart that there is no interaction between them at all. Because of this the maser cavity is very weakly coupled to the guide and when the pump power is applied the maser oscillates at the resonant frequency of the maser cavity.

Figs. 8.2, 8.3 and 8.4 are all of the same cavity combination.

Fig. 8.2 Shows a split resonance. No magnetic field. No pump power. From the symmetry of the double resonance it is apparent that the splitting is, at least in part, due to the coupling between the cavities.

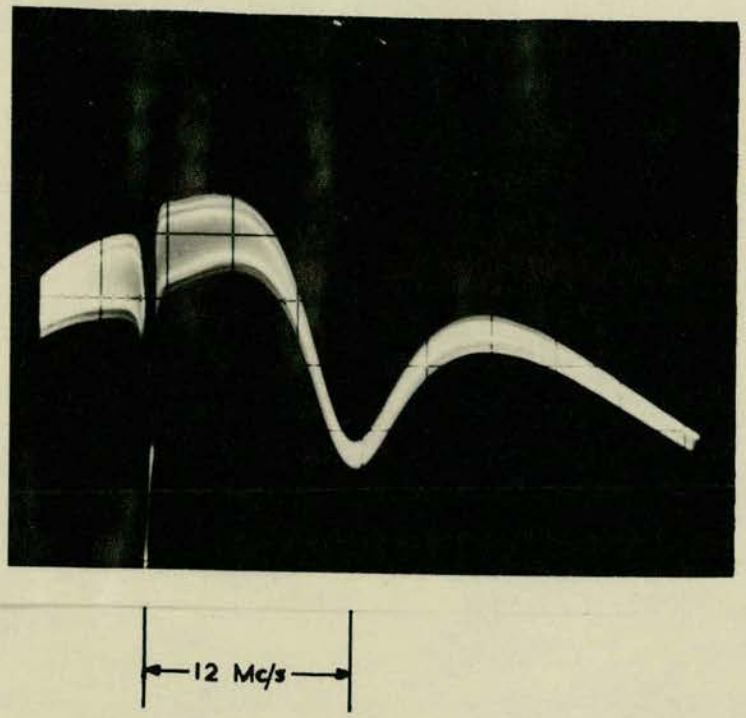

Fig.8.1

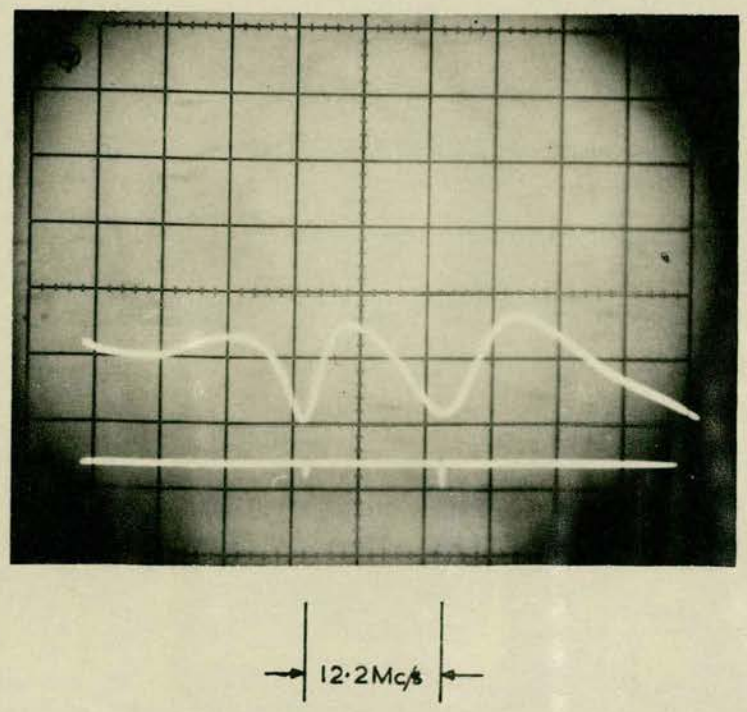

Fig.8.2

Fig. 8.3 Shows the cavity combination of Fig. 8.2 with a d.c. magnetic field of the appropriate value (4·13 Kg) applied. No pump. It is seen that the paramagnetic absorption occurs more strongly in the higher frequency half of the response. This indicates that, although there is coupling between the cavities, the splitting is due largely to the fact that the resonant frequency of the maser cavity is higher than that of the coupling cavity.

Fig. 8.4 Field on. Pump power on.
The application of the pump power confirms the above because amplification occurs at the higher frequency and of the response. Evidence of the coupling is present, however, for, although there is no amplification at the lower frequency, the paramagnetic absorption is reduced by the pump power.

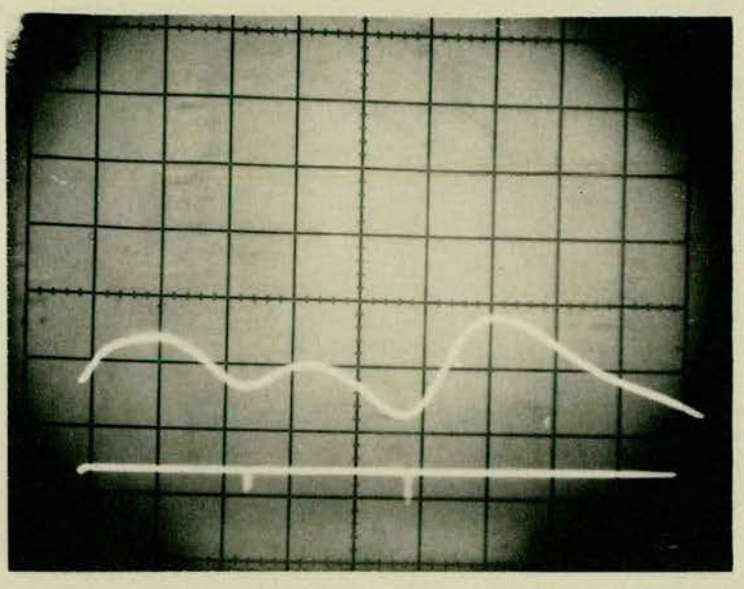

12·2 Mc/s

Fig.8.3

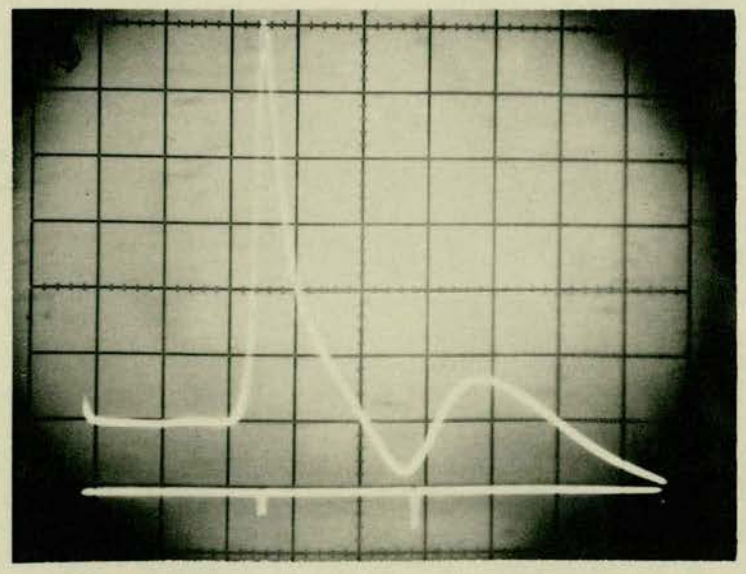

12·2 Mc/s

Fig.8.4

Figs. 8.5 and 8.6 are opposite extremes.

Fig. 8.5 Shows the two-cavity maser operating virtually as a single cavity maser. The coupling cavity is having little or no effect. The splitting is 10·6 Mc/s and the 3 dB bandwidth is 2·5 Mc/s. The gain is 15 dB.

Fig. 8.6 Shows a system with cavity splitting of 16·8 Mc/s. The bottom trace was taken with the pump and field off and the middle trace with the pump and field on. The gain is nominal but from the "squaring" of the response between the two resonances, it is apparent that both cavities are participating about equally. The maser cavity is resonant at a slightly lower frequency than the coupling cavity.

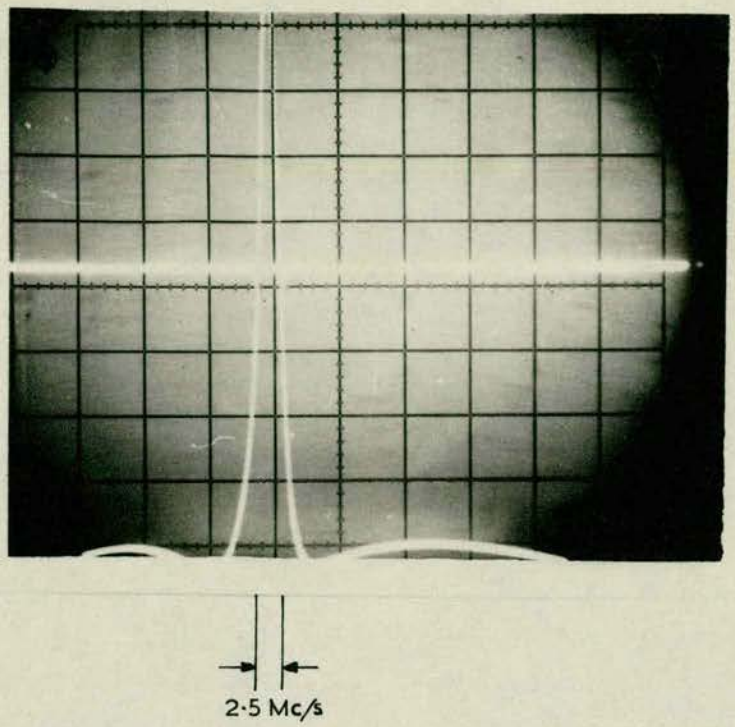

Fig.8.5

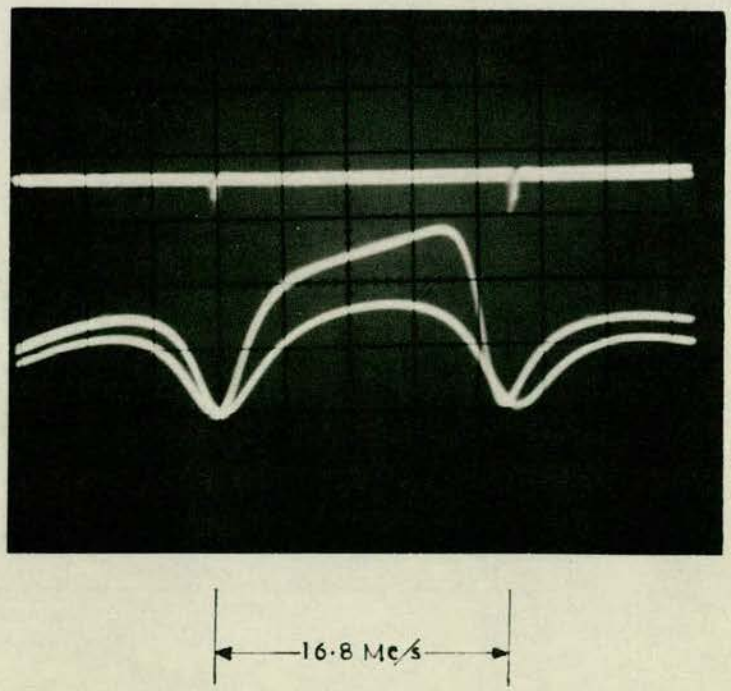

Fig.8.6

Figs. 8.7 to 8.12 are all of the same two-cavity combination.

Fig. 8.7 Shows an almost symmetrical splitting. No field. No pump.

Fig. 8.8 Shows the same maser with the magnetic field on. The paramagnetic absorption is towards the upper frequency.

Figs. 8.9 to 8.12 were all taken with the pump power on. The only differences in these photographs are due to slight changes in magnetic field and θ.

Fig. 8.9 Looks perfectly symmetrical which is surprising since the absorption shown in Fig. 8.8 is not.

Fig. 8.10 Shows the characteristic effect of altering the field slightly. In this case it was lowered.

Fig. 8.11 Shows the effect of increasing the field slightly and altering the angle θ by a very small amount. This should cause an effect similar to Fig. 8.10 but with the raised peak on the opposite side of the response curve. The comparatively high gain (7 dB) observed here indicates that the cavity alignment is not symmetrical and that the original field and angle settings used in Figs. 8.7 and 8.8 were slightly off the values for double pumping at the frequency of the applied pump power.

Fig. 8.12 This proves the above. The field strength and angle θ have been re-adjusted to give the desired

response shape. The gain here is only about 2 dB. The performance is limited by the fact that one parameter is deliberately being de-tuned to compensate for the misalignment of another.

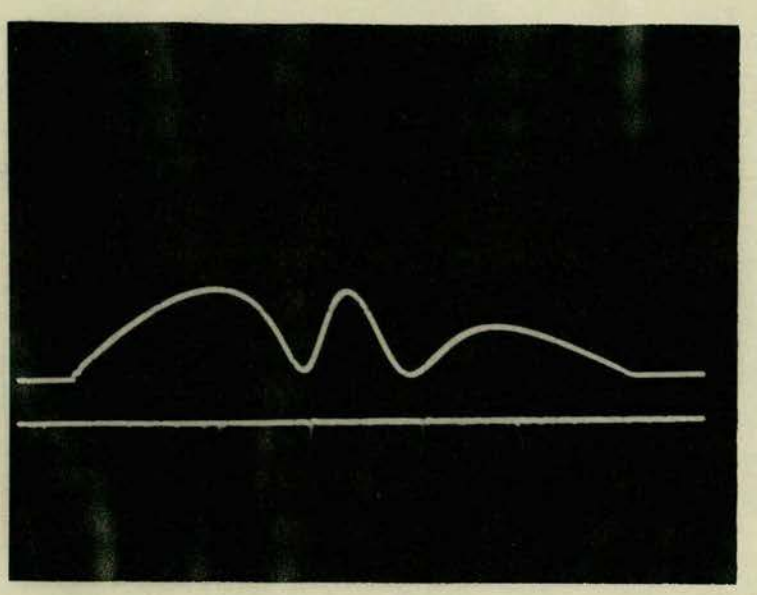

11·8 Mc/s

Fig.8.7

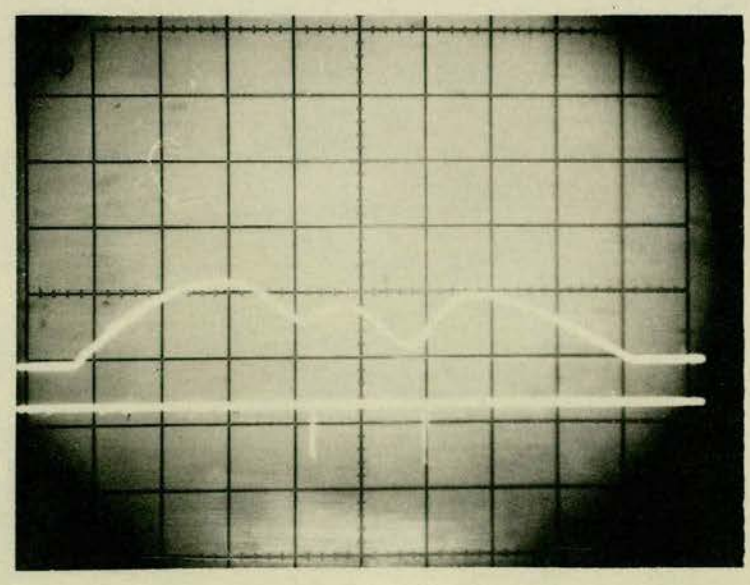

11·8 Mc/s

Fig.8.8

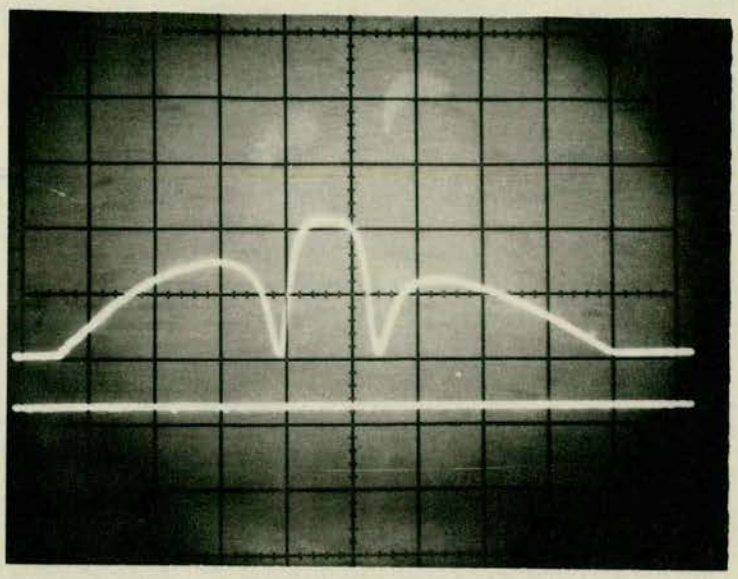

Fig.8.9

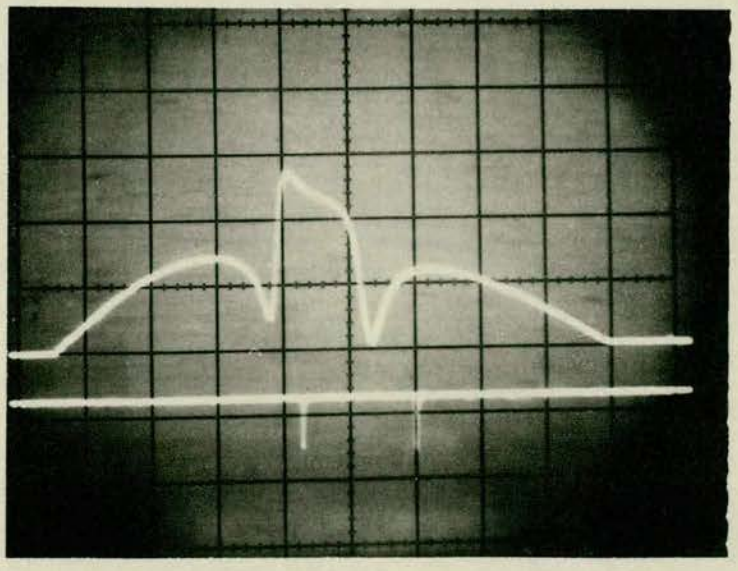

Fig.8.10

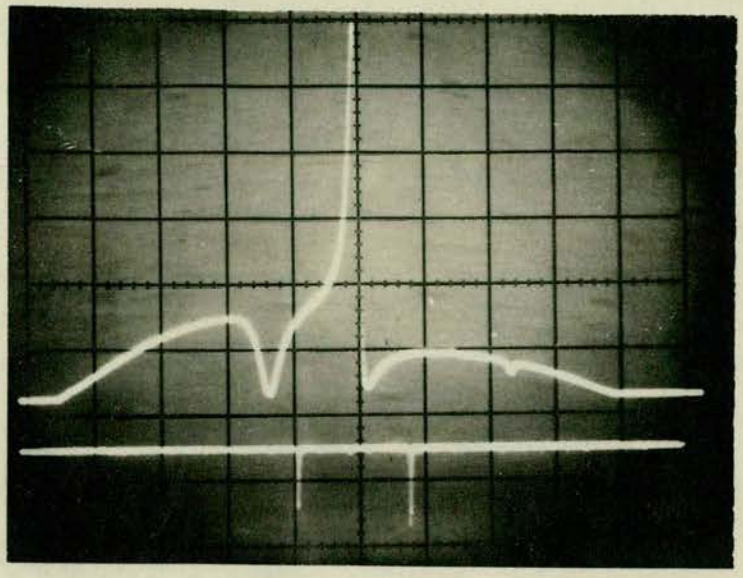

11·8 Mc/s

Fig:8.11

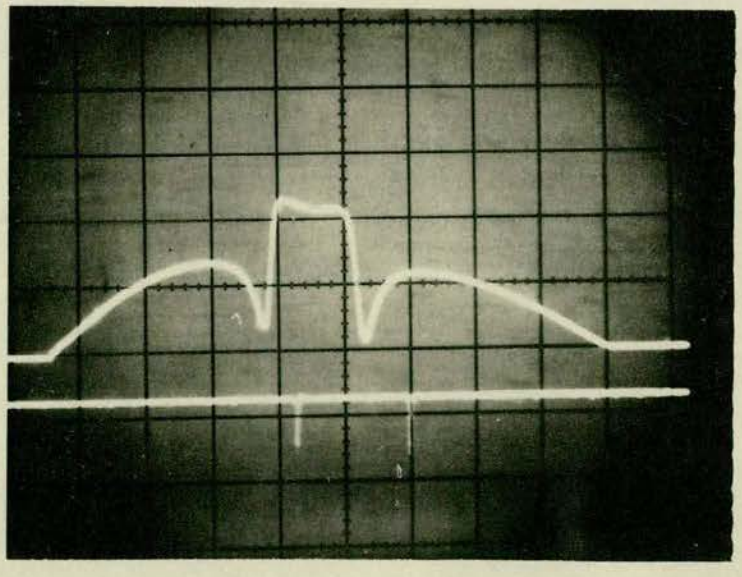

11·8 Mc/s

Fig.8.12

Figs. 8.13 and 8.14 Show a maser which is correctly aligned. As can be seen the field is very slightly too low in Fig. 8.13 and very slightly too high in Fig. 8.14. The optimum would be between the two. The gain of this maser was 12·7 dB. The width between the markers is 4·8 Mc/s and the 3 dB bandwidth was estimated to be about 4·6 Mc/s. It is seen that the required shape of response curve is produced, i.e. the gain is practically constant over about 4·5 Mc/s.

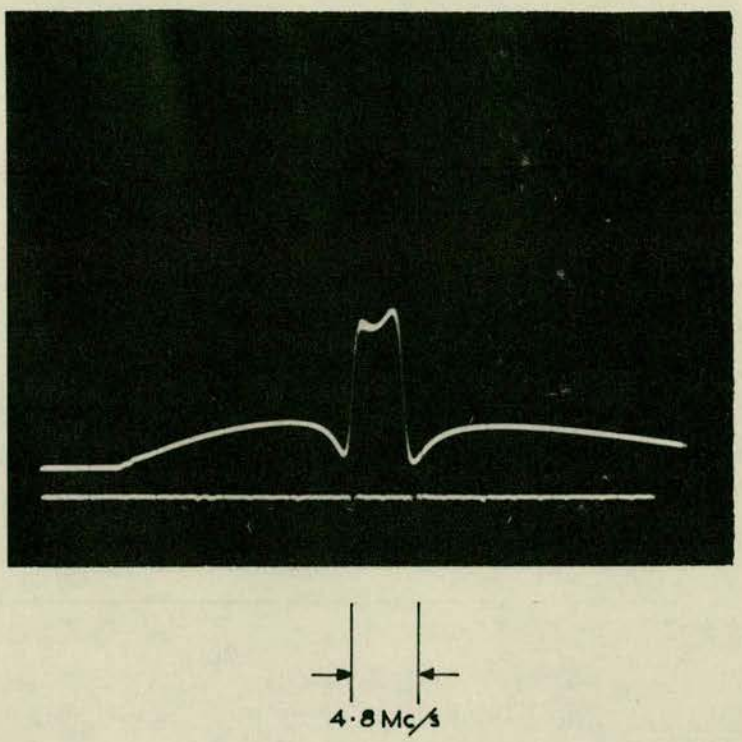

Fig.8.13

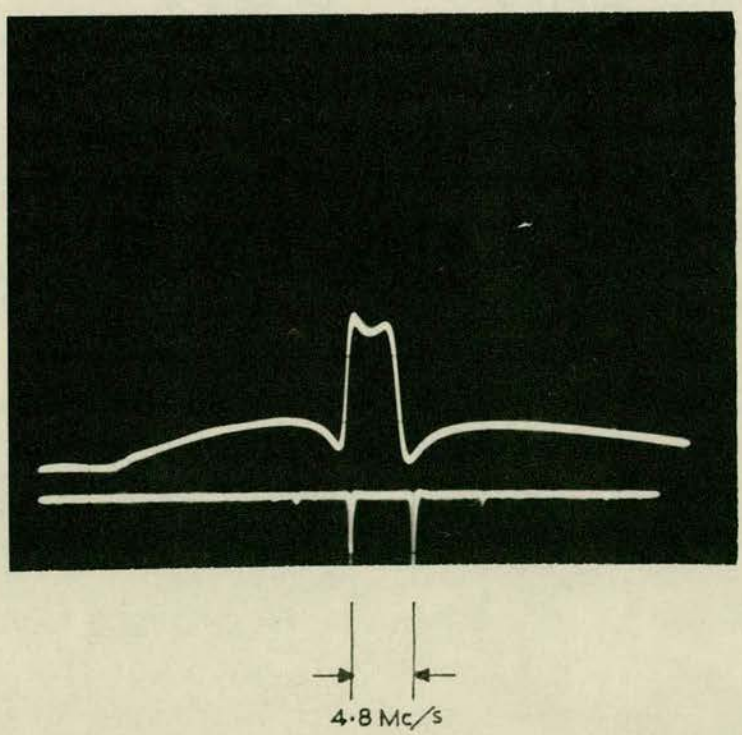

Fig.8.14

Fig. 8.15 Shows a single cavity maser response for comparison with Figs. 8.13, 8.14 and 8.16 (below). This maser was rather unstable which made accurate measurements difficult. The gain was about 10 dB and the 3 dB bandwidth about 2 Mc/s.

Fig. 8.16 Shows the two-cavity maser with the cavity splitting increased from the value used for Figs. 8.13 and 8.14. The gain was 6·5 dB and the 3 dB bandwidth was 8·8 Mc/s. The splitting in this case was perhaps slightly too large and the effect of this is seen in the way the edges of the response curve slope away. If the parameter k was even very slightly smaller the bandwidth close to the mid-band gain would be better defined.

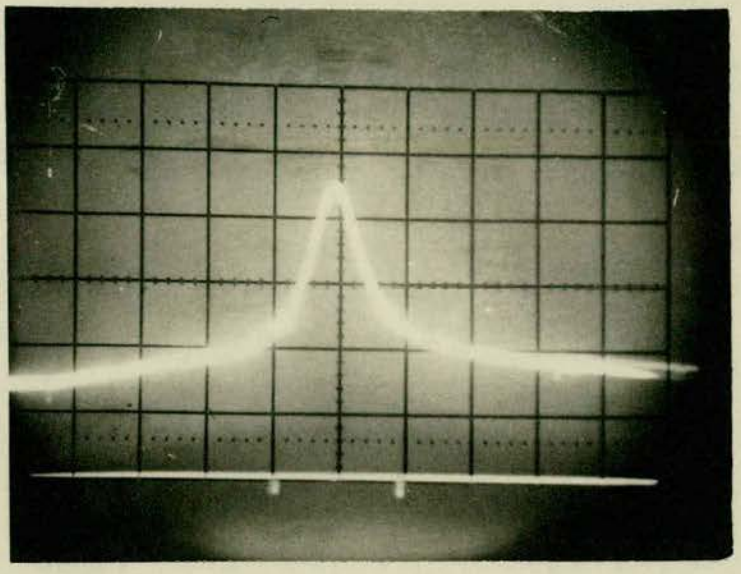

Fig.8.15

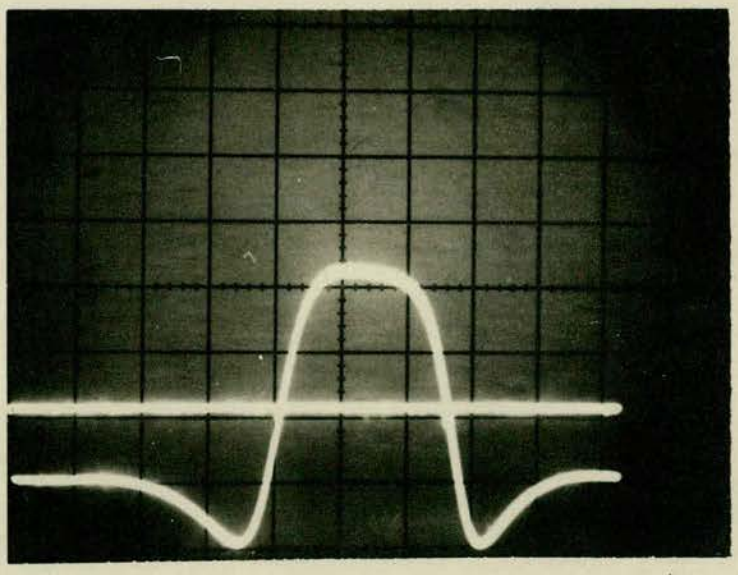

Fig.8.16

The best performances recorded are, therefore, 12·7 dB gain with a bandwidth of 4·6 Mc/s and 6·5 dB with a bandwidth of 8·8 Mc/s. As expected these are below the "best possible" values estimated at the end of Chapter 5.

It is felt that the gain measured may be less than the maximum gain of the maser due to signal saturation. The gain was measured with the crystal-video system which required that the maser input power be of the order of microwatts whereas the onset of signal saturation for a liquid-nitrogen-cooled maser occurs at about 4×10^{-8} watts. It was intended to investigate the variation of gain with signal input power and a low noise I.F. amplifier was obtained for this purpose. Unfortunately this amplifier developed a fault and it was not possible, in the limited time remaining, to have it repaired.

At the start of this project it was decided to use one passive cavity to increase the bandwidth because it was felt that the alignment problems involved would be difficult enough. During the course of this work Ammann[39] published results obtained with a liquid-nitrogen-cooled maser which had two passive cavities. Despite the fact that tuning adjustments were available on the cavities, Ammann was unable to produce the predicted flat response curve shape. It is clear from the thesis and the paper that this maser was well-designed and superbly engineered and it therefore may be inferred that a reactance compensated maser with two coupling cavities is very difficult, if not impossible, to align.

It is therefore claimed that it has been shown that the two-cavity liquid-nitrogen-cooled maser represents a significant improvement over the single cavity device both in increased bandwidth and in the near-rectangular response curve shape which is ideal for communication purposes.

REFERENCES

1. EINSTEIN, A.
   Phys. Zeits., 18, 121 (1917)
   "Zur Quantentheorie der Strahlung"

2. PLANCK, M.
   Ann. Phys. (Germany), 4, 553 (1901)
   "Uber das Gesetz der Energieverteilung im Normalspectrum"

3. SIEGMAN, A. E.
   "Microwave Solid State Masers"
   McGraw-Hill, 1964

4. GORDON, J. P., Zeiger, H. J. and Townes, C. H.
   Phys. Rev., 95, 284 (1954)
   "Microwave Molecular Oscillator and New Hyperfine Structure in the Microwave Spectrum of NH_3"

5. GORDON, J. P., Zeiger, H. J. and Townes, C. H.
   Phys. Rev., 99, 1264 (1955)
   "The Maser - A New Type of Microwave Amplifier, Frequency Standard and Spectrometer"

6. COMBRISSON, J., Honig, A. and Townes, C. H.
   C. R. Acad. Sci. 242; 2451 (1956)
   "Utilisation de la Resonance de Spins Electroniques pour Realiser un Oscillateur ou un Amplificateur en Hyperfrequences"

7. BLOCH, F.
   Phys. Rev., 70, 460 (1946)
   "Nuclear Induction"

8. CHESTER, P. F., Wagner, P. E. and Castle, J. G. (Jr.)
Phys. Rev., 110, 281 (1958)
"Two-Level Solid State Maser"

9. BLOEMBERGEN, N.
Phys. Rev., 104, 324 (1956)
"Proposal for a New Type of Solid-State Maser"

10. SCOVIL, H. E. D., Feher, G. and Seidel, H.
Phys. Rev., 105, 762 (1957)
"The Operation of a Solid-State Maser"

11. VUYLSTEKE, A. A.
"Elements of Maser Theory"
Van Nostrand, 1960

12. DE GRASSE, R. W., Schulz-du-Bois, E. O. and Scovil, H. E. D.
Bell Syst. Tech. J., 38, 305 (1959)
"The Three-Level Solid-State Travelling-Wave Maser"

13. McWHORTER, A. L. and Meyer, J. W.
Phys. Rev., 109, 312 (1958)
"Solid-State Maser Amplifier"

14. MAKHOV, G., Kikuchi, C., Lambe, J. O. and Terhune, R. W.
Phys. Rev., 109, 1399 (1958)
"Maser Action in Ruby"

15. GEUSIC, J. E.
Phys. Rev., 102, 1252 (1956)
"Paramagnetic Fine Structure Spectrum of Cr^{3+} in a Single Ruby Crystal"

16. CHANG, W.S.C. and Siegman, A. E. Special Supplement to: WEBER, J.
Rev. Mod. Phys. 31, 681 (1959)
"Masers"
(Also reprinted as a special supplement to Reference 3)

17. SCHULZ-DU-BOIS, E. O.
Bell. Syst. Tech. J., 38, 271 (1959)
"Paramagnetic Spectra of Substituted Sapphires - Part I: Ruby"

18. REITBOCK, H. J. P.
Ph. D. Thesis (1963) Max-Planck-Institut fur Biophysik. Frankfurt a. M.
"Ein X-band-Rubin Molekularverstarker mit einer Betriebstemperatur von 90°K fur biophysikalische Anwendungen"

19. KIKUCHI, C., Lambe, J. O., Makhov, G. and Terhune, R. W.
J. Appl. Phys., 30, 1061 (1959)
"Ruby as a Maser Material"

20. MORRIS, R. J., Kyhl, R. L. and Strandberg, M. W. P.
Proc. I.R.E., 47, 80 (1959)
"A Tunable Maser Amplifier with a Large Bandwidth"

21. KING, J. E. and Terhune, R. W.
J. Appl. Phys., 30, 1844 (1959)
"Operation of a Zero-Field X-band Maser"

22. NAGY, A. W. and Friedman, G. E.
Proc. I.E.E., 51, 361 (1963)
"Iron Sapphire Maser with No Magnetic Field"

23. NAGY, A. W. and Friedman, G. E.
Proc. I.E.E., 59, 1037 (1963)
"A No-Field Powder Maser"

24. GENNER, R. and Plant, J. G.
R.R.E. Memorandum No. 2070
"The Design of X-band Filled Cavity Ruby Masers with Special Reference to their Performance at Liquid Nitrogen Temperature"

25. MAIMAN, T. H.
J. Appl. Phys., 31, 222 (1960)
"Maser Behaviour: Temperature and Concentration Effects"
see also "Quantum Electronics" p. 324
C. H. Townes (Ed.)
McGraw-Hill

26. KRONIG, R. de L.
Physica, 6, 33 (1939)
"On the Mechanism of Paramagnetic Relaxation"

27. VAN VLECK, J. H.
Phys. Rev., 57, 426 (1940)
"Paramagnetic Relaxation Times for Titania and Chrome Alum"

28. PACE, J. H., Sampson, D. F. and Thorp, J. S.
Proc. Phys. Soc., 76, 697 (1960)
"Spin-Lattice Relaxation Times in Ruby at 34·6 Gc/s."

29. MIMS, W. B. and McGee, J. D.
Phys. Rev., 119, 1577 (1960)
"Cross-Relaxation in Ruby"

30. GEUSIC, J. E.
Phys. Rev., 118, 129 (1960)
"Harmonic Spin Coupling in Ruby"

31. MANENKOV, A. A. and Prokhorov, A. M.
Soviet Phys. J.E.T.P., 15, 54 (1962)
"Spin-Lattice Relaxation and Cross-Relaxation Interactions in Chromium Corundum"

32. ROBERTS, R. W., Burgess, J. H. and Tenney, H. D.
Phys. Rev., 121, 997 (1961)
"Cross-Relaxation and Concentration Effects in Ruby"

33. REITBOCK, H. J. P. and Redhardt, A.
Z. Naturforsch., 17a, 187 (1962)
"Ein Molekularverstarker fur eine Betriebstemperatur von 90°K"

34. WIEDERHOLD, G.
"Elektronenresonanz-Untersuchungen am Synthetischen Rubin" in "Hochfrequenzspektroscopie" by Losche, A. and Schutz, W.
Akademie Verlag, (Berlin) 1961, p. 148

35. DITCHFIELD, C. R.
Radio Electronic Engr., 27, 149 (1964)
"Prediction of the Optimum Noise Performance of a Reflection Cavity Maser"

36. FRUIN, A. S. and Ahern, S. A.
CVD Final Report No. VX8525
"Lightweight X-band Cavity Maser"

37. PAXMAN, D. H.
CVD Report RP8-17 (July, 1962)
"X-band Travelling-Wave Maser Assessment"

38. DILS, R. R., Martin, G. W. and Huggins, R. A.
Appl. Phys. Lett., 1, 75 (1962)
"Chromium Distribution in Synthetic Ruby Crystals"

39. AMMANN, E. O.
Ph. D. Thesis (1963), Electrical Engineering Department, Stanford University, California.
"Ruby as a Nitrogen-Temperature X-band Maser Material"
see also Trans. I.E.E., MTT-13, 186 (1965)
"Broad-Banded Solid-State Microwave Maser"

40. TABOR, W. J. and Sibilia, J. T.
Bell. Syst. Tech. J., 42, 1863 (1963)
"Masers for the 'Telstar' Satellite Communication Experiment"

41. BUTCHER, P. N.
Proc. I.E.E., 105, part B Supplement 11, 684 (1958)
"Theory of Three-Level Paramagnetic Masers" (Part 2)

42. SABISKY, E. S. and Gerritsen, H. J.
Proc. I.R.E., 49, 1329 (1961)
"A Travelling-Wave Maser Using Chromium-Doped Rutile"

43. HADDAD, G. I. and Paxman, D. H.
Trans. I.R.E., MTT-12, 406 (1964)
"Travelling-Wave Experiments Using Ruby"

44. HADDAD, G. I. and Rowe, J. E.
Trans. I.R.E., MTT-10, 3 (1962)
"X-band Ladder-Line Travelling-Wave Maser"

45. KYHL, R. L.
Proc. I.R.E., 48, 1157 (1960)
"Negative L and C in Solid-State Masers"

46. COOK, J. J., Cross, L. G., Bair, M. E. and Terhune, R. W.
Proc. I.R.E., 49, 768 (1961)
"A Low-Noise X-band Radiometer Using Maser"

47. NAGY, A. W. and Friedman, G. E.
Proc. I.R.E., 50, 2504 (1962)
"Reflection-Cavity Maser with Large Gain-Bandwidth"

48. KYHL, R. L., McFarlane, R.A. and Strandberg, M. W. P.
Proc. I.R.E., 50, 1608 (1962)
"Negative L and C in Solid-State Masers"

49. CROSS, L. G.

J. Appl. Phys., 30, 1459 (1959)

"Silvered Ruby Maser Cavity"

ACKNOWLEDGEMENTS

This research was carried out under the supervision of Professor W. E. J. Farvis whose advice and encouragement throughout the project is gratefully acknowledged.

Thanks are due to the S.R.C. for their generous financial support of the work.

The author would like to thank the Institution of Electronic and Radio Engineers for the award of the Mountbatten Research Studentship for three years.

It is felt that Mr. D. Anderson of the Mechanical Engineering Department deserves thanks for the skill which he exercised in making the special waveguide sections.